Microfluidics-Assisted Investigation of T-Lymphocyte Migration in Lymph Node Relevant Chemokine Gradients

A Thesis

submitted to the Faculty of Graduate Studies of

The University of Manitoba

in partial fulfilment of the requirements of the degree of

Doctor of Philosophy

by

Saravanan Andalur Nandagopal

Department of Biosystems Engineering

University of Manitoba

THE UNIVERSITY OF MANITOBA

FACULTY OF GRADUATE STUDIES

*****

COPYRIGHT PERMISSION

By

SARAVANAN ANDALUR NANDAGOPAL

A Thesis/Practicum submitted to the Faculty of Graduate Studies of the University of Manitoba in partial fulfilment of the requirement of the degree of Doctor of Philosophy

ABSTRACT

T-lymphocytes (T-cells) trafficking in the lymph nodes (LNs) is key for T-cells activation and their effector functions in adaptive immune responses. T-cells enter the LNs through high endothelial venules (HEVs) and interact with dendritic cells (DCs) for cognate antigens in the T-cell zone (TCZ). After scanning the TCZ for antigens, T-cells leave the LNs through efferent lymphatic vessel. CCR7 and its ligands, CCL19 and CCL21 are involved in the recruitment and compartmentalization of T-cells in LNs. However, their specific role(s) in mediating T-cells migration in LNs sub-regions remain unclear. In addition, the mechanism behind the passage of T-cells from the TCZ to the abluminal side of medullary sinuses (for their exit through medullary sinuses) is not well understood. Here, I hypothesize that different CCL19 and CCL21 fields in LNs sub-regions, orchestrate T-cells sub-regional migration in LNs..

In this study, I examined the CCL19 and CCL21 distribution profiles in mouse LNs sub-regions by immunofluoroscence staining and confocal microscopy. Using microfluidic devices that can flexibly configure well-defined single and co-existing chemical concentration gradients, I quantitatively analyzed the migration of activated human blood T-cells in LNs relevant CCL19 and CCL21 fields. The results suggested a novel CCL19 and CCL21 based combinatorial guiding mechanism for T-cells migration in different LNs sub-regions. In particular, this mechanism operates in the TCZ periphery region to guide T-cells migration away from the TCZ. Furthermore, the CCL19 and CCL21 fields mimicking the region beyond the TCZ toward the medulla result in disturbed chemotaxis, which prevents T-cells from being attracted back to the TCZ. Taken together, this microfluidics-based *in vitro* study shows the coordinated T-cells migration

in different single and combined CCL19 and CCL21 fields, leading to interesting new insights into the guiding mechanisms for T-cells trafficking in LNs sub-regions.

ACKNOWLEDGEMENTS

First, I sincerely express my thanks and gratefulness to my supervisor Dr. Francis Lin, Assistant Professor, Department of Physics and Astronomy, for his excellent guidance, mentorship and help. Dr. Lin celebrated my achievements and provided significant encouragement during the difficult times. I am grateful for his valuable support throughout my doctoral degree.

I express my heartfelt thanks to my co-advisor Dr. David Levin, Associate Professor, Department of Biosystems Engineering, for his valuable guidance and support during my Ph.D. study. Dr. Levin was always kind when I approached him in regard to matters both professional and personal.

I sincerely thank my doctoral committee member Dr. William L. Diehl-Jones, Associate Professor, Department of Biological Sciences, for his valuable guidance and constructive advice during my research. I also take an opportunity here to appreciate his support for providing space in his laboratory to conduct my experiments during my initial days.

I express my sincere thanks to my doctoral committee member Dr. Jason Morrison, Assistant Professor, Department of Biosystems Engineering, for his valuable suggestions and constructive advice during the course of my research.

I am grateful to my external examiner, Dr. Carolyn Ren, University of Waterloo, for examining my thesis and providing valuable comments.

I am also thankful to Dr. Jörg Stetefeld, Professor, Department of Chemistry, and Dr. John Wilkins, Director, Manitoba Centre for Proteomics and Systems Biology,

for supporting my research.

I also thank Dr. Jude Uzonna, Associate Professor, Department of Immunology, and Mr, Paul Perumal, Technician, Department of Human Anatomy and Cell Sciences, for providing mouse lymph nodes for this study and for cryo-sectioning sample preparation respectively.

I express my special thanks to Ms. Jing Li, M.Sc. student in the lab, for her support during this research; Dr. Dan Wu, Postdoctoral Fellow in the lab, for providing mathematical modelling results for this thesis; I also express my thanks to my other lab members Nitin Wadhawan, Jiandong Wu, Kanmani Natarajan and Xun Wu for their support and assistance.

I also want to thank Ms. Wanda Klassen, Ms. Susan Beshta, Mr. Gilles Roy and Mr. Maiko Langelaar, Department of Physics and Astronomy, and Ms. Debby Watson and Ms. Evelyn Fehr, Department of Biosystems Engineering, for their valuable support. In addition, I would like thank Dr. Adam Rogers, Department of Physics and Astronomy, for giving his valuable time for proof reading my thesis. I also thank all my friends in Winnipeg for their moral support during my stay here.

I express my thanks to Nano Systems Fabrication Laboratory (NSFL), University of Manitoba, especially Mr. Dwayne Chrusch, for support of microfluidic device fabrication. I thank the Victoria Institute of Clinical Research and Evaluation (Vic R&E), Winnipeg, especially Ms. Shauna Leeson for helping with human blood samples.

I am also thankful to the University of Manitoba, Manitoba Health Research Council, Manitoba Institute of Child Health, the Natural Sciences and Engineering Research

Council of Canada, and the Canada Foundation for Innovation, for their financial and research support.

In addition, I thank all my teachers (starting from elementary school) who made learning fascination and taught every subject, including science, with fashion.

Finally yet importantly, I acknowledge my family. I would like to articulate my deepest gratitude to my parents in India for inculcating the value of hard work and dedication in life and appreciate their hard work for bringing me up to this level. I express my greatest appreciation to my wife Suchitra and my daughter Khaashwini for their devotion in my every accomplishment and their support in my successes and difficulties.

TABLE OF CONTENTS

LIST OF TABLES

LIST OF FIGURES

LIST OF FIGURES IN APPENDIX

LIST OF ABBREVIATIONS

B-cells- B-Lymphocytes

CCR7- C-C Chemokine receptor type-7

C.I.- Chemotactic Index

CIP4- Cdc42 Interacting Protein 4

CNS- Central Nervous System

2D- Two-dimensional

3D- Three-dimensional

DCs- Dendritic Cells

ECs- Endothelial Cells

ECM- Extracellular Matrix

ELR- Glutamic acid-Lysine-Arginine

ERK- Extracellular Signal-Regulated Kinase

FITC- Fluoro-iso-thiocyanate

fMLP- formyl-Methionyl Leucyl-Phenylalanine

GDP- Guanosine Di Phosphate

GM-CSF- Granulocyte Macrophage Colony-Stimulating Factor

GPCRs- G-Protein Coupled Receptors

GTP- Guanosine Tri Phosphate

HEVs- High Endothelial Venules

ICAM- Intercellular Adhesion Molecule

IFN- Interferon

IL8- Interleukin 8

LFA- Lymphocyte Function-Associated Antigen

LNs- Lymph Nodes

LTB4- Leukotriene B4

MAdCAM- Mucosal Addressin Cell Adhesion Molecule

MAPK- Mitogen Associated Protein Kinase

M-CSF- Macrophage Colony-Stimulating Factor

MHC- Major Histocompatibility Complex

MLN- Mesenteric Lymph Nodes

MS- Multiple Sclerosis

NK-cells- Natural Killer Cells

PAF- Platelet-Activating Factor

PAK- p21-Activated Kinase

PBMC- Peripheral Blood Mononuclear Cells

PDGF- Platelet-Derived Growth Factor

PDMS- Polydimethylsiloxane

PECAM-1- Platelet Endothelial Cell Adhesion Molecule-1

PH- Pleckstrin Homology

PIP3- Phosphatidylinositol 3, 4, 5-trisphosphate

PI3K- Phosphatidylinositol 3, 4, 5-trisphosphate Kinase

PKB- Protein Kinase B

PLN- Peripheral Lymph Node

PTEN- Phosphatase and Tensin Homolog

RNAi- RNA interference

S1P- Sphingosine-1-Phosphate

S1P1- Sphingosine-1-Phosphate Receptor 1

SC- Sub-cortical zone

SDF- Stromal Cell Derived Factor

SLTs- Secondary Lymphoid Tissues

T-cells- T-Lymphocytes

TCR- T-Cell Receptor

TCZ- T-Cell Zone

TNF- Tumour Necrosis Factor

VCAM- Vascular Cell Adhesion Molecules

WASP- Wiskott–Aldrich Syndrome Protein

CHAPTER 1

INTRODUCTION

1.1. INTRODUCTION AND OUTLINE OF THE THESIS

Cell migration is critical for physiological processes such as embryogenesis, immune responses, wound healing and neuron guidance. Migration also causes pathological conditions including autoimmune diseases and cancers (Luster et al., 2005). Therefore, it is important to understand the mechanisms underlying directed cell migration. Cells can migrate directionally in response to different guiding factors such as chemical concentration gradients, electric field and mechanical stimulations (Li et al., 2012; Menon and Beningo, 2011; Zhao et al., 2006). While it is beneficial to study cell migration in physiological models, *in vivo* approaches are often invasive and difficult to measure or control the local cell migration environments. In addition, it is challenging to quantify cell migration *in vivo* due to limitations of light microscopy. By contrast, *in vitro* assays allow measurements of directed cell migration in simplified but controlled environments. Particularly, microfluidic devices can configure the chemical microenvironments to mimic the physiological conditions and allow quantitative cell migration analysis at the single cell level (Jeon et al., 2002). Such a microfluidics-based biomimetic approach enabled the research in this thesis concerning the migration of immune cells in chemical guiding environments simulating lymph nodes (LNs).

LNs play a crucial role in organising adaptive immune responses. In LNs, antigen carrying dendritic cells (DCs) present the cognate antigens to the resident T-lymphocytes (T-cells) to initiate the T-cells activation and proliferation as part of secondary immune

response (Cyster et al., 2005). C-C Chemokine receptor type-7 (CCR7) and its ligands CCL21 and CCL19 recruit T-cells to LNs and the importance of CCR7 and its ligands were further confirmed in the CCR7-deficient mouse model and the *plt/plt* (lack CCL21 and CCL19 expression) mouse model (Cyster, 2005; Forster et al., 2008; Otero et al., 2006; Weninger and von Andrian, 2003). CCL21, present in the high endothelial venules (HEVs) of LNs, recruits T-cells and B-lymphocytes (B-cells) (Gunn et al., 1999). After crossing the HEVs, the T-cells follow the CCL21 and CCL19 gradients to reach the T-cell zone (TCZ) (Cyster, 2005). Though the T-cells recruit mechanism is well defined, the process of T-cells sub-regional migration in LNs is not clear.

In the TCZ, T-cells scan for cognate antigens by interacting with dendritic cells (DCs). After scanning the TCZ, T-cells down regulate their CCR7 expression and reach the medullary sinuses or cortical sinusoids (egress ports) for their ultimate exit from LNs by the Sphingoisine-1-phosphate receptor 1 (S1P1) based mechanism (Cyster, 2005; Pham et al., 2008). Though the CCR7 ligands are involved in the recruitment of T-cells to LNs, the specific roles of CCR7 ligands in T-cells sub-regional migration in LNs is still not clear. Previous studies demonstrated that the S1P1 based mechanism is confined to the egress port, suggesting there must be an intermediate mechanism bringing T-cells to the vicinity of the egress port from the TCZ for their ultimate exit (Mandala et al., 2002; Pham et al., 2008; Wei et al., 2005; Worbs and Förster, 2009). Furthermore, previous studies indicated that CCL21 alone is sufficient to recruit T-cells to LNs (Britschgi et al., 2010; Gunn et al., 1999; Link et al., 2007). Despite the fact that CCL21 alone is enough to recruit the T-cells to the TCZ, the reason for the presence of CCL19, having similar action, in the TCZ remains unclear.

Conventional cell migration assays such as transwell assays lack the ability to configure complex chemical gradients and to quantitatively analyze cell migration at the single cell level. In this thesis, I employed a microfluidic system to examine activated human T-cells migration in different CCL21 and CCL19 fields that mimic the conditions in LNs sub-regions to understand the T-cells sub-regional migration in LNs. The microfluidics-based cell migration studies are supplemented by LNs sub-regional CCL21 and CCL19 distribution analysis, CCR7 expression analysis in T cells upon exposure to different CCL21 and CCL19 fields, and mathematical modelling (through collaboration). The results in this thesis suggested a combinatorial guiding mechanism by CCR7 ligands fields for T-cells migration in LNs sub-region relevant environments. Such a mechanism has particular importance in facilitating T-cells passage from the TCZ to the medulla for their exit from LNs.

Chapter 1 provides the biological and immunological background of directed immune cell migration and trafficking. In addition, this chapter provides the technological background of different *in vitro* cell migration assays and justifies the use of microfluidics-based approach. Finally, this chapter discusses the rationale, central hypothesis and objectives of the thesis. The details of experimental methods are described in Chapter 2. Chapter 3 and 4 are devoted to the results and discussion. Chapter 3 investigates the combinatorial guidance by CCR7 ligands fields for T-cells migration in co-existing chemokine fields relevant to LNs sub-regions. Chapter 4 further investigates this combinatorial guiding mechanism with a focus on its dependency on CCR7 ligands fields and its relevance to facilitating T-cells exit from LNs. In Chapter 4, I also report the CCL21 and CCL19 distribution profile analysis in mouse LN sub-

regions to support the chemokine field configurations in the microfluidic system. Finally, I conclude the thesis and discuss future directions in Chapter 5. The sub-regional T-cells migration analysis in the dual same-side CCL21 and CCL19 gradients and cell surface CCR7 expression analysis upon exposure to different CCL21 and CCL19 fields are provided as appendix after the main chapters.

1.2. BACKGROUND OF DIRECTED IMMUNE CELL MIGRATION AND IMMUNE CELL TRAFFICKING

1.2.1. Overview

Immune cell migration is essential for a variety of physiological functions including immune cell development, immunosurveillance, and host defence. However, misdirected immune cell migration can result in pathological problems such as ischemia and reperfusion injury stroke, myocardial ischemia and infarction, and disseminated intravascular coagulation, shock, systemic septicemia, transplantation, severe trauma and burns, acute lung injury (adult respiratory distress syndrome), and various autoimmune disorders (systemic lupus erythematosus, multiple sclerosis and rheumatoid arthritis) (Friedl and Weigelin, 2008; Geng, 2001).

The mechanism of immune cell migration is a multi-step process, that is highly tissue specific and tightly regulated. Circulating immune cells "sense" the environmental guiding cues such as adhesion and chemotactic signals, which initiates adhesion of immune cells on endothelial cells (ECs) followed by transmigration through endothelial barrier and chemotactic migration (chemotaxis) (Figure 1.1.). The adhesion process is mediated by sequential activation of adhesion proteins and their ligands on both leukocytes and ECs (Bretscher, 2008; Friedl and Wolf, 2010; Horwitz and Webb, 2003). In T-cells trafficking in LNs, CCR7 ligands orchestrate the T-cells entry into the LNs and their sub-regional compartmentalization (Cyster, 2005). Chemokine CCL21, a CCR7 ligand originating from HEVs of LNs, orchestrates the rolling process of naive T-cells on ECs of HEVs and activates Integrins on naive T-cells for adhesion (Gunn et al., 1998). Subsequently, attached naive T-cells undergo transendothelial migration and reach the

TCZ of LNs. In TCZ, T-cells migrate randomly to interact with antigen laden DCs for cognate antigens (Worbs et al., 2007). DCs process and present the captured antigens to T-cells through Major Histocompatibility Complex molecules (Guermonprez et al., 2002). Activated T-cells stay in LNs over an extended period of time, where they proliferate resulting in clonal expansion and the inactivated naive cells leave the LNs immediately for further surveillance (Cyster, 2005). The expanded T-cells populations then leave the LNs through efferent lymphatic vessel for effector functions (Pham et al., 2008).

1.2.2. Immune cell migration and chemotaxis

1.2.2.1. Gradient sensing

Chemotactic signals act as extracellular cues to guide immune cell movement, and this process is known as chemotaxis (Figure 1.1.). The chemotactic factors (chemoattractants) released during inflammation, injury, death of host cells and phagocytosis of pathogens trigger chemotaxis of immune cells. Immune cells can sense a gradient as low as a 2% variation of chemoattractant concentration across the cell body (Comer and Parent, 2002). The extracellular chemical factors (ligands) bind with their corresponding G-Protein Coupled Receptors (GPCRs) present on the surface of immune cells and activate the GPCRs. The GPCRs activation by ligand binding induces the Phosphoinositide-3-kinase (PI3K) pathway. Activated PI3K phosphorylates phosphatidylinositol 4, 5-disphosphate (PIP2) to phosphatidylinositol 3, 4, 5-trisphosphate (PIP3), and newly formed PIP3 molecules accumulate in the leading edge of the cell. When cells are placed in a gradient of chemoattractant, the delicate balance between the activation of PI3K and Phosphatase and Tensin Homolog (PTEN) leads to

the spatial enrichment of PIP3 at the leading edge (Wessels et al., 2007). PIP3 accumulation recruits pleckstrin homology (PH) domain proteins like Cytosolic Regulator of Adenylyl Cyclase (CRAC) and Protein Kinase B (PKB) from the cytosol to the leading edge and the PH domain-containing proteins act as adapters for a variety of downstream responses (Comer and Parent, 2002). This PIP3 mediated intracellular signalling process initiates the formation of pseudopodia at the leading edge and actomyosin contraction at the rear end of the cell that drive the cell to migrate (Van Haastert and Veltman, 2007). Cells can sense chemical gradients in both soluble and surface-bound states. Immune cells undertake chemotaxis in soluble chemoattractant gradients, and haptotaxis on immobilized surface-bound gradients (Friedl and Weigelin, 2008). Cell migration can occur either on a two-dimensional (2D) substrate or in a three-dimensional (3D) extracellular matrix (ECM). 2D, but not 3D, cell migration is integrin dependent (Klemke et al., 2010). In 2D migration, cells attach to the substrate and form a protrusion to move toward the target. In 3D migration, cells adjust their morphology to fit to the limited available space within the ECM or by remodelling the ECM (Friedl and Wolf, 2010; Klemke et al., 2010; Wolf et al., 2003) .

1.2.2.2. Cell adhesion and migration

Physical contact of immune cells to the ECM is critical for immune cell migration. Leukocytes arrest to ECs, preceding the migratory process (Figure 1.1.). Arrest and adhesion of leukocytes involve tethering, rolling and attaching on ECs. After sensing the chemical signals, immune cells respond by primary adhesion (tethering and rolling) followed by firm adhesion. Primary adhesion is mainly mediated by different selectin

molecules and firm adhesion is mediated by integrins (Grabovsky et al., 2000). Selectins P, E and L involve in the primary adhesion of leukocytes.

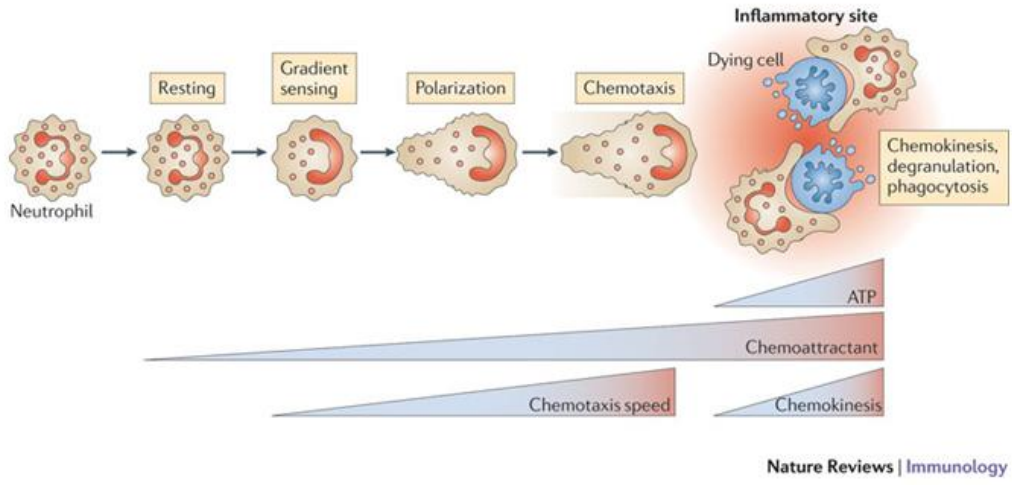

Figure 1.1. Illustration of the leukocyte recruitment process. The figure was reprinted by permission from Macmillan Publishers Ltd: [Nature Review] (Junger, 2011), copyright (2011).

Selectins are expressed on leukocytes (L-selectin), platelets (P-selectin) and vascular ECs (E and P selectins) (Tedder et al., 1995). Selectins help the attachment of leukocytes on venular (blood vessel) ECs near the site of injury or inflammation by binding with the carbohydrate moiety of different ligands. After primary adhesion, interaction between integrins and immunoglobulin superfamily members leads to firm attachment of immune cells on vascular endothelium. Integrins are transmembrane obligate heterodimers having α (alpha) and β (beta) subunits and bind with the cell surface and ECM components such as fibronectin, vitronectin, collagen, laminin, lymphocyte function-associated antigen (LFA-1), intercellular adhesion molecules (ICAM)-1 and ICAM-2, vascular cell adhesion molecules (VCAM)-1 and mucosal addressin cell adhesion molecule (MAdCAM) (Kinashi and Katagiri, 2005). Integrin activation is initiated by activation of selectins and chemoattractants such as leukotriene B4 (LTB4), platelet activating factor (PAF), Complement component 5a (C5a) and formyl-Methionyl-Leucyl-Phenylalanine (fMLP) and chemotactic cytokines (chemokines) (Laudanna and Bolomini-Vittori, 2009; Schaerli and Moser, 2005). Recently, it has been shown that many molecules other than chemoattractants are involved in integrin-based adhesion. Carreau et al. showed that nitric oxide expression in ECs during inflammation modifies cell adhesion (Carreau et al., 2010). In another study, Koduru et al. showed the importance of Cdc42 interacting protein 4 (CIP4) in integrin-dependent T-cells trafficking (Koduru et al., 2010). After the firm adhesion, a cascade of intracellular signalling events organises the pseudopod (leading edge) and the uropod (tail) formation in the arrested cells leading to organised transendothelial migration (diapedesis) and chemotaxis (Friedl et al., 2001). Platelet Endothelial Cell Adhesion Molecule-1 (PECAM-1) plays an important role in leukocyte diapedesis (Muller, 2009). The paracellular diapedesis occurs between ECs (junction

between individual cells) and the transcellular diapedesis process occurs through the individual ECs. After the diapedesis process, leukocytes follow the existing chemical gradient to reach the target (chemotaxis).

During chemotaxis, cell surface GPCRs are activated by chemoattractant gradients leading to cascade of intracellular signalling. GPCRs are seven transmembrane receptors having extracellular amino (-NH2) terminal and the intracellular acid (-COOH) C terminal. The G- Protein domain is attached to the C terminal of the receptor (Kroeze et al., 2003). In GPCRs, Gα proteins form complex with Gβ and Gγ to create a heterodimeric structure of the G-protein. GPCRs are inactive with Guanosine diphosphate (GDP) binding and become active when GDP is phosphorylated to Guanosine triphosphate (GTP) by chemokine binding (Murdoch and Finn, 2000). The GPCRs activation causes detachment of the G-protein from the receptor. When the G-protein detaches from the receptor, Gα and Gβγ separate from the detached G protein unit. Gα and Gβγ activate the membrane bound enzyme PI3K (Murdoch and Finn, 2000). Activated PI3K activates the Rho GTPase proteins namely RhoA, Rac1 and Cdc42. Rho family proteins, RhoA, Cdc42, and Rac1 are small GTP-binding proteins, which involve in actin polymerisation and myosin contraction during cell migration (Ridley et al., 2003). Rac1 and Cdc42 initiate actin polymerisation at the leading edge of the cell and RhoA interacts with Rho associated coiled–coil kinase (ROCK) and myosin at the rear end of the cell initiating myosin contraction. Upon activation by GTP binding, Rho family proteins interact with downstream molecules (effectors) such as kinases and scaffold proteins for actin polymerisation leading to lamellipodia and filopodia formation. Each Rho family proteins interact with their respective downstream

molecules. Activation of Cdc42 results in its interaction with p21-Activated Kinase (PAK) and Wiskott–Aldrich syndrome protein (WASP). Activated Rac1 interacts with downstream proteins namely PAK, IQGAP1 (scaffolding protein) and p140Sra-1. Activated RhoA interacts with ROCK (also known as ROK), the myosin-binding subunit of myosin phosphatase, protein kinase N, mDia, citron and rhotekin (Fukata et al., 2003). Subsequent activation and deactivation of Rho GTPases causes adhesion and detachment of leukocytes leading to forward migration of leukocytes (Alblas et al., 2001; Sanchez-Madrid and Angel del Pozo, 1999; Xu et al., 2003). In addition, PI3K activation causes the formation of diacyl-glycerol (DAG), which interacts with protein kinases to mediate cell polarization (Murdoch and Finn, 2000).

Apart from P13K activation pathway, the detached Gα sub-unit of G protein activates the mitogen associated protein kinases (MAPK) pathway (Murdoch and Finn, 2000). There are five different groups of MAPKs so far identified. ERK (extracellular signal-regulated Kinase) 1/2, c-Jun N-terminal kinases (JNKs), and p38 kinases are well documented groups (Roux and Blenis, 2004). Each group has a set of three kinases namely MAP kinase (MAPKs), MAPK kinase (MAPKKs), and MAPKK kinase (MAPKKKs). The detached Gα sub-unit activates the Rho GTPase family, which in turn phosphorylates MAPKKK. Phosphorylated MAPKKKs phosphorylate MAPKKs and phosphorylated MAPKKs subsequently phophorylate MAPKs (Roux and Blenis, 2004). The activated MAPKs interact with different downstream substrates, which ultimately lead to cell migration (Huang et al., 2004; Klemke et al., 1997; Roux and Blenis, 2004).

1.2.3. Chemotactic factors and their cell surface receptors

Chemotactic factors and their respective receptors play central roles in immune cell migration and trafficking. Knowledge of chemoattractants and their receptors are crucial to study immune cell migration. Chemoattractants include classical chemoattractants such as bacterial lipids, formylated peptides, and proteolytic fragments of complement proteins or specialized chemotactic cytokines (chemokines). The important classical chemoattractants include PAF, fMLP, C5a and LTB4. Formation of arachidonic acid during inflammation leads to the release and acylation of lysoglycerol-ether-phosphoryl choline, which produces PAF, a potent inflammatory chemoattractant acting through its receptor PAFR (Wardlaw et al., 1986). PAF is a potent attractor of monocytes, neutrophils and eosinophils. Another potent chemoattractant for monocytes and neutrophils is fMLP, which is derived from bacterial culture. fMLP acts through its receptor fMLPR (Schiffmann et al., 1975). Complement peptide (anaphylatoxin) C5a, a proteolytic fragment of complement component C5, is another potent chemoattractant for neutrophils, eosinophils, basophils, monocytes and macrophages (Ehrengruber et al., 1995). C5, the potent proinflammatory factor, is released by complement action during inflammation. Another extensively studied neutrophil chemoattractant is LTB4, which acts through its receptor LTBR. Inflammation leads to the formation of arachidonic acid, which is then converted to LTB4 by oxygenation and enzymatic hydration (Luster, 2001).

1.2.3.1. Chemokines

Chemokines maintain continuous trafficking of immune cells among various microenvironments to ensure proper immunosurveillance and homeostasis (Figure 1.2.). Chemokines and chemokine receptors also play important roles in mediating various

diseases (Table 1.1.). Some chemokines are homeostatic, which are produced and secreted constitutively and others are only produced by cells during infection or following pro-inflammatory stimulations. Chemokines are 8-10 kDa sized cytokines and are classified into four different groups based on the spacing of the first two cysteine residues (C) near the N terminal. They are CXC (alpha chemokines), CC (beta chemokines), CX_3C and C (Murphy et al., 2000).

In CXC chemokines, the two cysteines adjacent to N-terminal are separated by another amino acid. The CXC type is further subdivided into ELR positive and ELR negative chemokines. Glutamic acid-lysine-arginine (ELR) near the N-terminus (preceding the CXC sequence) determines this classification. ELR positive chemokines such as CXCL1, CXCL2, CXCL3, CXCL5, CXCL6, CXCL7, CXCL8, and CXCL15, facilitate neutrophil adhesion and chemotaxis. ELR negative chemokines, such as CXCL4, CXCL9, CXCL10, CXCL11, CXCL12, CXCL13, CXCL14, and CXCL16, are poor neutrophil chemoattractants (Laing and Secombes, 2004; Murphy et al., 2000).

There are 28 CC chemokines (CCL1-CCL28). They have adjacent cysteine residues next to the amino terminal. They are potent attractants of mononuclear immune cells. These CC chemokines are subdivided into four sub-groups- allergenic, pro-inflammatory, developmental, and homeostatic based on their functional diversity (Laing and Secombes, 2004). Normally, CC chemokines have four cysteine residues but there are a few exceptions, such as CCL21, which have six cysteine residues. Lymphactin and fractalkine are the two chemokines found in “C” and CX3C types of chemokines, respectively (Kelner et al., 1994 and Bazan et al., 1997).

1.2.3.2. Chemokine receptors

Based on the specific binding to the chemokines, the chemokine receptors are divided into different groups. They are classified as CCR, CXCR, XCR and CX3CR (Murphy et al., 2000). In CXCR, CXCR1 and CXCR2 are the only receptors for ELR positive CXC chemokines such as interleukin 8 (IL8) (Hammond et al., 1995). Apart from chemotaxis, CXCR1 is also involved in superoxide production during IL8 induced chemotaxis. In addition, CXCR1 responds to growth-regulated oncogene (GRO) α at high concentrations and CXCR2 responds to GRO α and neutrophil-activating peptide 2 (NAP2) at lower concentrations (Murphy et al., 2000). CXCR3 is a receptor for ELR negative CXC chemokines and is found on circulating T-cells, B-cells, and natural killer (NK) cells (Qin et al., 1998). CXCR4 (a HIV co-receptor) is found on T-cells and B-cells, as well as monocytes and neutrophils, and responds to CXCL12 (SDF-1) (Bleul et al., 1996). CXCR5 is specific to the B-cell attracting chemokine BLC (Breitfeld et al., 2000).

CCR1 was the first CCR receptor to be identified in 1993. CCR1 binds with multiple chemokines. It is an important inflammatory receptor and its role in neutrophil guiding mechanism is well known (Ramos et al., 2005). Another important CCR is CCR2. CCR2 RNAs are detectable in monocytes, DCs, NK cells, and T-cells, but not in resting neutrophils or eosinophils. CCR3 is an eoisnophil chemokine receptor and plays important roles in asthma and antihelminthic host defense. CCR7 is another important CCR receptor. It plays an important role in the homing of naive lymphocytes and DCs into secondary lymphoid organs and in thymocytes maturation (Cyster, 2005).

1.2.3.3. CCR7 and its ligands (CCL21 and CCL19)

CCR7 is expressed on various immune cells, including naive and memory T-cells. CCR7 and its ligands CCL21 and CCL19 are responsible for T-cells migration in thymus and LNs (Figure 1.2.). Lack of CCR7 results in devoid of T-cells in LNs, and excessive accumulation of T-cells in non-lymphoid tissues (Höpken et al., 2007). CCR7 deficiency also causes delayed immune response and oral tolerance (Martin et al., 2009). Furthermore, CCR7 over-expressing cells are retained in LNs and CCR7 down-regulation is critical for T-cells egress from LNs (Cyster, 2005; Pham et al., 2008). Deficiency of CCR7 and its ligands causes reduced motility of T-cells in LNs (Okada and Cyster, 2007; Worbs et al., 2007). CCR7 is also critical for localizing the T-helper cells within LNs for effective secondary immune response (Randolph et al., 1999). CCR7 and its ligands also involve in the migration of other immune cells. CCR7 and its ligand CCL21 facilitate the homing of antigen captured DCs into secondary lymphoid tissues (SLTs). Recently, the involvement of CCR7 was implicated in neutrophil migration into LNs (Beauvillain et al., 2011). Moreover, CCR7 is essential for peripheral tolerance against environmental agents and the functions of T regulatory cells (Martin et al., 2009). The involvement of CCR7 and its two chemokine ligands are implicated in various pathological conditions such as multiple sclerosis, rheumatoid arthritis, cancer metastasis and various inflammations.

CCL21 and CCL19 are the two ligands for CCR7. CCL21 and CCL19 are CC family homeostatic chemokines produced in LNs. CCL21 has six cysteine residues rather than four normal cysteine residues in CC family (Bazan et al., 1997; Kelner et al., 1994). CCL21 has a extended C terminus with 40 amino acid residues while the CCL19 lacks this C terminus moiety (Schumann et al., 2010). The extended C terminus moiety helps

CCL21 to bind with fibro reticular structure in the paracortex zone of LNs and create immobilized gradient. On the other hand, lack of the C terminus moiety in CCL19 renders it a soluble chemokine. In human peripheral LNs, CCL21 and CCL19 are co-expressed by TCZ reticular cells while TCZ homing DCs produce CCL19 to a lesser extent (Cyster, 2005; Luther et al., 2000; Ngo et al., 1998). In murine models, HEV ECs produce CCL21. By contrast, human HEV ECs lack the ability to produce CCL21 (Manzo et al., 2007). In addition, the protein expression levels of CCL21 and CCL19 varies to a greater extent in the LNs. CCL21 protein levels in the LNs are up to 100-fold higher than CCL19 (Britschgi et al., 2008; Luther et al., 2002). Though both CCL21 and CCL19 are potent T-cells chemoattractants (Cyster, 2005; Förster et al., 2008), they vary in their capacity for CCR7 internalization and desensitization. CCL19 causes a more robust CCR7 desensitization and internalization than CCL21 (Kohout et al., 2004; Otero et al., 2006).

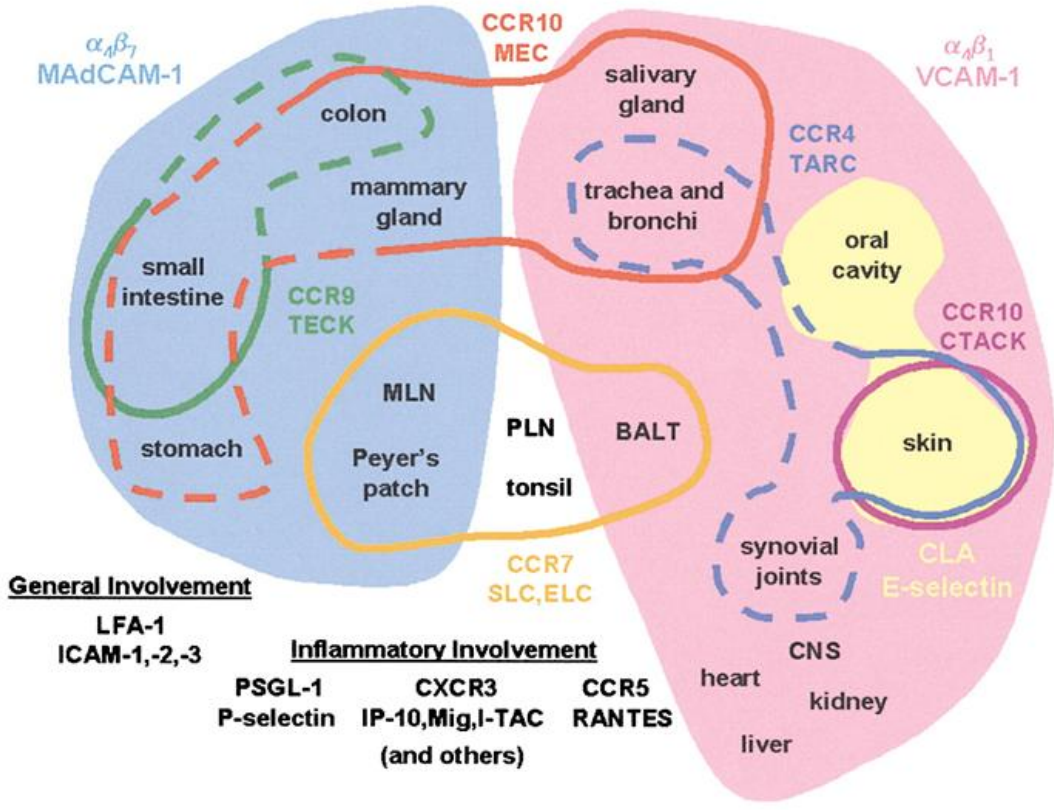

Figure 1.2. Chemokines, chemokine receptors and adhesion molecules for guiding lymphocyte migration and trafficking in tissues. "Reprinted from "Immunity", 16, Eric J Kunkel, Eugene C Butcher, Chemokines and the Tissue-Specific Migration of Lymphocytes,4, Copyright (2002), with permission from Elsevier.

1.2.4. Immune cell trafficking in tissues

Immune cell trafficking leads to the distribution of immune cells (immune cell trafficking) into different physiological systems such as circulatory system (lymph and blood), nervous system and respiratory system, and mediates immune system development, homeostasis, immune surveillance and immune responses.

1.2.4.1. Immune cell development

Immune cell migration distributes the progenitor and immature immune cells to the appropriate tissues for their development and maturation. CXCR4 associated migration play a crucial role in neutrophil development. Immature neutrophils are produced in bone marrow and express CXCR4. The immature neutrophils are retained by SDF-1 (ligand for CXCR4) produced by the bone marrow stromal cells until their maturation. Upon maturation, the CXCR4 expression is down regulated and neutrophils enter the peripheral blood for immune surveillance (Borregaard, 2010).

Similarly, cell migration plays a crucial role in DC maturation. DCs are derived from monocytes and are differentiated by the presence of specific cytokines and growth factors. The sources for DCs are bone marrow CD34+ myeloid progenitors and CD34+ lymphoid progenitors. These progenitors produce CD14+, CD11c+, CD1+, CD14-, CD11-, CD1c- and IL3Rα+ precursors. Precursor cells are modified to different immature DCs by different combination of macrophage colony-stimulating factor (M-CSF), granulocyte-macrophage colony stimulating factor (GM-CSF), interleukin (IL)-4, IL-15, tumor necrosis factor (TNF)-α, tumor growth factor (TGF)-β, and IL-3 (Banchereau et al., 2000). Immature DCs express CCR1, CCR2, CCR4, CCR5, (Langerhans DCs also express CCR6) CXCR1 and CXCR4, and reach the site of

infection with the activation of these receptors (Barratt-Boyes et al., 2000). Upon capturing antigens, the immature DCs become mature cells and express CCR7 (Banchereau et al., 2000), which mediates DCs trafficking to SLTs for interaction with T-cells (Banchereau and Steinman, 1998).

Trafficking among different microenvironments such as thymus and SLTs is a vital process for T-cells development and activation. Premature thymocytes enter into the cortical–medullary junction (CMJ) of the thymus, which is mediated by CXCR4, CCR7 and CCR9 (Calderón and Boehm, 2011; Stein and Nombela-Arrieta, 2005). From the junction, the premature cells reach the subcortical zone (SC) by CCR7 based mechanism for their massive proliferation and development. During the developmental process and clonal selection in SC, the CCR7 expression is down regulated. The developed naive T-cells reach the cortex zone with CCR7 upregulation. Finally, T-cells reach the medulla and exit from there to the circulatory system as positively selected naive T-cells (Takahama, 2006).

Positively selected naive T-cells then enter SLTs for antigen scanning. Their entry to SLTs through HEVs is orchestrated by CCR7 based cell migration mechanism (Cyster, 2005; Girard and Springer, 1995). In the spleen, naive T-cells directly enter the marginal zone from blood since spleen lacks HEVs (Gunn et al., 1998). The entered naive T-cells migrate randomly in TCZ and scan for cognate antigens by interacting with antigen laden DCs (Cyster, 2005; Worbs et al., 2007). The random migration is coordinated by CCR7 and its ligands (Kaiser et al., 2005; Worbs et al., 2007). If activated, T-cells will remain in the SLTs for extended period and undergo proliferation and clonal expansion before leaving the SLTs. The non-activated naive T-cells immediately leave the SLTs to the

circulatory system for surveillance. The T-cells exit migration mechanism through efferent lymphatic vessel is organised by S1P and its receptor S1P1 (Mandala et al., 2002; Pham et al., 2008).

B-cell development takes place in bone marrow and B-cell trafficking to SLTs plays crucial roles in B-cell activation and antibody production. B precursor cells are produced in the bone marrow. During this pro B-cell stage, the expression of adhesive molecules such as C- kit ligand (also known as stem cell factor - SCF) help to retain the pro B-cells in bone marrow. With the expression of immunoglobulin M (IgM) and immunoglobulin D (IgD) on precursor cells, the cells become immature B-cells and leave the bone marrow. IL7 production facilitates the journey of immature B-cells from bone marrow to blood. The circulating immature B-cells reach SLTs through HEVs and their entry to SLTs is facilitated by CCR7 and its ligands (Okada and Cyster, 2006). After entering the paracortex zone, they follow the CXCL13 signal (B-cells express CXCR5, the receptor for CXCL13) to reach the follicular zone. After activation, immature B-cells become mature B-cells (plasma cells) and leave the SLTs.

1.2.4.2. Homeostasis

Immune cell migration maintains circulation of different immune cell populations at equilibrium in specific tissues such as LNs. T-cells and B-cells circulate between blood and SLTs for antigen scanning. Naive T and B-cells are kept in base line population by maintaining a balance between cell entry and exit of LNs. Other immune cell populations such as DCs, monocytes, macrophages, and mast cells are also maintained in balance in various tissues by immune cell migration (Shaykhiev and Bals, 2007).

1.2.4.3. Immune response

Immune cell migration brings immune cells to the site of infection or injury to elicit immune responses. It is well-known that neutrophils recruitment to the sites of inflammation or injury is important for host defense (Borregaard, 2010). In monocyte-mediated immune response, CXCL12 (SDF-1) and its receptor CXCR4 play a key role in the recruitment of monocytes into different tissues. Stromal cells in central nervous system (CNS), lung, liver, and kidney produce SDF-1 and attract the monocyte population by activating CXCR4 (Sánchez-Martín et al., 2011). Macrophages are also a major player in the recruitment of other immune cells to the site of infection or injury. During initial stress or infection, NK-cells at the site of injury produce interferon (IFN) γ to recruit macrophages. Initial activation by IFNγ induces the expression of toll-like receptors in macrophages causing secretion of autocrine and paracrine cytokines and other molecules such as IFNβ for their own activation and for the recruitment of other immune cells to the site of infection (Dale et al., 2008; Mosser and Edwards, 2008).

1.2.4.4. Immune cell migration and pathogenesis

Misdirected immune cell migration is responsible for many pathological problems such as ischemia and reperfusion injury (stroke, myocardial ischemia and infarction, and disseminated intravascular coagulation), shock, systemic septicemia, transplantation, severe trauma and burns, acute lung injury (adult respiratory distress syndrome), and various autoimmune disorders such as systemic lupus erythematosus, multiple sclerosis and rheumatoid arthritis (Friedl and Weigelin, 2008; Geng, 2001; Luster et al., 2005).

Rheumatoid arthritis (RA), a chronic inflammatory disease associated with immune cell migration (Wan et al., 2006), is characterised by increased infiltration of T-cells, B-cells,

and macrophages (Tran et al., 2005). Interleukin 17 (IL17), produced by CD4 positive memory T-cells, induces the production of many inflammatory cytokines at the site of RA, which further recruits immune cells (Afzali et al., 2007). In respiratory diseases, IL17 also plays a critical role in neurtophil infiltration during respiratory tract infection, which causes extensive damage to the lung tissues (Afzali et al., 2007). Excessive free radical produced by the invading neutrophils during influenza infection causes severe damages to the lung tissues (Narasaraju et al. 2011; Smith, 1994).

1.2.5. Immune cell migration in complex chemoattractant fields

Immune cells navigate in complex microenvironments and are exposed to multiple guiding signals with complex spatiotemporal profiles (Foxman et al., 1997). It has been shown that immune cells express multiple chemoattractant receptors and can effectively integrate or prioritize multiple complex chemotactic signals for chemotactic migration and positioning in various immunological contexts (Foxman et al., 1997; Lin and Butcher, 2006). Neutrophils can navigate through an array of multiple chemoattractant sources in a step-by-step manner to effectively reach the distant target (Foxman et al., 1997; Foxman et al., 1999). The ability of neutrophils to migrate away from the local target in response to the distant target is suggested to be enabled by ligand-induced homologous receptor desensitization mechanism (Lin and Butcher, 2008; Wu and Lin, 2011). In thymus, combinations of CCL21, CCL19, CCL22, CCL25 and CXCL12 coordinate the development of thymocytes to naive T-cells (Takahama, 2006). In SLTs, CCL19, CCL21, CXCL13 and S1P are co-presented in a sub-region dependent manner to guide internodal migration and positioning of T and B-cells (Cyster, 2005). Balance between CCR7 and S1P1 determines the residing time of T-cells in LNs and over

expression of CCR7 causes prolonged retention of T-cells in LNs (Cyster, 2005; Pham et al., 2008).

As some examples, Foxman et al. used an under-agarose assay to study the sequential migration of neutrophils in conflicting chemoattractant gradients (Foxman et al., 1997). Using a microfluidic device, Jeon et al. studied the migration of neutrophils in different complex chemoattractant gradient profiles (Jeon et al., 2002). The similar microfluidic device was also used to study neutrophil migration in single or superimposed gradients of IL8 and LTB4 (Lin et al., 2005). More recently, microfluidic devices were used to study DCs migration in co-existing chemokine gradients (Haessler et al., 2011; Ricart et al., 2011).

In addition to studying immune cells in complex spatial arrangements of chemoattracatant gradients, several studies have examined cell migration in response to temporal variations of chemoattractant fields. For example, Irimia et al. studied neutrophil migration in response to fast gradient switching using a sophisticated microfluidic device (Irimia et al., 2006b).

Using microfluidic maze device, bifurcating and trifurcating migration paths toward the chemoattractant source were configured to study directional-decision making behaviour of neutrophils (Ambravaneswaran et al., 2010). In another study, Han et al. developed a microfluidic system to mimic the physiological environments for neutrophil transendothelial migration during inflammation (Han et al., 2012).

In summary, this chapter provides the relevant biological and immunological background of immune cell migration and trafficking. Since the research in this thesis is largely based on *in vitro* cell migration analysis, in the next section I will discuss

different conventional *in vitro* cell migration assays and the microfluidics-based approach for quantitative immune cell migration analysis.

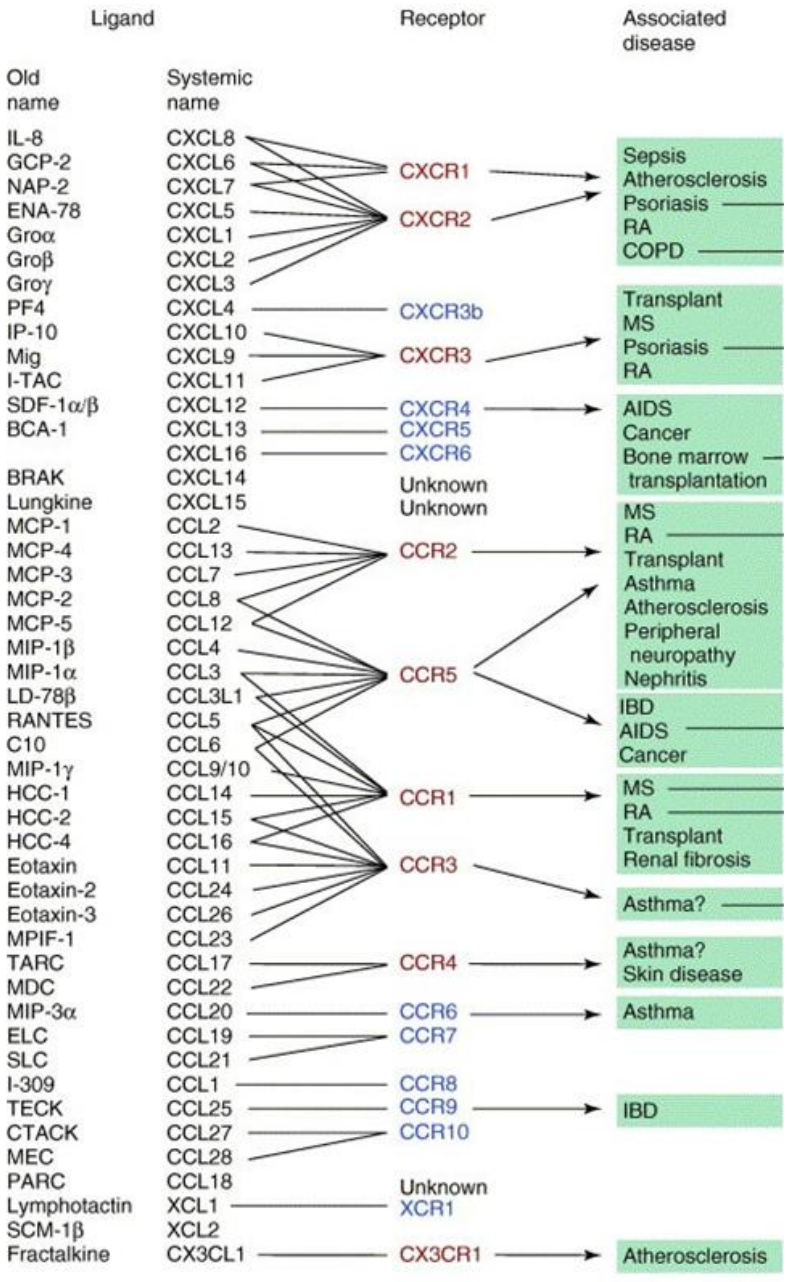

Table 1.1. Roles of chemokines and their respective receptors in diseases. Reprinted from Trends in Pharmacological Sciences , 27, Timothy N.C. Wells, Christine A. Power, Jeffrey P. Shaw, Amanda E.I. Proudfoot, Chemokine blockers – therapeutics in the making?,7, Copyright (2006), with permission from Elsevier.

1.3. *IN VITRO* CELL MIGRATION ANALYSIS PLATFORMS

In vitro cell migration analysis provides an important approach to study the mechanisms of immune cell migration. Such cell migration analysis requires experimental platforms that can create and control the cellular guiding environments such as chemical gradients. In this chapter, I describe both conventional cell migration assays and microfluidic cell migration devices.

1.3.1. Conventional cell migration assays

1.3.1.1. 2D whole population assays

Various assays are developed to measure cell migration on a 2D substrate at the population level. In the microcarrier assay, cells are grown on microcarrier beads to an optimal confluence and the beads are placed in 24 well plates. After incubation for a defined period of time, beads are removed from the wells (by wash or by slow suction). Cells that have migrated to the plastic surface in the wells are visualised by staining and quantified by optical measurements (Rosen et al., 1990). The wound healing assay is another commonly used 2D whole population assay for cell migration analysis. A monolayer cell population is grown to optimal confluence on a glass slide. Wounding (scratch) is done using a pipette tip or a syringe needle, or using electrical current, across the monolayer. Cell migration to heal the wound is analyzed by determining the movement of wound edge or by counting the colonies or cells across the wound zone (Keese et al., 2004; Yarrow et al., 2004). In the ring assay, teflon or glass ring are placed in 6 well plates. To attain optimum confluence, the cell suspension is dropped inside the ring followed by incubation. Then the ring is removed and the monolayer is washed to remove the unattached cells. The setup is incubated at 37°C for several hours and the cell

monolayer is then analyzed for the total area expansion (Cai et al., 2000). In the cell aggregate assay, cell aggregates are prepared by centrifugation or sedimentation. Then the aggregates are examined for cell spreading on a glass slide similar to the ring assay (Zagzag et al., 2002).

Though 2D whole population methods are simple and easy to operate, each has their own limitations. In these assays, it is difficult to manipulate cells or conditions during the experiment. In addition, most of these assays are generally incapable of visualizing and analyzing the dynamic process of cell migration. Furthermore, these assays cannot distinguish cell proliferation from migration.

1.3.1.2. 2D single cell locomotion assays

In contrast to 2D whole population assays, 2D single locomotion assays can measure cell migration on a 2D substrate at the single cell level. In the colloidal gold migration assay, a glass cover slip is covered with gold particles. A monolayer of cells is grown on the gold particle coating. After several hours, the cells are stained and the cover slip is fixed on a glass slide for measuring individual cell tracks (Albrecht-Buehler, 1977). The Zigmond chamber allows chemotaxis measurement in a chemical gradient (Figure 1.3A.). In the Zigmond chamber, two channels are etched on the surface of a glass slide. The gap between the channels (ridge) is set as 1 mm. Cells are seeded on the glass coverslip and placed onto the glass slide. The media is added to one of the channels (sink) and the chemoattractant solution is added to the other channel (source) in the glass slide. The spacing between the coverslip and the ridge is around 5-10μm. A linear gradient forms on the ridge connecting the sink and source (Zigmond, 1977). Cell migration towards the source channel can be observed and measured by live cell

imaging. The Dunn chamber is a variant of the Zigmond chamber that replaces the parallel sink and source channels with concentric rings, and a linear chemokine gradient forms over the ridge (the ridge connects the sink and source rings) (Zicha et al., 1991).

Other methods include under-agarose assay and micropipette-based method. The under-agarose assay consists of an agarose gel cast on a glass substrate. Wells are punched into the gel for cells and chemical solutions. A gradient is created by chemical diffusion from the wells through the gel. Cells can migrate under the agarose in response to the gradient. (Nelson et al., 1975). In the micropipette-based method, chemoattractants are slowly released using micropipettes (tips) into a dish filled with medium and seeded with cells (Figure 1.3B.). Gradual release of liquid from the micropipette forms a radial diffusive gradient to attract cells (Lokuta et al., 2003). Both the under-agarose assay and the micropipette-based assay are capable of configuring multiple co-existing chemoattractant gradients. Furthermore, the micropipette-based assay has the advantage in locally stimulating cells with temporal controls.

Despite of the ability of 2D single cell locomotion assays for single cell migration and chemotaxis analysis, it generally suffers from poor gradient controls. For example, the gradient stability in these assays is limited due to chemical equilibration and evaporation of the liquids. In addition, the mechanical structures of the assays (e.g. ridge in Zigmond chamber and Duun chamber) affect the migration of cells. The micropipette-based assay further suffers from poor reproducibility in gradient generation and the gradient can be easily disturbed.

1.3.1.3. Cell migration assays in 3D environments

Transwell assay and Boyden chamber are popular methods for 3D cell migration analysis (Figure 1.3C.). Transwell method is a modified version of the Boyden chamber and commonly used to test chemotaxis and invasion. The assay is conducted in wells, where a membrane (pore sizes ranging from 3-12 μm) is inserted. Chemoattractant solution is placed in the bottom chamber and cell suspension is added to the top chamber. A gradient forms across the membrane and cells can squeeze through the pores (Figure 1.3A.). To mimic *in vivo* 3D environments, ECM such as hydrogel or matrigel or endothelial cell monolayer or tissue slice is placed on the membrane. Cells penetrate these 3D structures through the membrane (Limame et al., 2012). At the end of the assay, cells migrated to the bottom well are counted to indicate the level of migration. Despite of the wide use of these assays and its advantages in high-throughput, these assays have several limitations. As end-point assays, they do not allow visualization and cell migration analysis at the single cell level. Thus, it is difficult to distinguish the chemokinetic and chemotactic cell populations. In addition, these assays cannot maintain stable chemical gradients and it is difficult to manipulate gradient conditions in a controlled manner. Cells directly falling through the membrane further complicate migration analysis in these assays.

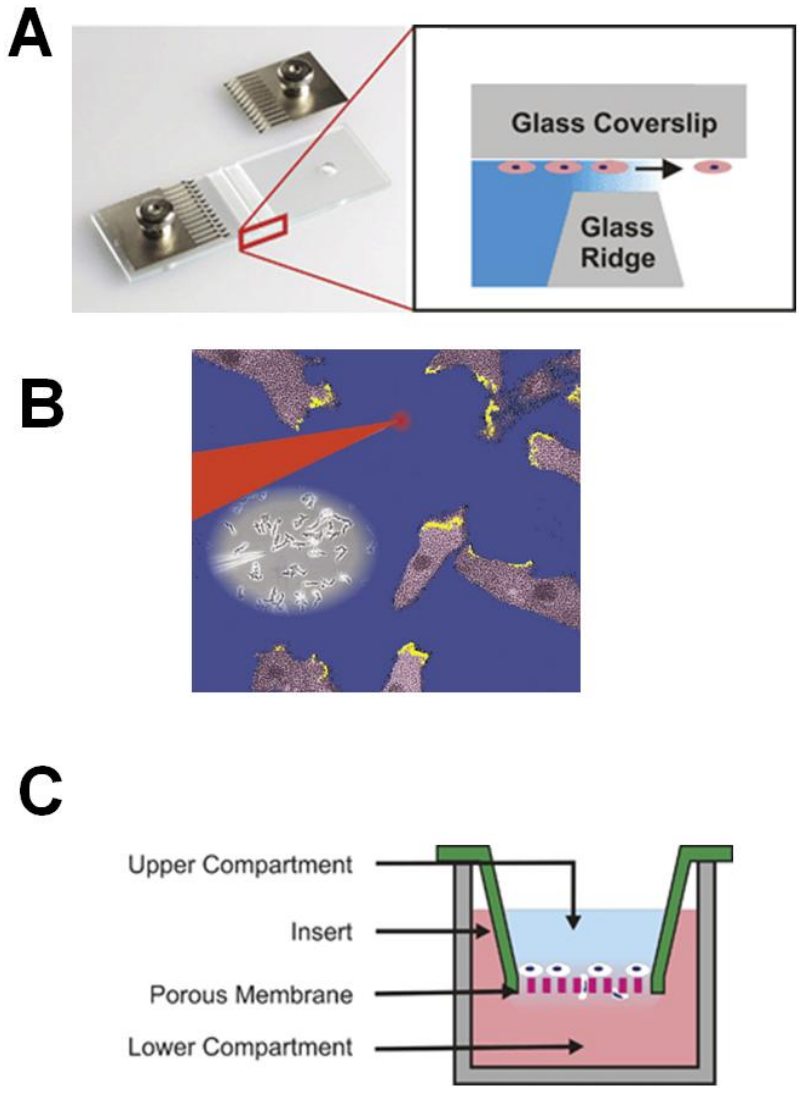

Figure 1.3. Conventional cell migration assays (A) Zigmond chamber (Keenan and Folch, 2008) -Reproduced by permission of The Royal Society of Chemistry; **(B)** Micropipette-based assay. Reprinted from Current Biology, 9, Jeffrey E Segall, Cell polarization: Chemotaxis gets CRACking, 3, Copyright (1999), with permission from Elsevier; **(C)** Transwell assay (Keenan and Folch, 2008)-Reproduced by permission of The Royal Society of Chemistry.

1.3.2. Microfluidic gradient generating devices

The conventional cell migration assays lack the ability to maintain and manipulate chemical gradients. The emerging microfluidic devices and systems offer a powerful experimental platform for quantitative cell migration analysis in well-controlled cellular microenvironments. Particularly, microfluidic devices can generate stable gradients with simple or complex spatiotemporal profiles, reduce reagent consumption and has the potential to increase experimental throughput (Figure 1.4.). Therefore, the microfluidics-based approach is uniquely suited for studying cell migration in mimicked physiologically relevant chemical guiding environments. Depending on the nature of gradient generation methods, microfluidic devices can be categorized into flow based devices and flow free devices.

1.3.2.1. Flow based microfluidic gradient generating devices

In the flow based gradient generators. The gradient is generated by mixing between parallel laminar flows in the microfluidic channel (Ismagilov et al., 2000; Kim et al., 2010). Syringe pumps are typically used for chemical infusion. The commonly used designs of flow based microfluidic gradient generators include the Y shape and the network device (Jeon et al., 2000). The simple Y shape device can create stable single or co-existing chemical gradients by mixing between two chemical flows in the microfluidic channel. The gradient shape can be controlled to evolve slowly along the lateral length of the channel. The Y shape device has been previously used to quantitatively study T-cells chemotaxis in single or competing chemokine gradients (Lin and Butcher, 2006) and therefore it was chosen as the platform for experimental cell migration studies in this thesis.

The network device incorporates one or multiple networks of mixing channels, which produce streams of different chemical concentrations to generate gradients of different shapes in the downstream channel (Figure 1.4A-B.). The network device has been successfully used to study chemotaxis of various cell types such as neutrophils (Jeon et al., 2002). In addition, various other flow based microfluidic gradient generators (many are variants of the network device) have been developed for flexible gradient generation all based on the principle of controlled laminar flow mixing. For example, Irimia et al. constructed a "universal gradient generator" to generate arbitrary shapes of gradients. In this device, by placing several parallel dividers, the inter-diffusion between adjacent streams of various concentrations was controlled to generate different gradient profiles (Irimia et al., 2006a). Cambell and Groisman constructed a "planar network microfluidic device" to generate various types of gradients. While passing through series of stages, the source solutions are spilt and mixed to generate different gradient shapes such as exponential, linear and two fused branches of a parabola (Campbell and Groisman, 2007). Amarie et al. developed a microfluidic device for spatiotemporal gradient generation. Bifurcated and trifurcated channels are used to split the flow to generate different gradients in one setup. The small length of microfluidic channel length allows fast switching of different gradients (temporal variation) (Amarie et al., 2007).

The main disadvantages with the flow-based systems are that the gradient generation is limited to 1D, and the flow induces shear stress on cells. In addition, the flow continuously removes autocrine, paracrine and other cell secreting extracellular molecules although such simplification of the experiment condition can also be used as an advantage to examine cell migration in response to externally applied gradients.

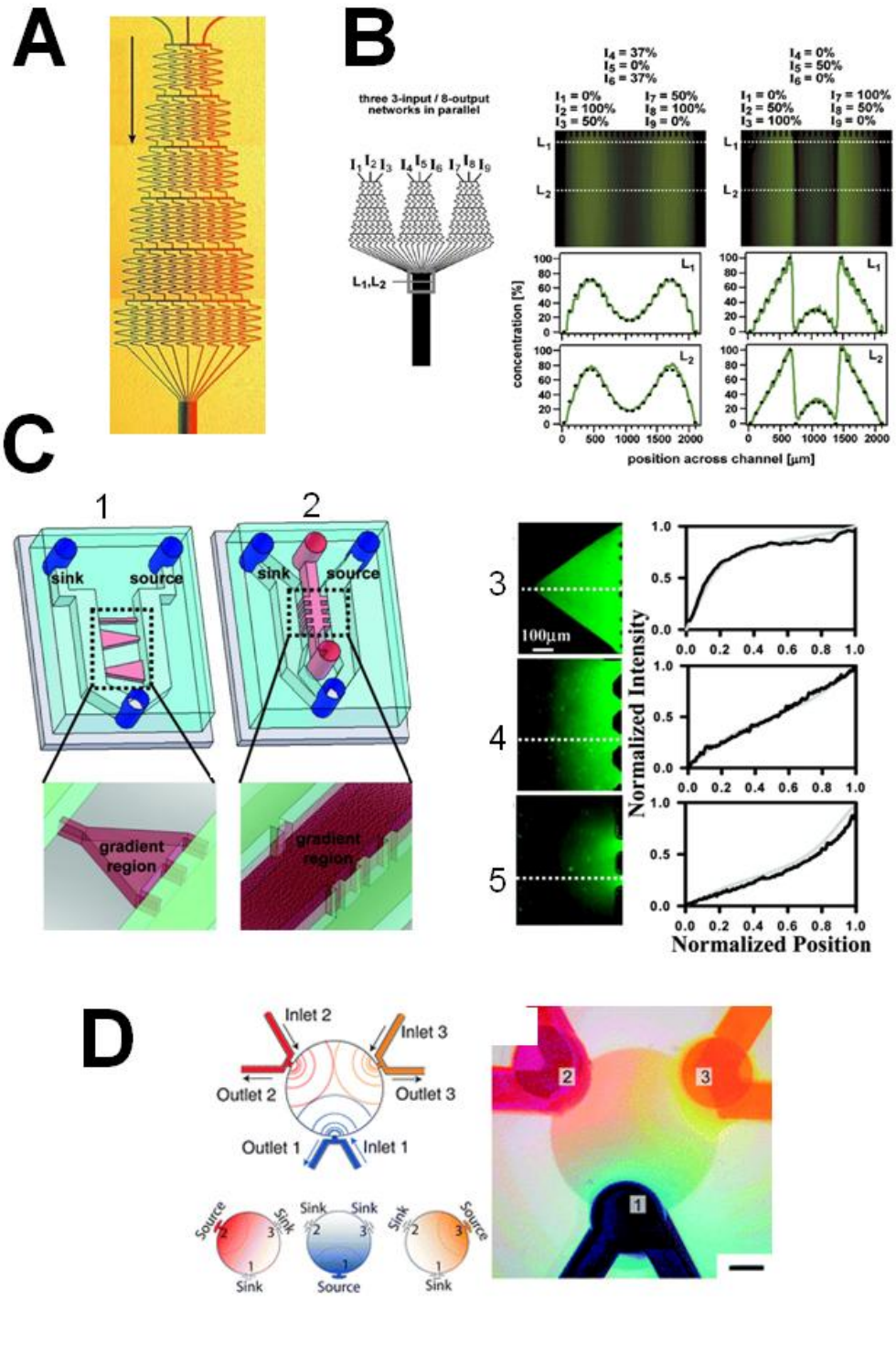
A
B
three 3-input / 8-output networks in parallel
I1 I2 I3 I4 I5 I6 I7 I8 I9
L1,L2
I4 = 37%
I5 = 0%
I6 = 37%
I1 = 0%
I2 = 100%
I3 = 50%
I7 = 50%
I8 = 100%
I9 = 0%
I4 = 0%
I5 = 50%
I6 = 0%
I1 = 0%
I2 = 50%
I3 = 100%
I7 = 100%
I8 = 50%
I9 = 0%
L1
L2
concentration [%]
position across channel [μm]
C
1
2
sink
source
gradient region
3
4
5
100μm
Normalized Intensity
Normalized Position
D
Inlet 2
Inlet 3
Outlet 2
Outlet 3
Outlet 1
Inlet 1
Source
Sink
1
2
3

Figure 1.4. Microfluidic devices for creating complex gradient environments (A) The microfluidic network device for generating single or superimposed linear gradients. Reprinted with permission from (Dertinger et al., 2001). Copyright (2001) American Chemical Society; **(B)** The microfluidic network device for generating complex gradient shapes. Reprinted with permission from (Dertinger et al., 2001). Copyright (2001) American Chemical Society; **(C)** Microfluidic devices for generating gradients in a flow free environment. In these devices, multiple groove channels are designed to directly connect the sink and source channels or to connect the source and sink channels to the centre gradient channel. Varying the shapes of the groove channels or their matched or mismatched configurations on the two sides of the centre channel result in different gradient shapes in the 3D gel environment. Reprinted with permission from (Mosadegh et al., 2007). Copyright (2007) American Chemical Society; **(D)** Microfluidic palette device for generating superimposed gradients on a 2D plane (Atencia et al., 2009) - Reproduced by permission of The Royal Society of Chemistry.

1.3.2.2. Flow free based microfluidic gradient generating devices

In contrast to flow based devices, microfluidic devices have been developed to generate chemical gradients in a flow free environment. In these type of devices, the gradient forms by free diffusion of molecules between the sink and the source. Resistant structures such as porous, semipermiable membrane, gels, or thin microchannels connecting the source and sink are often used in these devices to help control the chemical diffusion rate. Stable gradients are achieved at the equilibrium state. To maintain the source and sink reservoirs relative to the gradient region, manual pipetting or external pumping are sometimes used to provide the liquids intermittently in sink and source (Shamloo et al., 2008).

As some examples, Abayankar et al. developed a PDMS based microfluidic device that integrates polyester membranes to control diffusion from the source/sink to the gradient channel in a flow free manner (Abhyankar et al., 2006). Saadi et al. developed a "ladder chamber" for gradient generation in 2D or 3D flow free environments (Saadi et al., 2007). In this device, the sink and source channels are inter connected by narrow microgroove channels to allow gradient generation in these channels filled with medium or 3D gels. Mosadegh et al. further modified this approach to generate different chemical gradient shapes in a flow free 3D gel environment (Figure 1.4C.) (Mosadegh et al., 2007). In this device, the sink and source channels are connected with microgrooves of different shape and size to generate different gradient profiles. In addition, varying the matched or mismatched configurations of the groove channels connecting the source and sinks to the centre gradient channel further offer the flexibility of gradient shape control. In another method, using a chamber containing multiple microfluidic channels, depleting

gradient was generated in 3D hydrogel by flow free method. In this assay, after filling hydrogels such as collagen or fibrin in microfluidic channels, test cells are seeded on one end of the 3D gel and chemoattractant is place on the other end of the gel. The diffusion of chemoattractant from one end generate depletion gradient to attract the test cells into the ECM (Keenan and Folch, 2008). Interestingly, a microfluidic device employing stacked-flows was developed to generate flow-based stable gradients but in a low shear force environment. This device was integrated with a breast cancer cell culture platform to study breast cancer cell migration (Sip et al., 2011).

Several new approaches have been recently developed to permit generation of single or superimposed chemical gradients on a 2D plane. Atenica et al. developed a "microfluidic palette", (Figure 1.4D.) in which complex gradient formation on a 2D plane is implemented by separating the central gradient chamber from the fluid chamber (Atencia et al., 2009). As another example, Choi et al. used self-assembled particles as resistance barrier between the chemical sources and the centre gradient forming region to allow gradient generation on a 2D plane (Choi et al., 2012). These flow free based microfluidic gradient generators offer flexibilities to create more physiologically-relevant chemical guiding environments and in many cases, the experimental setup is simplified by eliminating the requirement of external flow controls. On the other hand, the main drawback of having no external flows in these devices is the reduced ability to maintain stable gradient over long time and to manipulate gradient conditions.

1.3.3. Microfluidic systems for studying immune cell migration

Microfluidic devices have been widely used for studying immune cell migration. As some examples, Jeon et al. applied the network device to study neutrophil migration in

different simple or complex chemokine gradient profiles (Jeon et al., 2002). Multiple mixing network modules are combined to generate complex gradient shapes and the results of the study suggested the interesting memory effect of neutrophil migration when encountering a "hill" type gradient versus a "cliff" type gradient. Using similar network devices, Lin et al. examined the effects of IL8 gradient profile characteristics in neutrophil chemotaxis (Lin et al., 2004). Furthermore, neutrophil migration in opposing IL8 and LTB4 gradients was tested and the results confirmed the previously reported preferential cell migration toward the distant attractant and further revealed a subtle hierarchy of the potency between IL8 and LTB4 in directing neutrophil migration (Lin et al., 2005). The network-based microfluidic devices have also been applied to study neutrophil migration in response to "fast-switching" gradients, and the repulsive neutrophil migration from high-dose chemoattractant gradients (Irimia et al., 2006b; Tharp et al., 2006). Similarly, the network device was used to study DCs migration in different single and competing chemokine gradients (Ricart et al., 2011).

Besides the network-based devices, the simple Y shape microfluidic device was used to study the migration of activated human blood T cells in single and competing chemokine gradients (Lin and Butcher, 2006). A modified version of the Y shape device was used to study T cell migration in competing chemokine and direct current electric fields (dcEF) (Li et al., 2012). Haessler et al. developed a 3D microfluidic platform to evaluate DCs migration in co-existing CCL19, CCL21, CXCL12 gradients (Haessler et al., 2011). Butler et al. used a flow free microfluidic device to study the alteration of neutrophil directional motility in burn injury patient cell samples (Butler et al., 2010). Recently,

Sackmann et al. developed a novel microfluidic strategy to perform integrated on-chip neutrophil capturing and subsequent chemotaxis analysis (Sackmann et al., 2012).

In addition to testing primary immune cells, Herzmark et al. used a flow based microfluidic device to create fMLP gradient of an exponential profile to study the migration of differentiated neutrophil-like HL-60 cell line. The results demonstrated the effect of gradient profiles in HL-60 cell chemotaxis (Herzmark et al., 2007). Cheng et al. used a 3D gel-based microfluidic device to study HL-60 cell migration in fMLP gradients (Cheng et al., 2007).

Taking together, microfluidic devices are proven a useful tool for *in vitro* experimental cell migration analysis. Its ability to configure well-defined gradient profiles and combinations of multiple chemical fields is particularly suited for quantitative studies of immune cell migration in mimicked physiological chemical fields. Among the diverse microfluidic cell migration devices, I chose the simple Y shape device in this thesis to study T cell migration in different CCL21 and CCL19 fields for its demonstrated effective use for T cell migration analysis, the simplicity in the device design and the flexibility of generating single or combined gradients.

1.4. RATIONALE, HYPOTHESIS AND OBJECTIVES OF THE THESIS

T-cells trafficking in LNs is crucial for secondary immune responses. It requires an effective mechanism to guide the journey of T-cells in and out of LNs. CCR7 expressed in T-cells and its dual ligands CCL21 and CCL19 are important mediators responsible for T-cells recruitment to LNs and their organization within LNs. However, the specific roles of CCR7 and its ligands in coordinating T-cells migration in different LNs sub-regions are not clearly defined. Particularly, the possible CCR7 ligands fields mediated

T-cells exit from LNs has not been explored. This is in part due to the lack of knowledge of LNs sub-regional CCL21 and CCL19 distribution profiles and the lack of ability of conventional cell migration assays to examine T-cells migration in mimicked LNs sub-region relevant CCL21 and CCL19 fields. Toward better understanding the guiding mechanism by CCR7-ligands fields for T-cells migration in LNs, the research in this thesis focused on quantitatively evaluating the migration of T-cells in different CCL21 and CCL19 fields that mimic LNs sub-regions. Such research was enabled by the use of a microfluidic system that can configure different well-defined CCL21 and CCL19 fields. I used activated human blood T-cells as a model cell system for cell migration analysis in this thesis to mimic the situation, wherein acutely activated and clonally expanded T-cells in LNs need to be directed out of the LNs for their subsequent adaptive immune functions.

The central hypothesis underlying the research of this thesis is:

"Different CCL21 and CCL19 gradient fields in different LNs sub-regions provide a novel combinatorial guiding mechanism for T cell trafficking in LNs."

Guided by this hypothesis, the research in the thesis was designed to achieve two closely connected objectives:

Objective 1: The focus of this objective is to quantitatively characterize T-cells migration in different mimicked LNs sub-region relevant CCL21 and CCL19 fields, Based on the results, a CCR7 ligands fields based combinatorial guiding mechanisms for T-cells migration in LNs will be defined.

Objective 2: The research under the second objective is to further investigate the proposed combinatorial guiding mechanism from the previous objective. This will be achieved by 1) directly characterizing the CCL21 and CCL19 distributions profiles in mouse LNs sub-regions; and 2) further testing T-cells migration for its dependency on the CCL21 and CCL19 fields with a focus to better understand its relevance to T-cells exit from LNs. Based on the results, the combinatorial guiding mechanism will be updated accordingly.

CHAPTER 2

METHODOLOGIES

This chapter is based, in-part, on the following publication: "Nandagopal, S., Wu, D., and Lin, F. (2011). Combinatorial Guidance by CCR7 Ligands for T Lymphocytes Migration in Co-Existing Chemokine Fields. PLoS ONE 6(3), e18183".

2.1. Cell preparation

Human peripheral blood samples were collected from healthy donors in collaboration with The Victoria Institute of Clinical Research and Evaluation (Vic R&E) at Winnipeg with an approved human ethics protocol. Peripheral blood mononuclear cells (PBMC) were isolated using standard gradient centrifugation method. T-cells from total PBMC were selectively activated by anti-CD3/CD28 antibodies for 2 days in culture medium (RPMI-1640 with 1% PS and 10 % FBS) in a 37^{o}C incubator with 8% CO_2 injection. Activated T-cells were expanded with IL-2 and were cultured for at least 3 days before cell migration experiments. Unless specified otherwise, T-cells used in the experiments of this thesis refer to activated human blood T-cells.

2.2. Microfluidic device and gradient generation

A previously reported Y shape microfluidic device was used for cell migration experiments in this study (Lin and Butcher, 2006) (Figure 2.1.). The microfluidic device was designed in Freehand 9.0 (Macromedia) and the design was printed to a transparency mask by a high resolution printer. The masters were fabricated at Stanford Nanofabrication Facility (SNF) at Stanford University and The Nano Systems Fabrication Laboratory (NSFL) at the University of Manitoba. The design was patterned

on a Si wafer by the standard contact photolithography technique with SU-8 photoresist (Micro Chem, MA) through the transparency mask. The SU-8 pattern yields ~100 μm thickness. Next, the master was used for Polydimethylsiloxane (PDMS) based device fabrication using the soft-lithography technique. The master was covered by PDMS (Sylgard 184, Dow Coring, MI) and baked for 3 hours at 70^{o}C. The cured PDMS replica was cut and separated from the master. Two 1 mm diameter holes for the two fluidic inlets and one 4 mm diameter hole for the fluidic outlet were punched out of PDMS respectively in the device. An additional 1 mm hole was punched for loading cells. The PDMS replica was bonded to a glass slide using an air plasma cleaner (PDC-32G, Harrick, NY).

Polyethylene tubing (PE-20, Becton Dickinson, MD) was inserted into the inlet holes to connect the microfluidic device to syringe pumps (Model V6, Kloehn, Inc., NV) with two 250 μL Kloehn syringes containing medium or chemokine solutions for fluidic infusion. Chemokine solutions (Recombinant Human CCL19/MIP-3 beta and Recombinant Human CCL21/6Ckine from R&D Systems) of suitable concentrations were prepared in migration medium (RPMI-1640 with 0.4% BSA). Fluorescent-Iso thiocyanate dextran (FITC-Dextran) 10kDa, which has molecular weight similar to the chemokine molecule, was added to the chemokine solution. The migration medium and chemokine solutions were continuously infused into the device by syringe pumps through tubing and the inlets of the device at the total flow rate of 0.2μL/min. The defined stable chemokine gradients are generated by controlled mixing of chemokines and medium. The low flow rate is expected to reduce shear stress to cells. On the other hand, I often observe a bias of cell movement along the flow direction although I assume

such a flow effect does not significantly affect cell migration along the gradient direction, which is perpendicular to the flow. I have attempted to use a flow free microfluidic device for the T-cells migration experiments. However, T-cells motility was much lower in the flow free device due to un-identified reasons. Another advantage of the flow based device is that the flow reduces the effects of autocrine and paracrine signalling allowing cell migration analysis in response to externally applied and well-defined chemical gradients. Therefore, I decided to use the Y shape device for the research in this thesis.

The chemokine gradient was confirmed by measuring the fluorescence intensity profile of FITC-Dextran inside the microfluidic channel and the cells were imaged at ~3mm downstream of the "Y" junction, where the gradient yields a smooth profile. The gradient profile was quantitatively characterized in a previous publication and was shown to be effective in inducing chemotaxis of human activated T-cells chemotaxis to chemokines including CCL19 and CXCL12 (Lin and Butcher, 2006). Although the gradient characteristics (e.g. nonlinearity; basal concentration) can potentially affect T-cells migration, it is beyond the focus of the research in this thesis. For generating superimposed CCL21 and CCL19 fields, solutions of one or both chemokines with specific concentrations were used for both inlets (i.e. CCL21 and CCL19 were infused to both inlets for "double-uniform" fields; CCL19 was infused to one inlet and CCL21 were infused to both inlets for generating a CCL19 gradient with a uniform background of CCL21; CCL21 and CCL19 were infused to one inlet and migration medium was infused to the other inlet for generating the dual CCL21 and CCL19 gradients along the same side)

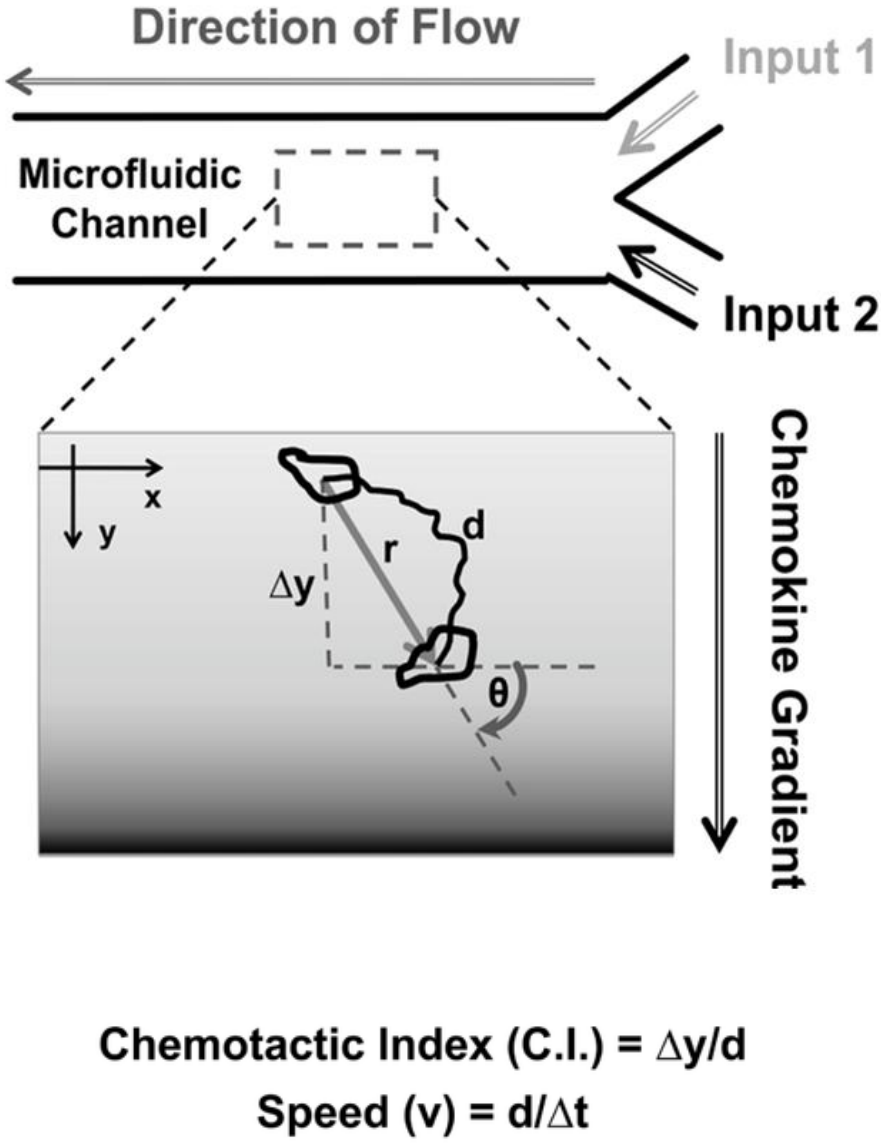

Figure 2.1. Illustration of cell migration experiments using microfluidic devices and data analysis methods.

2.3. Cell migration experiment setup

The fluidic channel was coated with fibronectin (BD Biosciences, MA) for 1 hour at room temperature and blocked with BSA for another hour before the experiment. For each experiment, T-cells were loaded into the microfluidic device from the wells and allowed to settle in the fibronectin-coated channel for ~5 min. The device was maintained at 37^{o}C by attaching a transparent heater to the back of the cover slide (Thermal-Clear Transparent Heater, Model No. H15227, Minco, MN). The heater was powered by a DC power supply (Model No. 6204A, Harrison, Canada) and was controlled by a sensorless temperature controller (Model No. CT198, Minco, MN). The temperature was calibrated to 37^{o}C using a digital thermometer (VWR, Canada). Medium and chemokine solutions were infused into the device by syringe pumps through tubing and the inlets of the device. The device was placed on a microscope stage (Model No. BX60, Olympus). The system was allowed to equilibrate for ~5min (wait until no flowing cells were seen in the channel) and cell migration was recorded by time-lapse microscopy at 6 frames/min for 19 to 44min using a CCD camera (Model No. 370 KL 1044, Optikon, Canada). This frame rate matches well with the average migration speed of activated T-cells on a fibronectin-coated surface under flow inside the microfluidic channel (i.e. typically less than or close to a cell body length per minute). The image acquisition was controlled by NIH ImageJ (v.1.34s). The temperature of both the glass surface and the medium in the outlet of the device was monitored and was confirmed to be ~37^{o}C throughout the experiments.

2.4. Data analysis

Movement of individual cells was tracked using NIH ImageJ (v.1.34s). The background noise of the image was removed using the “despeckle” function. Then the images were

calibrated to distance. Only the cells that migrated within the microscope field were selected and tracked using the "Manual Tracking" plug-in in NIH ImageJ. The tracking data were exported to Excel for analysis. Following previously established analysis methods (Lin et al., 2008; Lin and Butcher, 2006) the movement of cells was quantitatively evaluated by (a) the percentage of cells that migrated toward the chemokine gradient; (b) the Chemotactic Index (C.I.), which is the ratio of the displacement of cells toward the chemokine gradient (Δy), to the total migration distance (d) using the equation C.I. = $\Delta y/d$, presented as the average value ± standard error of the mean (s.e.m); (c) the average speed (V) calculated as $d/\Delta t$ and presented as the average value ± s.e.m. of all cells; and (d) statistical analysis of migration angles performed using MATLAB and Origin 8.5 to examine the directionality of the cell movement.

Specifically, migration angles (calculated from x-y coordinates at the beginning and the end of the cell tracks) were summarized in a direction plot, which is a rose diagram showing the distribution of angles grouped in defined intervals, with the radius of each wedge indicating cell number. Unless it is specified for each wedge, it indicates 1 at the most inner wedge with increment of 1 for the outer wedges. The parameters between different conditions were compared by the 2 sample t test. 20-85 cells were analyzed for each experiment. Two-three independent experiments were repeated for each condition with similar results. The figures were generated using one representative experiment for each condition.

2.5. Immunofluorescence staining and confocal microscopy for analyzing chemokine distributions in mouse lymph node sections

Fresh peripheral LNs were isolated from BALB/c mice and 8-10 μm thick frozen (cryosections) sections were made. The frozen samples were fixed with 4% formaldehyde for 10 minutes at room temperature. The fixed samples were washed with 1X PBS buffer and blocked with 10% donkey serum for 45 minutes at room temperature. To analyze the CD3 and CCL21 distribution, the blocked samples were stained with the mixture of anti-mouse CD3 rat IgG (Rat IgG2b,K, eBioscience, CA) antibody and anti-mouse 6Ckine (FL-134) rabbit IgG antibody (Santa Cruz Biotechnology, CA) for 2 hours at room temperature. Similarly, to analyze the CD3 and CCL19 distribution, the blocked samples were stained with the mixture of anti-mouse CD3 rat IgG antibody (Rat IgG2b,K, eBioscience, CA) and anti-mouse MIP-3β goat IgG antibody (Santa Cruz Biotechnology, CA) for 2 hours at room temperature. After the primary antibody exposure, the samples were washed with 1X PBS and stained with the secondary antibodies for 1 hour in dark at room temperature. For CD3 and CCL21, mixture of Alexa-flour 488 tagged anti-rat donkey IgG antibody (Invitrogen, NY) and Texas Red tagged anti-rabbit donkey IgG antibody (abcam, MA) was used. For CD3 and CCL19, mixture of Alexa-flour 488 tagged anti-rat donkey IgG antibody (Invitrogen, NY) and Texas Red tagged anti-goat donkey IgG antibody (Abnova, Taiwan) was used. The stained samples were washed with 1X PBS and stained with DAPI for nucleus staining for 15 minutes in dark at room temperature. Iso type control experiments were performed with mixture of serum of the primary antibody sources in place of the primary antibodies. The negative control sample was prepared without primary antibodies staining.

Confocal images (10X) were taken using a Nikon C1 Plus confocal system installed on a Nikon Ti-U inverted microscope. The CCL21 and CCL19 distribution relative to TCZ in LNs from the confocal images was analyzed using ImageJ software following a previously reported method (Okada et al., 2005). Briefly, CD3 staining was analyzed to outline the TCZ boundary. This was done by applying the "outline" plug-in in ImageJ to the CD3 channel of the confocal image after converting it to a binary image. The outlined CD3 staining was manually corrected and connected to determine the estimated TCZ boundary (Figure 4.1.and 4.2.). Next, the TCZ outline was overlapped to the CCL19 and CCL21 staining channels of the confocal images to measure the CCL21 and CCL19 distribution profile relative to the TCZ boundary. The pixel intensity profile of CCL21 and CCL19 staining were measured along lines from the inner TCZ to the medulla, and the intensity at each point along the line was averaged across the 50μm line width (shown at the end of each line in the CCL21 and CCL19 staining images in Figure 4.1. and 4.2.). Then the CCL21 and CCL19 staining intensity profiles were plotted against the distance along the lines relative to the TCZ boundary using Origin 8.5 software (Figure 4.1. and 4.2.). The figures were generated using the data from two representative lines for CCL21 and CCL19 respectively.

CHAPTER 3

INVESTIGATION OF COMBINATORIAL GUIDANCE BY CCR7 LIGANDS FOR T-CELLS MIGRATION IN CO-EXISTING CHEMOKINE FIELDS

This chapter is based, in-part, on the following publication: "Nandagopal, S., Wu, D., and Lin, F. (2011). Combinatorial Guidance by CCR7 Ligands for T Lymphocytes Migration in Co-Existing Chemokine Fields. PLoS ONE 6(3), e18183".

3.1. Preamble

In this chapter, I explore the effect of co-existing CCL21 and CCL19 concentration fields on guiding T-cells migration. Using microfluidic devices that can configure single and superimposed chemokine fields, I show that under physiological gradient conditions, human peripheral blood T-cells chemotax to CCL21 but not to CCL19. Furthermore, T-cells migrate away from the CCL19 gradient in a uniform background of CCL21. This repulsive migratory response is predicted by mathematical modelling based on the competition of CCL21 and CCL19 for CCR7 signalling and the differential ability of the two chemokines for desensitizing CCR7. The details of the modelling and computer simulation methods and results were described in the above mentioned journal article (Nandagopal et al., 2011). These results suggest a new combinatorial guiding mechanism by CCL21 and CCL19 for the migration and trafficking of CCR7 expressing leukocytes.

3.2. Introduction

Migratory responses of cells to cellular guiding signals play important roles in regulating a wide range of physiological and pathological processes such as inflammation and

autoimmune diseases, wound healing, neuron guidance, embryogenesis, and cancer metastasis (Ayala et al., 2007; Behar et al., 1994; Dekker and Segal, 2000; Hatten, 2002; Knapp et al., 1999; Luster et al., 2005). In particular, chemoattractant gradients guide the migration of immune cells (i.e. chemotaxis), orchestrating cell trafficking and positioning in tissues (Kunkel and Butcher, 2002; Kunkel and Butcher, 2003). It has been shown that leukocytes express multiple different chemoattractant receptors in a cell subset dependent manner, and can integrate multiple co-existing chemotactic signals to direct their migration to specific targets in tissues that enable immune surveillance and immune responses (Foxman et al., 1997; Foxman et al., 1999). Such a multiple chemoattractants-based guiding mechanism relies on chemotactic signalling transduction through chemoattractant and their different specific cell surface receptors. In contrast, some chemoattractants share a common receptor for triggering chemotactic signalling such as chemokines CCL21 and CCL19 and their shared receptor CCR7 expressed in lymphocytes subsets and DCs (Cyster, 2005; Forster et al., 2008; Otero et al., 2006; Weninger and von Andrian, 2003). However, the mechanism of multiple chemoattractants with a common cell receptor for guiding cell migration is unclear.

Chemokine receptor CCR7 and its two ligands, chemokine CCL21 and CCL19, are important players in regulating lymphocytes and DCs trafficking in SLTs such as LNs (Cyster, 2005; Forster et al., 2008; Otero et al., 2006; Weninger and von Andrian, 2003). CCL21 and CCL19 are co-expressed in LNs with different expression patterns. CCL19 is only produced and presented in TCZ in humans and mouse LNs (Britschgi et al., 2008; Cyster, 2005; Forster et al., 2008; Ngo et al., 1998). In contrast, CCL21 is produced in TCZ and is transcytosed to HEVs in human (Carlsen et al., 2005; Forster et al., 2008;

Manzo et al., 2007), and is produced and presented in both TCZ and HEVs in mouse LNs (Gunn et al., 1999; Luther et al., 2002). Inside TCZ, it has been shown that CCL21 and CCL19 are co-expressed by reticular cells with more CCL21-expressing cells than CCL19-expressing cells in the periphery of TCZ (Luther et al., 2000), suggesting the size of the CCL21 producing tissue in TCZ is possibly larger than the CCL19 producing tissue. Therefore, the profiles of overlapping CCL21 and CCL19 fields can be different in different sub-regions of TCZ. Furthermore, the production levels of CCL21 and CCL19 in SLTs are significantly different with up to 100-fold higher of CCL21 production than CCL19 (Luther et al., 2002; Ngo et al., 1998) but the exact difference is not defined in sub-regions. In addition, CCL19 only exhibits soluble patterns in SLTs, whereas CCL21 is found in both soluble and immobilized forms (Schumann et al., 2010). At the cellular level, CCL21 and CCL19 have similar binding affinity with CCR7 and they are similar in inducing calcium immobilization and G protein activation (Ott et al., 2006). However, only CCL19 but not CCL21 robustly desensitizes and internalizes CCR7 (Britschgi et al., 2008; Kohout et al., 2004; Otero et al., 2006). Although both CCL21 and CCL19 are potent chemoattractants for T-cells as shown using *in vitro* chemotaxis assays, their distinct roles in regulating T-cells trafficking in SLTs remain unclear. It has been shown that CCL21 but not CCL19 is required for T-cells and DCs recruitment to SLTs using CCL19/21 deficient mice and CCL19 deficient mice (Britschgi et al., 2010; Gunn et al., 1999; Link et al., 2007). This finding together with the significantly lower production level of CCL19 further complicates the role of CCL19 in lymphocytes and DCs trafficking in SLTs. Altogether, the differential expression patterns of CCL21 and CCL19 in SLTs and their differential ability for desensitizing

CCR7 for recruiting T-cells and DCs to SLTs present a complex and unclear picture of CCR7 ligands guided T-cells migration and trafficking in SLTs.

In this chapter, I hypothesize that the different profiles of co-existing CCL21 and CCL19 fields in sub-regions of LNs together with the differential ability of CCL21 and CCL19 for desensitizing CCR7 provide a mechanism for fine tuning T-cells trafficking in LNs. I employed a microfluidics-based approach to quantitatively analyze T-cells migration *in vitro* in different configurations of co-existing CCL21 and CCL19 fields that mimic the physiological conditions in different regions of LNs and (in collaboration with Dr. Dan Wu, Postdoctoral Fellow in the lab) used mathematical modelling and computer simulations to explain the results.

3.3. Results

3.3.1. Physiological CCL21 but not CCL19 gradient attracts T-cells

As illustrated in Figure 2.1., I employed a microfluidic device that can precisely configure stable single or superimposed chemokine gradients by controlled mixing of continuous flows inside a microfluidic channel for quantitative cell migration analysis, and I used activated human peripheral blood T cells as a model cell system. In the first, I tested the migration of T cells in a CCL19 or a CCL21 concentration field with physiological doses (i.e. 100nM for CCL21 and 5nM for CCL19, which were selected based on *in vivo* studies of CCL21 and CCL19 expression (Luther et al., 2002) and the saturation chemokine concentration for T cell chemotaxis *in vitro* (Debes et al., 2005; Weninger and von Andrian, 2003). The results showed that T cells strongly chemotax to the 100nM CCL21 gradient (Figure 3.1.). In the uniform field of 100nM CCL21, T cells migrate randomly (Figure 3.1.). The speed of cells is similar in the gradient and uniform

CCL21 field. These results confirm CCL21 as a potent chemoattractant for T cells and suggest its role in T cell recruitment to TCZ. In contrast, T cells migrate randomly in a 5nM CCL19 gradient (Figure 3.2.). In a super-physiological 100nM CCL19 gradient, T cells show strong chemotaxis (Figure 3.2.). Interestingly, T cells maintain similar migration speeds in the 5nM CCL19 gradient when compared with those observed in a 100nM CCL21 gradient or 100nM uniform CCL21 field (Figure 3.2.). These results confirm that CCL19 can act as a chemoattractant for T cells at a super-physiological concentration. However, the much lower physiological dose of a CCL19 gradient is not sufficient to attract T cells. To further validate the 100nM CCL21 gradient as a chemoattractant for T cells in SLTs, I tested the condition of competing gradients of 100nM CCL21 and 5nM CCL19. The results show 60% of cells migrate toward the 100nM CCL21 gradient, suggesting that the 100nM CCL21 gradient attracts cells even in the presence of an opposing 5nM CCL19 gradient. In addition, I found that the chemotactic index (C.I.) toward the CCL21 gradient is significantly reduced (i.e. 0.04±0.04) comparing to it in the single CCL21 gradient (i.e. 0.24±0.04). I speculate that although the opposing 5nM CCL19 gradient does not attract cells by itself, it may still have an effect on cell chemotaxis to the 100nM CCL21 gradient at the quantitative level. While it is interesting, this aspect of the study is beyond the focus of this thesis and thus is not discussed further. Collectively, the results from the cell migration experiments in single and competing CCL21 and CCL19 fields indicate that at physiological concentrations, CCL21 but not CCL19 serves as a chemoattractant for T cell migration, which is consistent with previous *in vivo* studies showing CCL21 alone is sufficient for T cells and DCs recruitment to SLTs (Britschgi et al., 2010; Gunn et al., 1999; Link et al., 2007).

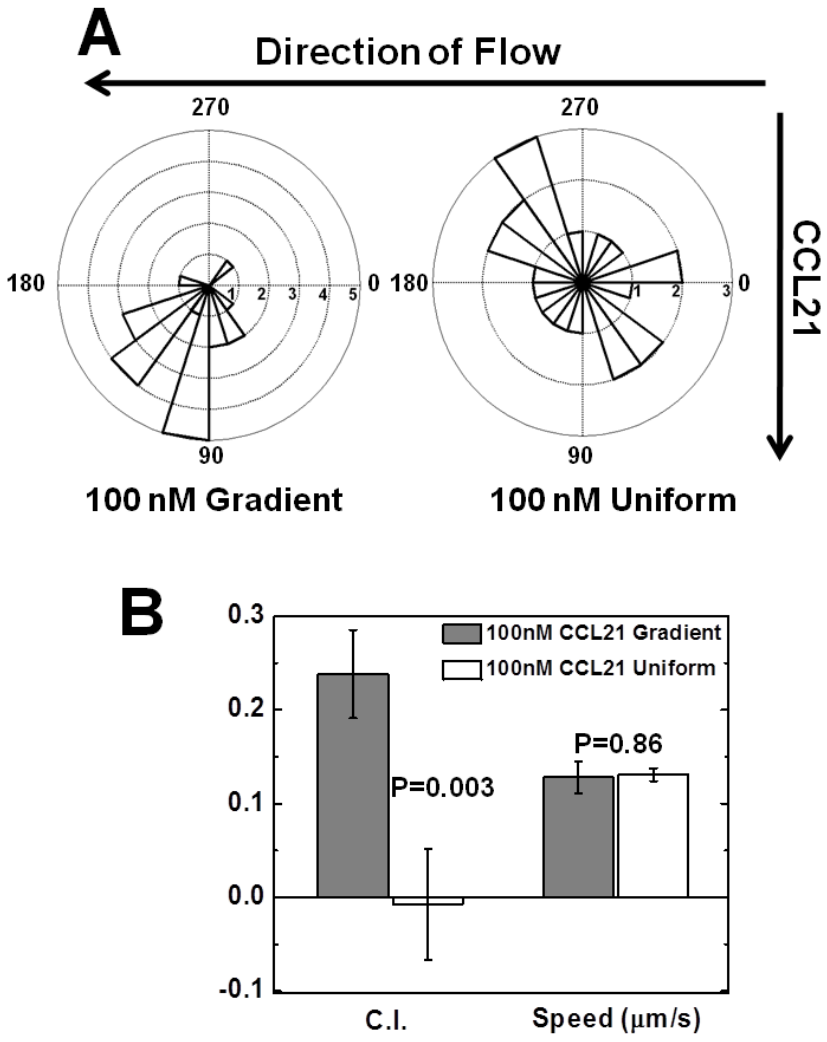

Figure 3.1. T-cells migration in a gradient or a uniform field of CCL21. (A) Angular histograms show T-cells orient randomly in a 100nM uniform CCL21 field, but toward a 100nM CCL21 gradient; **(B)** Comparison of chemotactic index (C.I.) and speed of cells in a 100nM uniform CCL21 field or a 100nM CCL21 gradient show random migration in the 100nM uniform CCL21 field, but chemotaxis in the 100nM CCL21 gradient with similar speed. The error bars represent the standard error of the mean (s.e.m.). The *p*-values for each comparison from 2-sample *t*-test are shown. Positive C.I. indicates cells migrate toward the gradients.

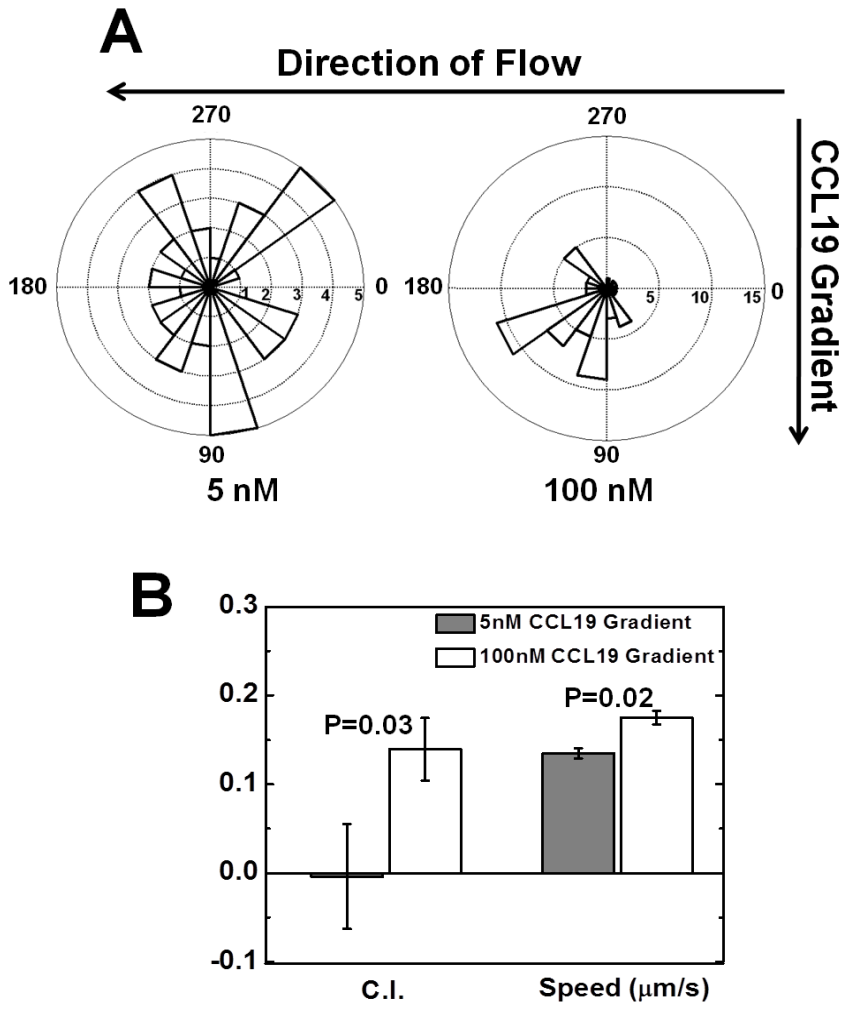

Figure 3.2. T-cells migration in CCL19 gradients. (**A**) Angular histograms show T cells orient randomly in a 5nM CCL19 gradient, but toward a 100nM CCL19 gradient; (**B**) Comparison of chemotactic index (C.I.) and speed of cells in a 5nM CCL19 gradient or a 100nM CCL19 gradient show random migration in the 5nM CCL19 gradient, but chemotaxis in the 100nM CCL19 gradient with higher speed in the 100nM CCL19 gradient. The error bars represent the standard error of the mean (s.e.m.). The *p*-values for each comparison from 2-sample *t*-test are shown. Positive C.I. indicates cells migrate toward the gradients.

3.3.2. T-cells migrate randomly in superimposed CCL21 and CCL19 uniform fields at physiological relevant concentrations

Both CCL21 and CCL19 are produced in TCZ, wherein uniform concentration fields of both chemokines are expected. Thus, I tested T-cells migration in superimposed CCL21 and CCL19 uniform fields at physiological concentrations (i.e. 100nM for CCL21 and 5nM for CCL19) using microfluidic devices. The results show that T-cells exhibit random orientation and migration in the "double uniform" chemokine fields (Figure 3.3.). However, the speed of T-cells is similar to it in single CCL19 or CCL21 gradient or uniform fields at the physiological concentrations. Thus, CCL19 does not necessarily enhance T-cells motility in TCZ.

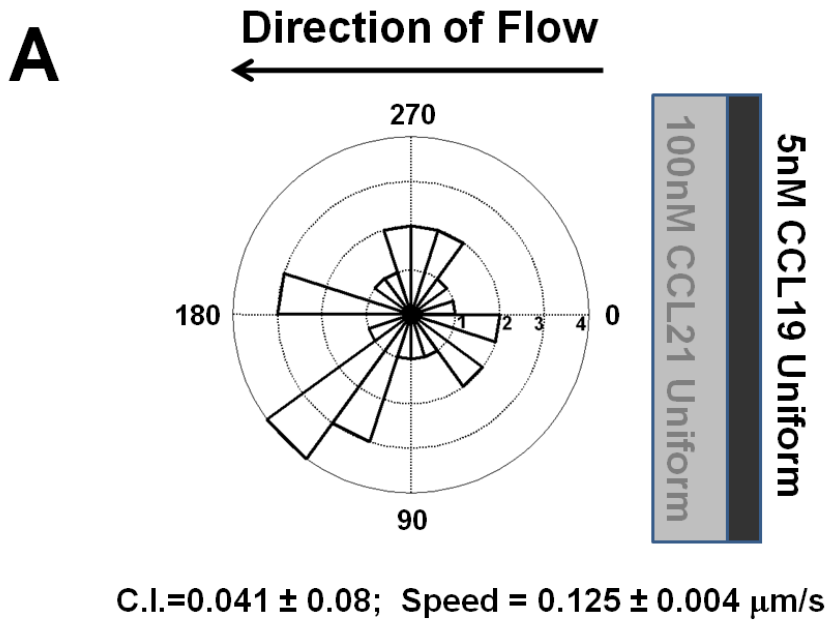

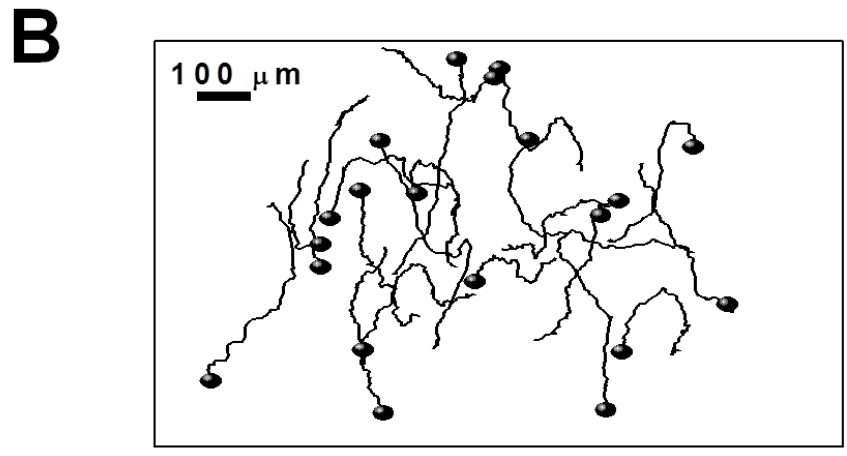

Figure 3.3. T-cells migration in "double-uniform" fields of CCL21 and CCL19. (A) Angular histogram shows random orientation of T-cells in superimposed 5nM CCL19 and 100nM CCL21 uniform fields. Chemotactic index (C.I.) and the speed of cells are shown with the errors represented as the standard error of the mean (s.e.m.). Positive C.I. indicates cells migrate toward the gradients; **(B)** Selected cell tracks from a representative experiment showing cells migrate randomly.

3.3.3. T-cells migrate away from the physiological CCL19 gradient in the presence of a uniform background of 100nM CCL21

As discussed in the Introduction (Chapter 1), because of more CCL21 producing cells than CCL19 producing cells in the periphery of TCZ (Luther et al., 2000), I speculate that the chemokine field in this region to be the superposition of a CCL19 gradient and a uniform CCL21 field. Therefore, I next tested T cell migration in this gradient configuration (i.e. a 5nM CCL19 gradient with a uniform background of 100nM CCL21) using microfluidic devices. Unexpectedly, more T cells oriented and migrated away from the 5nM CCL19 gradient (Figure 3.4.) and this repulsive effect is shown by the relatively high negative chemotactic index, the migration angle distribution and individual cell tracks. The speed of these cells is similar to it in other chemokine fields tested in this chapter. If a super-physiological concentration (i.e. 250nM) of uniform CCL21 field is used, cells will not migrate away from the 5nM CCL19 gradient, but migrate randomly (Figure 3.4.). Taking together, these results suggest that CCL21 and CCL19 may play an interesting role together in regulating T cell migration in the periphery of TCZ.

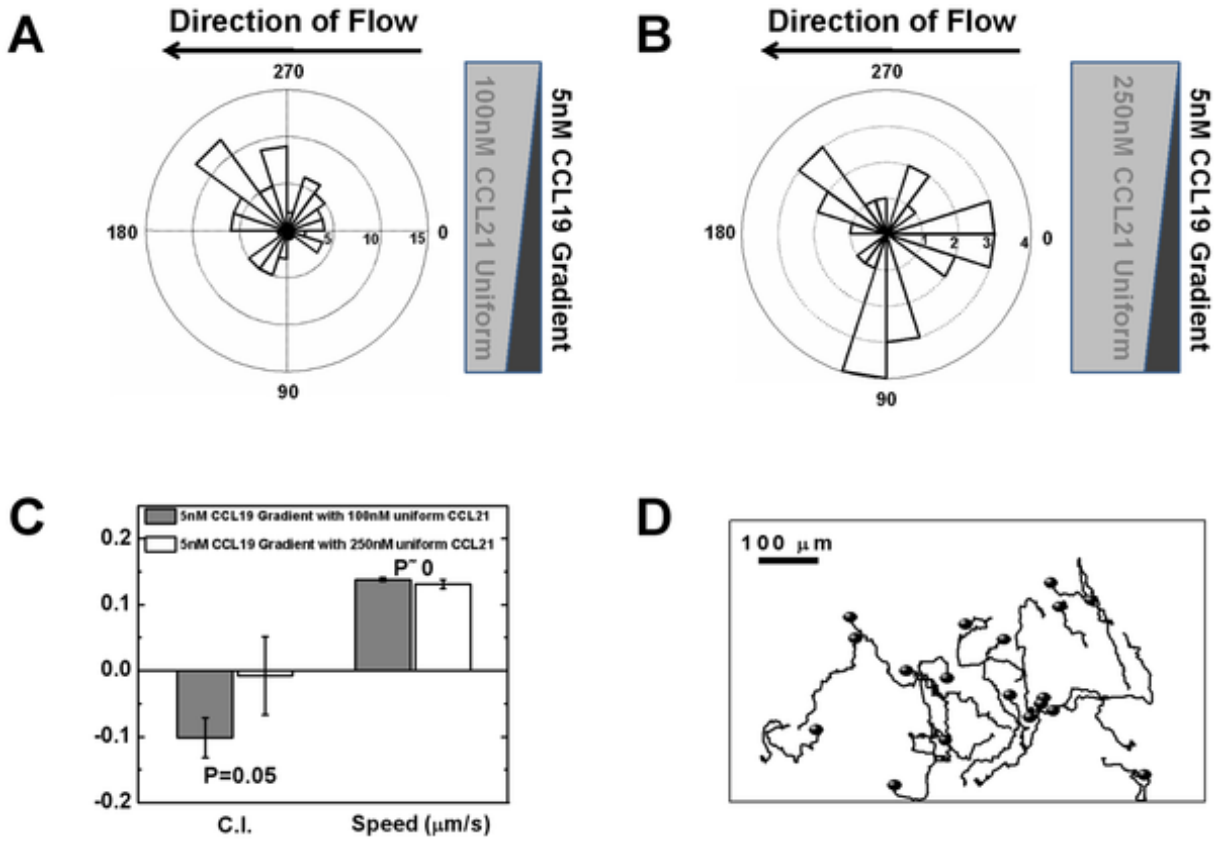

Figure 3.4. T-cells migration in a CCL19 gradient with a uniform background of CCL21. (A) Angular histogram shows more T-cells orient against a 5nM CCL19 gradient with a uniform background of 100nM CCL21; **(B)** Angular histogram shows T-cells orient randomly in a 5nM CCL19 gradient with a super-physiological 250nM uniform CCL21 field; **(C)** Comparison of chemotactic index (C.I.) and the speed of cells between 5nM CCL19 gradient with a uniform background of 100nM CCL21 and 5nM CCL19 gradient with a super-physiological 250nM uniform CCL21 field. The error bars represent the standard error of the mean (s.e.m.). Positive C.I. indicates cells migrate toward the gradients; **(D)** Selected cell tracks from a representative experiment showing more cells migrate away from the 5nM CCL19 gradient in a uniform background of 100nM CCL21.

3.3.4. Differential CCR7 desensitization by CCL21 and CCL19 as an underlying mechanism

To further understand the observed repulsive migration of cells from the CCL19 gradient in the uniform background of CCL21, we adapted a previous mathematical model to consider the ligand-induced chemoattractant receptor modulations for mediating cell orientation and migration in ligand fields (Lin and Butcher, 2008). The previous model is modified to consider 2 ligands L_1 and L_2 with a common cell receptor R. We assume only L_1, but not L_2, can desensitize R to simulate the differential ability of CCL21 and CCL19 for desensitizing CCR7. In a high dose L_2 gradient, the model predicts that cells orient and migrate toward the L_2 gradient. In a superimposed field of low dose uniform L_1 and high dose uniform L_2, the model predicts that cells orient and migrate randomly. These predictions are in agreement with the experimental results of T cell migration in single 100nM CCL21 gradient and in "double-uniform" CCL21 and CCL19 fields. Furthermore, the model predicts that cells orient and migrate randomly in a low dose L_1 gradient or a high dose uniform field of L_2, consistent with experimental results of random migration of T cells in a 5nM CCL19 gradient or a 100nM uniform CCL21 field. In the configuration of a low dose L_1 gradient with a uniform background of high dose L_2, the model predicts the repulsive migration of cells from the L_1 gradient and this prediction is in consistency with the experimentally observed repulsive migration of T cells from the 5nM CCL19 gradient in a uniform background of 100nM. Thus, the modelling predictions and experimental results are in good agreement.

Mathematical modelling provides an explanation for the repulsive migration of cells in a low dose desensitizing ligand gradient (L_1 in the model and CCL19 in the experiment) with a high dose uniform background of a nondesensitizing ligand (L_2 in the model and

CCL21 in the experiment). The desensitizing ligand gradient (L_1 in the model and CCL19 in the experiment) causes a differential receptor binding and activation between the front and the back of the cell with more activated receptors in the front. Although the difference of receptor activation across the cell does not lead to chemotaxis toward the gradient at the low ligand dose, it causes a difference of available free receptors between the front and the back of the cell with less free receptors in the front. As a result, when a nondesensitizing uniform ligand field (L_2 in the model and CCL21 in the experiment) is superimposed to the desensitizing ligand gradient, the high dose nondesensitizing ligands bind and activate more receptors in the back than the front of the cell. Additionally, the nondesensitizing ligand activated receptors stay active on the cell surface for chemotactic signalling that reverses the difference of activated receptors between the front and the back of the cells with more activated receptors in the back facing the low concentration side of the desensitizing gradient. Thus, the model suggests that the differential ability of CCL21 and CCL19 for desensitizing CCR7 combined with the hypothesized physiological configuration of superimposed CCL21 and CCL19 fields (possibly in the periphery of TCZ) enable the repulsive migration of T cells.

3.4. Hypothesized combinatorial guidance by CCR7 ligands for T-cells migration

Taking together the experimental and our modelling results and the previous results of others, I propose a possible combinatorial guiding mechanism by different configurations of CCL21 and CCL19 gradient fields for T-cells migration in different sub-regions of LNs (Figure 3.5.): CCL21 mediates the entry of T-cells to LNs through HEVs. Once inside LNs, T-cells follow gradients of CCL21 and possibly CCL19 to migrate to TCZ. Because CCL21 is produced in much higher amounts than CCL19 in

LNs and CCL21 desensitizes CCR7 at low level, CCL21 gradient alone may be sufficient to direct T-cells into TCZ. This is consistent with previous experimental results (Gunn et al., 1999; Link et al., 2007) and is supported by the results showing T-cells chemotax to a 100nM CCL21 gradient (Figure 3.1.) but not a 5nM CCL19 gradient (Figure 3.2.). Inside TCZ, T-cells migrate randomly in uniform fields of CCL21 and CCL19 to maximize sampling efficiency with antigen presenting cells (APCs) for immune synaptic interactions (Miller et al., 2003; Shankaran et al., 2007; Worbs et al., 2007). As expected, the results show random migration of T-cells in "double-uniform" CCL21 and CCL19 fields (Figure 3.3.). Thus, CCR7 and CCL21 play important roles in T-cells recruitment to LNs, and in T-cells migration to and within TCZ. However, CCL19 is not necessarily required for these processes.

Previous studies suggested that CCR7 down-regulation combined with additional chemotactic signals and S1P signalling mediate the exit of T-cells from LNs for recirculation and immune responses (Cyster, 2005; Dustin and Chakraborty, 2008). The exit process will be facilitated if T-cells first migrate out of TCZ through a CCR7-dependent mechanism. Here I suggest that T-cells will migrate away from TCZ when they reach (by random migration) the periphery region of TCZ, wherein the gradient fields is speculated to be a superposition of a low dose CCL19 gradient and a high dose uniform CCL21 field. This mechanism is enabled by the competition of CCR7 binding between CCL21 and CCL19, together with the differential ability of CCL21 and CCL19 for desensitizing CCR7 and the unique superimposed chemokine field profiles. Interestingly, this CCR7-dependent mechanism for T-cells exit from SLTs responds well to the previously reported CCR7-dependent T-cells exit from peripheral tissues (Brown

et al., 2010; Debes et al., 2005), suggesting the importance of CCR7 in T- cell trafficking and recirculation. Furthermore, it has been previously reported that leukocytes exhibit repulsive migration from high concentration chemoattractant gradients, termed "chemofugetaxis" (Mathias et al., 2006; Poznansky et al., 2002; Tharp et al., 2006; Vianello et al., 2005) and that receptor desensitization may play a role in such chemorepulsive migration (Raffaghello and Pistoia, 2009). Thus, other mechanisms for the repulsive cell migration differ from the proposed mechanism here based on combined chemokine fields. Altogether, this combinatorial guiding mechanism argues for the importance and necessity of co-expression of CCL21 and CCL19 in TCZ and the robust design for T-cells entry to LNs, navigation within LNs, and exit from LNs using a united CCR7-dependent mechanism in combination with other important mechanisms such as S1P signalling.

In this chapter, the physiological concentrations of CCL21 and CCL19 in LNs were approximated according to previous studies (Luther et al., 2000). In addition, it is difficult to test cell migration in complex co-existing chemokine fields using conventional assays such as transwell assays. The microfluidic devices used this study allowed me to test T-cells migration quantitatively in different chemokine gradient conditions that mimic possible scenarios in LNs. The results of such studies in conjunction with mathematical modelling and computer simulations offer novel insights into the complex process of T-cells migration and trafficking in SLTs.

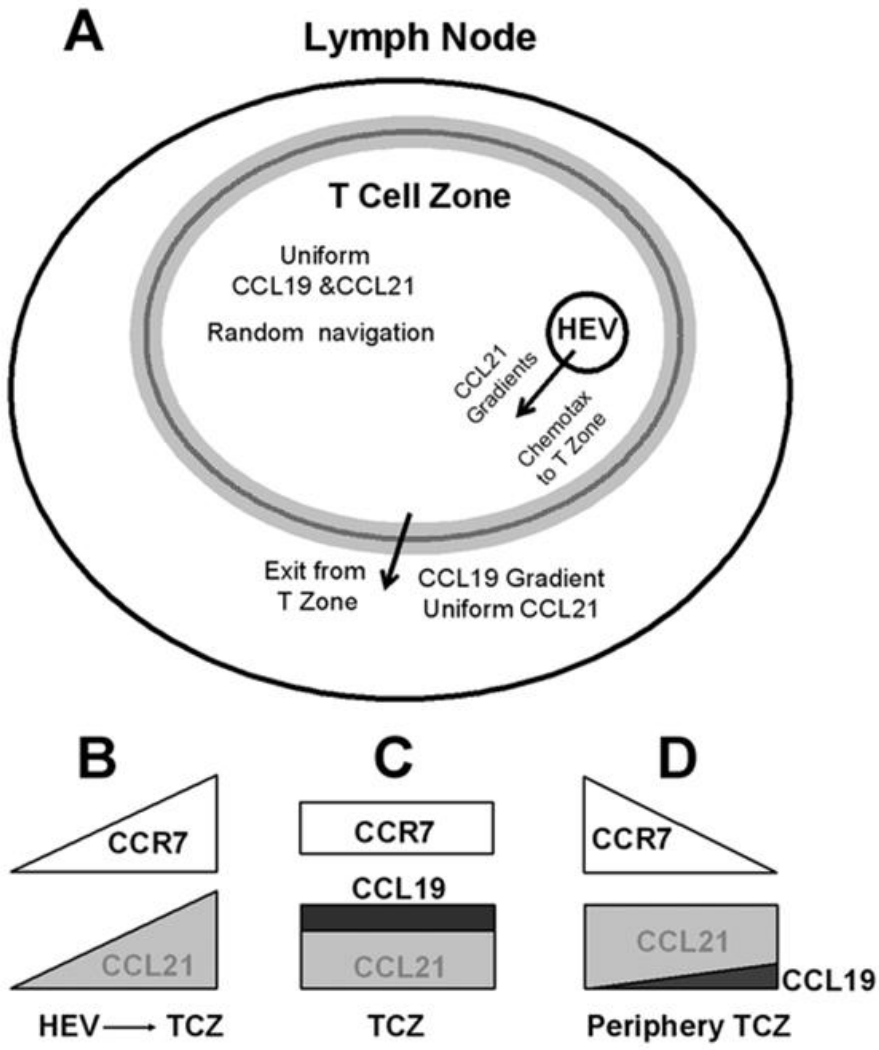

Figure 3.5. The proposed combinatorial guidance mechanism. (A) I propose a possible combinatorial guiding mechanism by different configurations of CCL21 and CCL19 gradient fields for T-cells migration in different sub-regions of lymph nodes. CCL21 mediates the entry of T-cells to LNs through HEVs. Once inside LNs, T-cells follow gradients of CCL21 and possibly CCL19 to migrate to TCZ. Inside TCZ, T-cells migrate randomly in uniform fields of CCL21 and CCL19 to maximize sampling efficiency with antigen presenting cells (APCs) for immune synaptic interactions. The T-cells exit from LNs is facilitated by first migrating out of TCZ through a CCR7-

dependent mechanism. Specifically, T-cells migrate away from TCZ when they reach (by random migration) the periphery region of TCZ, wherein the gradient fields is likely to be a superposition of a low dose CCL19 gradient and a high dose uniform CCL21 field. This mechanism is enabled by the competition of CCR7 binding between CCL21 and CCL19, together with the differential ability of CCL21 and CCL19 for desensitizing CCR7 and the unique superimposed chemokine field profiles. Such combinatorial guiding mechanism argues the importance and necessity of co-expression of CCL21 and CCL19 in TCZ and the robust design for T-cells entry to LNs, navigation within LNs, and exit from LNs using a united CCR7-dependent mechanism; **(B-D)** Schematic illustration of the hypothesized chemokine fields in different regions in the lymph nodes and the corresponding distributions of signalling CCR7 on the cell surface indicating the cell orientation and migration direction.

3.5. Conclusion

In conclusion, in this chapter, I experimentally investigated T-cells migration in different single and superimposed CCL21 and CCL19 fields using microfluidic devices. The results show that the CCL21 gradient, but not the CCL19 gradient at physiological concentrations similar to those observed in LNs, attract T-cells *in vitro*. T-cells migrate randomly in "double-uniform" fields of CCL21 and CCL19. However, T-cells migrate away from the CCL19 gradient in the presence of a uniform background of CCL21. The experimental results are consistent with mathematical modelling and computer simulations, and the T-cells repulsive migration is explained by mathematical modelling based on the chemokine field profiles, competition of CCL21 and CCL19 for activating CCR7 and the differential ability of CCL21 and CCL19 for desensitizing CCR7. Based on these results, I proposed a combinatorial guiding mechanism by CCL21 and CCL19 for T-cells migration in LNs.

CHAPTER 4

INVESTIGATING THE ROLE OF CCR7 LIGANDS FIELDS IN ASSISTING T-CELLS EXIT FROM LYMPH NODES

4.1. Preamble

The results presented in Chapter 3 demonstrate the role of CCL21 and CCL19 in T-cells sub-regional migration in LNs. Based on these results; I proposed a combinatorial guiding mechanism by CCL21 and CCL19 fields for T cell migration in LNs. However, some critical issues remained to be addressed.

In Chapter 3, the CCL21 and CCL19 distribution profiles in LNs sub-regions were speculated based on the reported different distribution patterns of CCL21 and CCL19 producing follicle reticular cells, (Luther et al., 2000; Luther et al., 2002). However, direct measurements of CCL21 and CCL19 distribution profiles in LNs sub-regions along the axis from the TCZ to the medulla are not available. Such knowledge is critically required to support the experimental design of *in vitro* cell migration analysis. To address this issue, I directly analyzed the CCL21 and CCL19 distribution profiles in mouse LNs sections by immunofluorescence staining technique and confocal microscopy.

In the cell migration experiments presented in Chapter 3, I selected 5nM CCL19 and 100nM CCL21 as the physiological concentrations in LNs for constructing different CCL21 and CCL19 fields in microfluidic devices. The selection of 5nM for CCL19 was meant to reflect the upper estimate of the CCL19 production level in peripheral LNs (Luther et al., 2002). The lower estimate of the CCL19 production in peripheral LNs can

be at the level of 1nM (Luther et al., 2002). In addition, the observed repulsive T-cells migration from the 5nM CCL19 gradient with a uniform background of 100nM CCL21 was rather surprising. Therefore, it is interesting and necessary for further examination of cell migration in different CCL21 and CCL19 fields with 1nM CCL19 as the physiological concentration. Similarly, additional experiments to test cell migration in a CCL19 gradient at a super-physiological concentration (e.g. 25nM) with a uniform background of CCL21 are needed. These experiments form an important part of the cell migration analysis in this chapter.

More importantly, the repulsive T-cells migration from the TCZ periphery relevant CCL21 and CCL19 fields suggested that these CCR7 ligands fields may provide a mechanism to facilitate T-cells exit from TCZ to the medulla for their eventual egress. However, such a mechanism is possibly contradicted by the scenario that T-cells will encounter the expected dual same-side CCL21 and CCL19 gradients upon their exit from the TCZ periphery, which will attract T-cells back to the TCZ. Therefore, T-cells migration in such dual same-side gradients at both physiological and super-physiological concentration of CCL19 needs to be examined and compared. These experiments form another important part of the cell migration analysis in this chapter.

As shown in the later sections of this chapter, the results showed the surprising random T-cells migration in the dual same-side gradients at the physiological concentration of CCL19. While such an observation supports the CCR7 ligands fields mediated T-cells exit mechanism, it further raised the question of its underlying molecular mechanism. Toward this direction, I attempted to address this question by evaluating cell surface CCR7 expression upon exposure to different CCL21 and CCL19 fields in microfluidic

devices by immunofluroscence surface CCR7 staining and confocal microscopy. The results suggested the possible role of CCR7 down-regulation by CCL21 and CCL19 fields' exposure to enable different observed T-cells migration patterns in LN sub-regions relevant CCL21 and CCL19 fields. However, as the results from the CCR7 expression studies are not conclusive and addressing the molecular mechanism for the T-cells exit model is beyond the focus of this thesis, I provide the CCR7 expression results in the Appendix in this thesis.

4.2. Introduction

CCR7 ligands CCL21 and CCL19 play important roles in T-cells recruitment and their compartmentalization in LNs (Cyster, 2005; Forster et al., 2008; Otero et al., 2006; Weninger and von Andrian, 2003). T-cells enter the LNs through HEVs and reside in TCZ for antigen scanning. After scanning the TCZ, T-cells exit the LNs via efferent lymphatic vessels by S1P1-based mechanism (Cyster, 2005; Pham et al., 2008). Earlier reports indicated that the S1P1-based mechanism was restricted to the egress port (medullary sinuses) and the inhibition of S1P1 based mechanism did not arrest the T-cells' journey from the TCZ to the medulla (Pham et al., 2008; Wei et al., 2005; Worbs and Förster, 2009). Hence, a SIP1-independent guiding mechanism is needed to orchestrate T-cells migration from TCZ to the medulla for facilitating their exit from LNs. In Chapter 3, microfluidics-based *in vitro* cell migration analysis showed that T-cells migrated away from the low-dose CCL19 gradient with a uniform background of high-dose CCL21 that mimics the possible CCL21 and CCL19 fields in the TCZ periphery (Figure 3.4.). This interesting repulsive migration motivated me to further investigate the possible relevance of the combinatorial guiding mechanism for guiding T-

cells migration from TCZ to medulla, wherein the S1P1-based mechanism takes effect for T-cells exit from LNs. In addition, direct evidence of CCL21 and CCL19 distribution profiles in LNs sub-regions along the axis from the inner TCZ to the medulla is needed to support the design of *in vitro* cell migration analysis. Furthermore, the dependency of T-cells migration on CCL19 gradient strength needs to be examined.

In this chapter, I first show the mouse LNs section staining results for CCL21 and CCL19 distribution profiles in LNs sub-regions. Next, I show the microfluidic experiment data for T-cells migration in different LNs sub-region relevant CCL21 and CCL19 fields at physiological or super-physiological CCL19 gradient strength. A particular focus is on testing T-cells migration in the dual same-side CCL21 and CCL19 gradients that mimic the region beyond the TCZ periphery toward the medulla. Furthermore, cell surface CCR7 expression altered by exposure to different CCL21 and CCL19 fields was also studied (the method and the results are discussed in the Appendix).

4.3. Results

4.3.1. CCL21 and CCL19 distribution in mouse lymph node sub-regions

Understanding chemokine distribution in a physiological environment is crucial for constructing an effective *in vitro* experimental model to study immune cell migration in chemokine fields. In the previous study in Chapter 3, I designed the LNs sub-region relevant CCL21 and CCL19 profiles based on the available literature reporting the difference in the total CCL21 and CCL19 protein levels in SLTs and the difference in CCL21 and CCL19 expressing follicle reticular cells in LNs sub-regions. Here, I directly analyzed CCL21 and CCL19 distribution profiles in LNs sub-regions in BALB/c mouse

peripheral LNs sections by immunofluoroscence staining and confocal microscopy. The CD3 staining allowed me to identify the T-cells concentrated region (TCZ) and locate the TCZ boundary (Figure 4.1A. and 4.2A.). The CCL21 and CCL19 staining revealed their distribution profiles along the axis from the inner TCZ to the medullary region relative to the TCZ boundary (Figure 4.1B. and 4.2B.). At the conceptual level, the results confirmed the expected CCL21 and CCL19 distribution profiles in LNs sub-regions (Figure 4.1C. and 4.2C.): 1) uniform fields of CCL21 and CCL19 in the inner region of TCZ; 2) a CCL19 gradient, but a relatively uniform field of CCL21 in the TCZ periphery region i.e. the region immediately within the TCZ boundary; 3) dual gradients of CCL21 and CCL19 from the TCZ boundary toward the medulla. The significantly different CCL21 and CCL19 staining intensity is consistent with the reported different CCL21 and CCL19 protein production levels in LNs. On the other hand, such analysis does not provide further quantitative characteristics for the CCL21 and CCL19 distribution profiles. In addition, as CCL19 is only presented in soluble form at low level in LNs (Schumann et al., 2010) while CCL21 is presented in both soluble and surface-bound forms at much higher level in LNs, both CCL21 and CCL19, especially CCL19, might be significantly modified or lost during the LNs section preparation. Finally, the current data are based on CD3 staining with CCL19 or CCL21 staining on separate LNs sections from the same LNs due to the availability of antibodies for fluorescence tag selections. I did try triple-staining of CD3, CCL21 and CCL19 in the same LNs section using a different set of antibodies in the later stage of the study. However, the results were complicated by the noisy CCL21 staining, possibly due to the specific antibody used in the experiments or the different LNs section preparation. I decided to not further pursue triple staining at this time. In spite of these issues, the results at least provide the

direct experimental support for the possible CCL21 and CCL19 fields in LNs sub-regions as I hypothesized. These results support the physiological relevance of the experimental design of the study in Chapter 3, and motivate me to further examine the combinatorial guiding mechanism in this chapter.

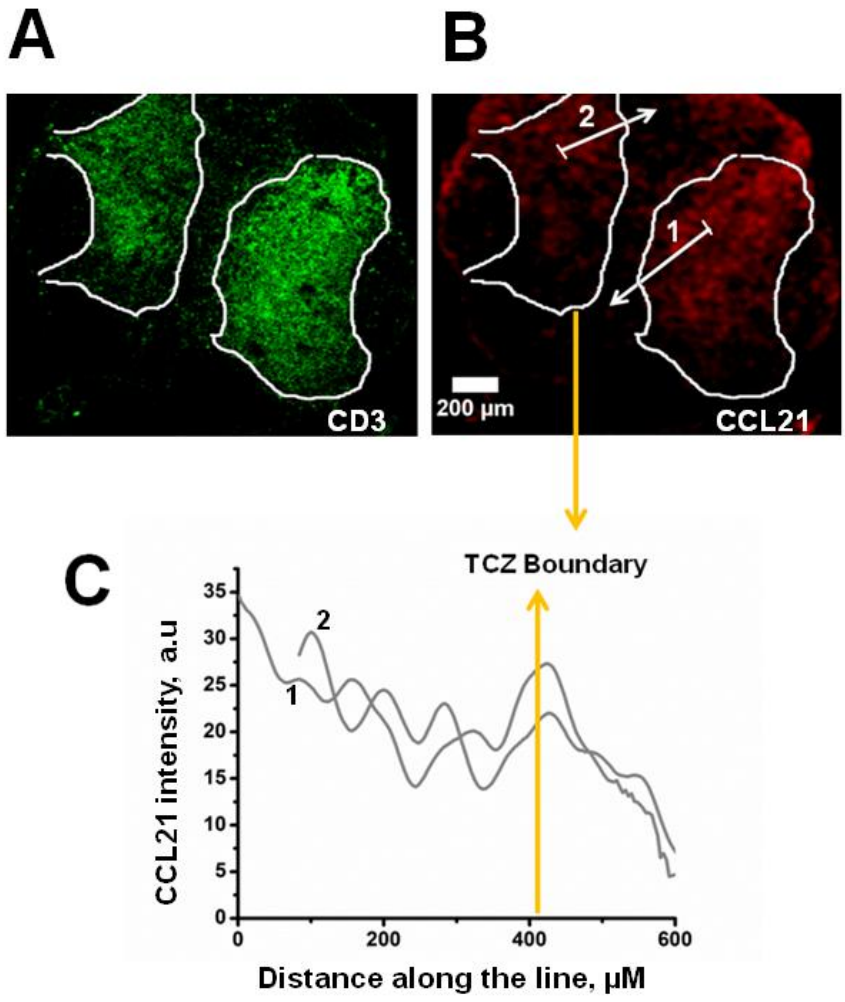

Figure 4.1. Immunostaining of mouse LNs section for CCL21 distribution analysis. **(A)** Alexa-Fluor 488 tagged secondary antibody staining of CD3 shows the TCZ in LNs and locates the TCZ boundary as indicated by the white outline; **(B)** Texas Red tagged secondary antibody staining shows the CCL21 distribution relative to the TCZ boundary as identified by CD3 staining. Two representative lines along the axis from the inner TCZ toward the medulla are shown to measure the CCL21 distribution profile. The CCL21 staining intensity along the line was average over the 50µm line width (as

indicated at the beginning of the arrow line inside the TCZ); **(C)** The CCL21 staining intensity along the two lines in (B).

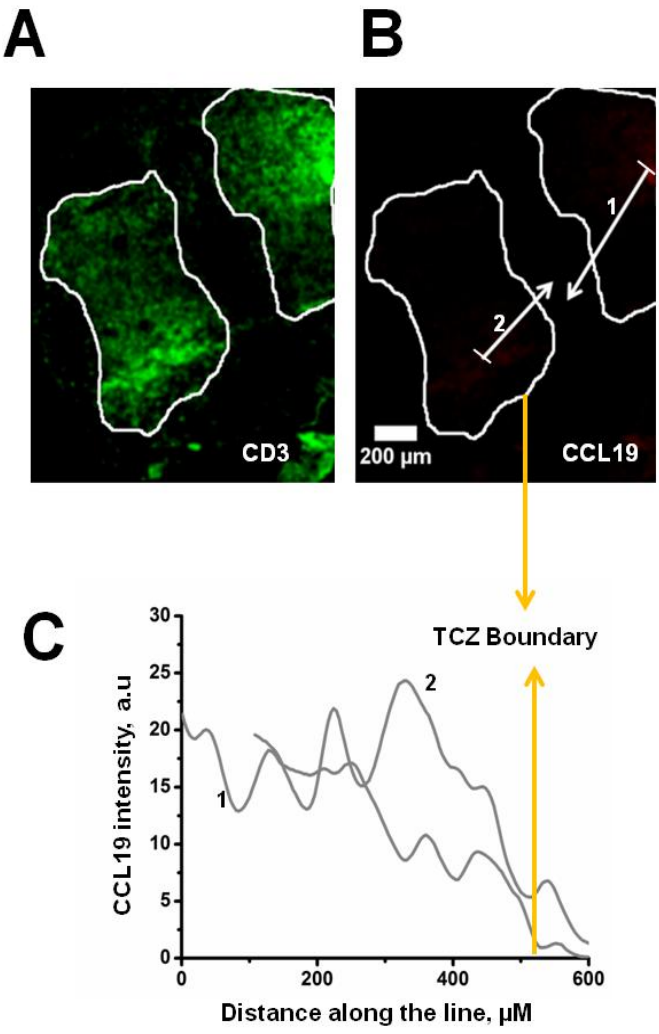

Figure 4.2. Immunostaining of mouse LNs section for CCL19 distribution analysis. **(A)** Alexa-Fluor 488 tagged secondary antibody staining of CD3 shows the TCZ in LNs and locates the TCZ boundary as indicated by the white outline; **(B)** Texas Red tagged secondary antibody staining shows the CCL19 distribution relative to the TCZ boundary as identified by CD3 staining. Two representative lines along the axis from the inner TCZ toward the medulla are shown to measure the CCL19 distribution profile. The CCL19 staining intensity along the line was average over the 50µm line width (as

indicated at the beginning of the arrow line inside the TCZ); **(C)** The CCL19 staining intensity along the two lines in (B). (Note that the CCL19 staining image is better visualized in the electronic copy, but not the hard printing copy of this thesis).

4.3.2. Confirmation of random T-cells migration in a 1nM CCL19 gradient or in double uniform fields of CCL21 and CCL19

The above mouse LNs staining result showed possible uniform distribution of CCL21 and CCL19 in the inner TCZ. To mimic this chemokine profile in the TCZ, I constructed uniform fields of CCL19 and CCL21 at its respective physiological concentrations (i.e. 100nM for CCL21 and 1nM for CCL19) using microfluidic devices. Here I used 1nM as the physiological CCL19 concentration, which has been indicated in previous study (Luther et al., 2002). I then tested T-cells migration in the double uniform fields of 100nM CCL21 and 1nM CCL19. As expected, the results showed the random migration of T-cells in this CCL21 and CCL19 fields (Figure 4.3.). These results is consistent with the previously published results (Kaiser et al., 2005; Worbs et al., 2007), and with the results of the previous study in double uniform fields of 5nM CCL19 and 100nM CCL21 (Figure 3.3.). The migration speed (Figure 4.3B.) is slightly lower than it in the double uniform fields of 5nM CCL19 and 100nM CCL21 (Figure 3.3A.), which is consistent with the use of lower CCL19 concentration (1nM) in the current experiment. Furthermore, the results show random T-cells migration in the 1nM CCL19 gradient with lower migration speed (Figure 4.2.), compared to it in the 5nM CCL19 gradient (Figure 3.2B.). Taking together, these results confirmed the expected random migration of T-cells in uniform CCL21 and CCL19 fields in TCZ, and that the low-dose CCL19 gradient is not sufficient to induce T-cells chemotaxis.

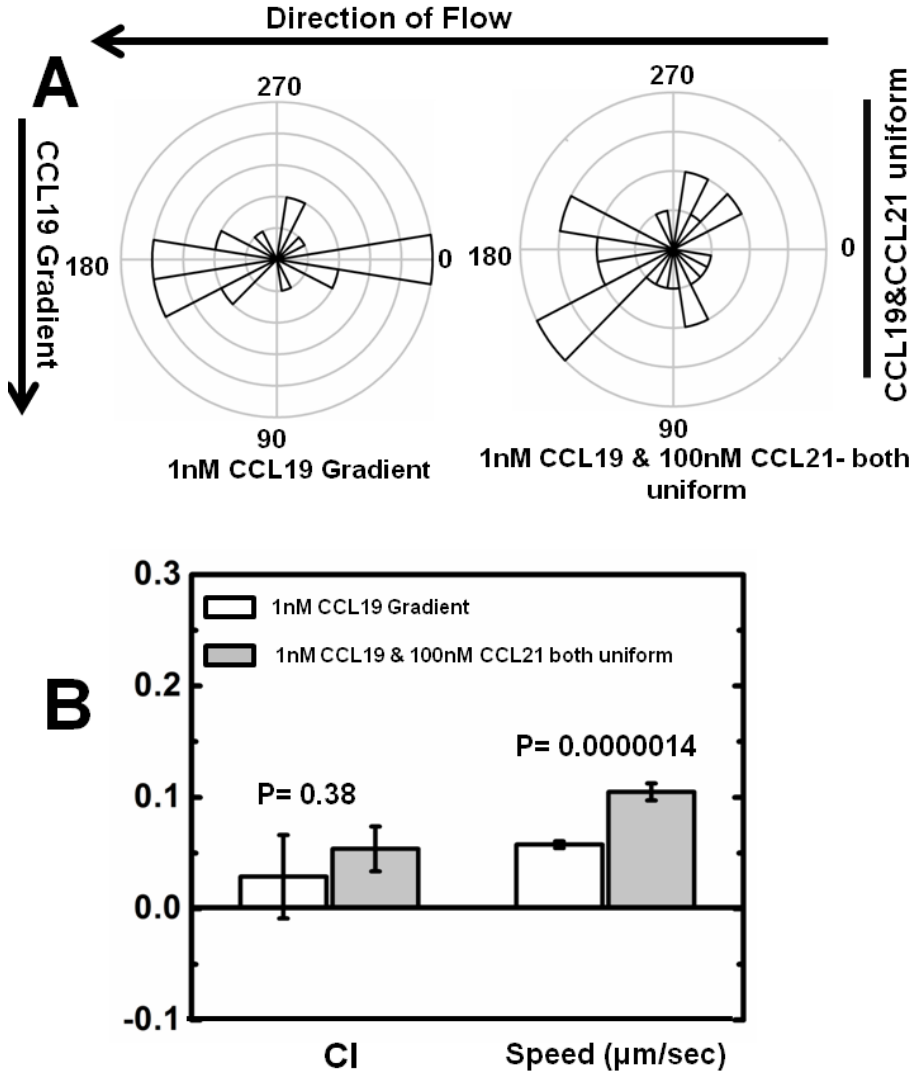

Figure 4.3. T-cells migration in a 1nM CCL19 gradient or double uniform fields of 1nM CCL19 and 100nM CCL21. (A) Angular histograms show T-cells orient randomly in a 1nM CCL19 gradient and double uniform fields of 1nM CCL19 and 100nM CCL21; **(B)** Chemotactic index (C.I.) and migration speed of cells in a 1nM CCL19 gradient or double uniform fields of 1nM CCL19 and 100nM CCL21. The C.I. show that cells migrated randomly under both conditions. The error bars represent the standard error of the mean (s.e.m.). The *p* values for each comparison from 2-sample *t* test are shown.

4.3.3. Bi-directional T-cells migration in a CCL19 gradient with a uniform CCL21 background depends on the CCL19 gradient strength

The mouse LNs staining results showed a possible configuration of a CCL19 gradient with a uniform background of CCL21 in the TCZ periphery. The previous study in Chapter 3 showed that T-cells migrated away from the 5nM CCL19 gradient with a uniform background of 100nM CCL21 (Figure 3.4.). In the current experiment, I tested T-cells migration in the similar CCL21 and CCL19 fields but used the even lower 1nM CCL19 as its physiological concentration. The results again showed the repulsive T-cells migration from the 1nM CCL19 gradient with the 100nM uniform CCL21 background (Figure 4.4.). By contrast, T-cells migrated toward the super-physiological 25nM CCL19 gradient with the same uniform background of 100nM CCL21 (Figure 4.4.). The migration speed is comparable under both conditions, possibly dominated by the same high dose CCL21 uniform field (Figure 4.4.). Thus, the repulsive T-cells migration holds true at an even lower CCL19 gradient, but not at a significantly higher CCL19 gradient, provided a high dose CCL21 uniform background is present. These results support the hypothesis that physiological CCL21 and CCL19 fields in the TCZ periphery region coordinate T-cells exit from the TCZ.

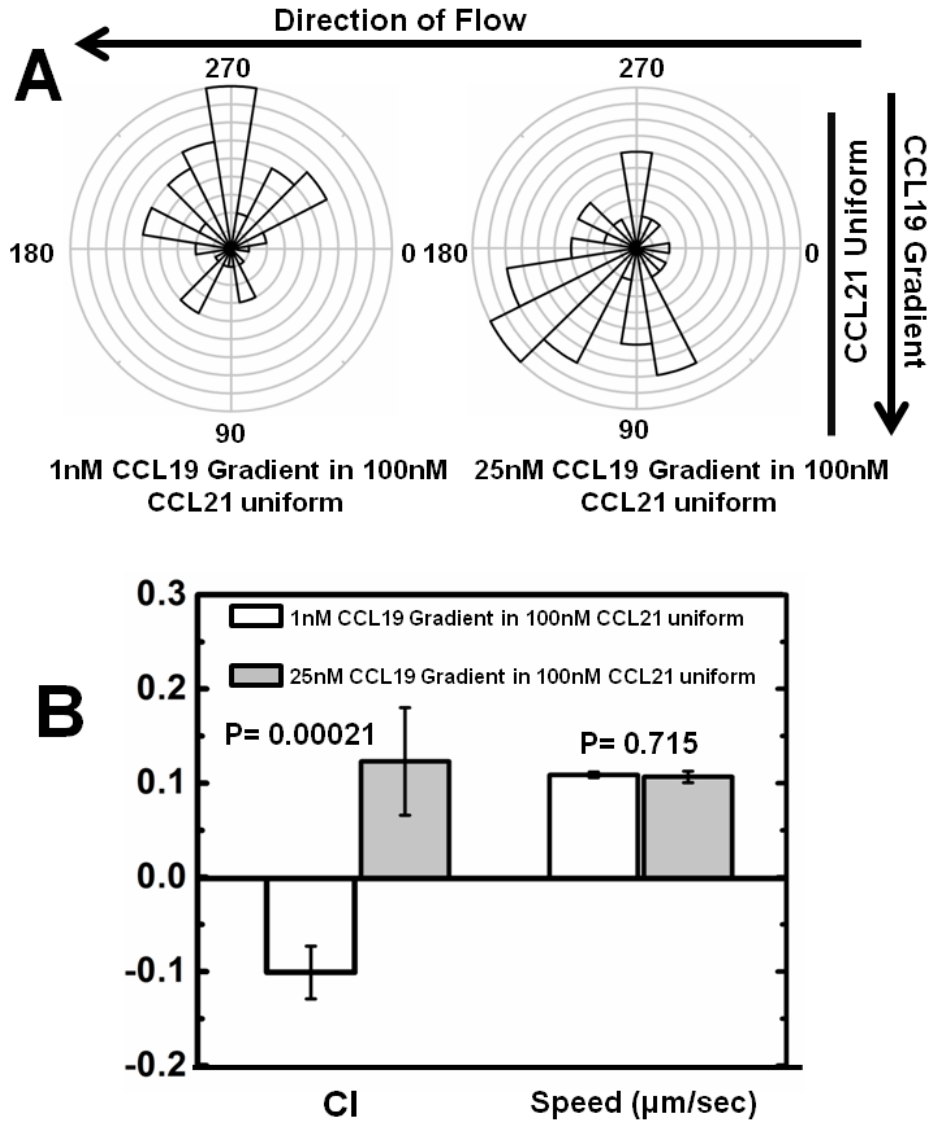

Figure 4.4. T-cells migration in different CCL19 gradients with a uniform background of CCL21. (A) Angular histogram shows more T-cells orient away from a 1nM CCL19 gradient with a uniform background of 100nM CCL21; T-cells orient toward a 25nM CCL19 gradient with a uniform background of 100nM CCL21; **(B)** Comparison of chemotactic index (C.I.) and the speed of cells between 1nM CCL19 gradient with a uniform background of 100nM CCL21 versus a 25nM CCL19 gradient

with a uniform background of 100nM CCL21. The error bars represent the standard error of the mean (s.e.m.). Negative C.I. indicates cells migrate away from the gradient and positive C.I. indicates cells migrate toward the gradient. The *p* values for each comparison from 2-sample *t*-test are shown.

4.3.4. T-cells migration in dual same-side CCL21 and CCL19 gradients depends on the CCL19 gradient strength

The mouse LNs staining indicated the possible configuration of dual CCL19 and CCL21 gradients along the axis from the TCZ toward the medulla (Figure 4.1.; Figure 4.2.). I have showed that the high dose CCL21 gradient (Figure 3.1.), but not the low dose CCL19 gradient (Figure 3.2.; Figure 4.3.), is effective to induce T-cells chemotaxis. Therefore, intuitively, a dual same-side CCL21 and CCL19 gradient configuration is expected to enhance or at least not disrupt T-cells chemotaxis. In this case, I would predict that T-cells migrated out of the TCZ through the repulsive migration mechanism by the TCZ periphery CCL21 and CCL19 fields will be attracted back to TCZ by the dual same-side CCL21 and CCL19 gradients. To test such a scenario, I examined T-cells migration in the dual same-side gradients of 1nM CCL19 and 100nM CCL21 using microfluidic devices. Surprisingly, the results show the overall random T cell migration under this CCL21 and CCL19 field configuration (Figure 4.5.). By contrast, the dual same-side gradient of 100nM CCL19 (super-physiological) and 100nM CCL21 (physiological) induces robust T-cells chemotaxis (Figure 4.5.).

Experiments in the dual same-side gradients of 5nM CCL19 and 100nM CCL21 showed similar overall random migration. On the other hand, further analysis show interesting different cell migration patterns in different sub-regions of the gradients (Appendix A.1), Specifically, in the high concentration region of the CCL21 and CCL19 gradients, cells exhibit repulsive migration away from the gradients; In contrast, in the low concentration region of the CCL21 and CCL19 gradients, cells chemotax to the gradients; in the middle region of the gradient fields, cells migrate randomly. These results demonstrate

the differential cell migratory behaviours in different combinations of CCL21 and CCL19 fields in a single experimental setup.

The observed overall random T-cells migration in the dual same-side CCL21 and CCL19 gradients, although surprising, would prevent T-cells from being attracted back to TCZ. One possible enabling mechanism is through CCR7 down-regulation. Previous studies have shown that CCL19 induces robust CCR7 desensitization and internalization even at low concentrations; and high concentration of CCL21 also induces CCR7 internalization (Kohout et al., 2004; Otero et al., 2006). Thus, in principle, a combination of CCL21 and CCL19 gradients can significantly down-regulate cell surface CCR7 expression, which blocks chemotactic responses to CCR7 ligands fields. Toward this direction, I performed immunofluorescence staining experiments and confocal microscopy analysis to examine cell surface CCR7 expression upon exposure to different CCL21 and CCL19 fields in microfluidic devices. The experimental method and the results of this study are discussed in Appendix A.2. Although not conclusive with several interesting unexpected observations, the current results confirmed the significantly reduced cell surface CCR7 expression upon exposure to the CCL19 and CCL21 fields relevant to the region beyond TCZ periphery. Further studies are required to clarify this CCR7 down-regulation based mechanism. Additionally, this random T-cells migration in the dual same-side CCL21 and CCL19 gradients can be consistent with our previously developed mathematical model based on the differential CCR7 desensitization by CCL21 and CCL19. In this case, the CCL19 gradient will more strongly desensitize and internalize CCR7 in the front of the cell (facing the high concentration of CCL19 in the gradient), leaving less free CCR7 for binding with CCL21 at higher CCL21 concentration. By contrast, the rear

side of the cell will have more free CCR7 to bind with CCL21 but at lower CCL21 concentration. This may possibly result in a balance of activated CCR7 occupancy across the cell body, leading to poor gradient sensing.

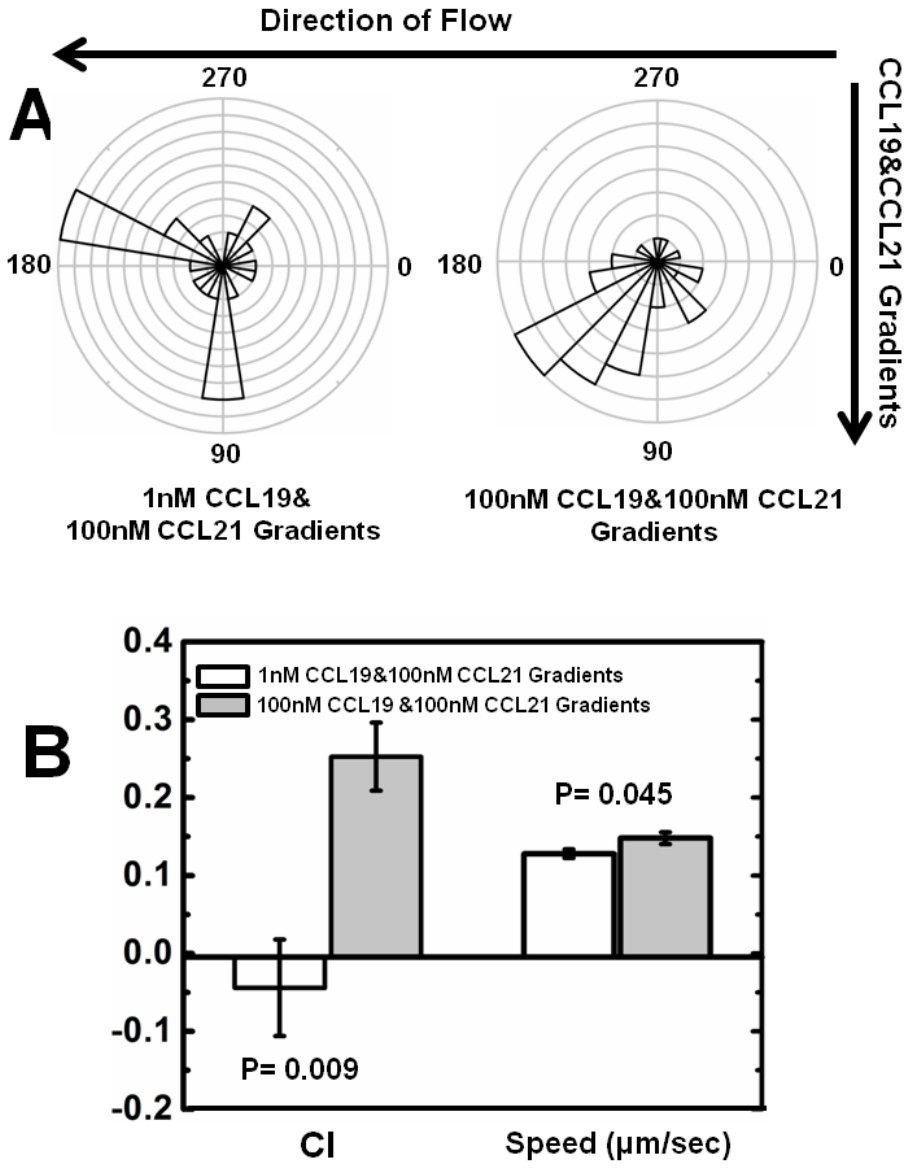

Figure 4.5. T-cells migration in dual same-side gradients of CCL21 and CCL19. (A) Angular histogram shows T-cells orient randomly in the dual 1nM CCL19 and 100nM CCL21 gradients along the same side; T-cells orient toward the dual 100nM CCL19 and 100nM CCL21 gradients along the same side; **(B)** Comparison of chemotactic index (C.I.) and cell migration speed between the dual 1nM CCL19 and 100nM CCL21 gradients along the same side versus the dual 100nM CCL19 and 100nM CCL21

gradients along the same side. The error bars represent the standard error of the mean (s.e.m.). Positive C.I. indicates cells migrate toward the gradients. The *p*-values for each comparison from 2-sample *t*-test are shown.

4.4. The updated combinatorial guidance model for facilitating T-cells exit from lymph nodes

Taking together the results in Chapter 3 and 4, here, I provide a comprehensive combinatorial guiding mechanism for T-cells migration in LNs. As illustrated in Figure 4.6., in this combinatorial guidance model, CCL21 alone mediates the entry of T-cells to LNs through HEVs. T-cells follow gradients of CCL21 and possibly CCL19 to the T-cells compartment (TCZ) within the LNs. Within TCZ, uniform fields of CCL21 and CCL19 do not present directional signals to allow random T-cells migration to efficiently interact with antigen presenting cells (APCs) corroborating previous results (Kaiser et al., 2005; Worbs et al., 2007). The antigen encountered T-cells are activated followed by clonal expansion over an extended period of time in LNs, and will eventually exit LNs. Naive cells (without activation) will egress LNs rather quickly (naive cells remain in LNs for 5-6 hours) (Cyster, 2005). Both activated and naive T-cells leave the TCZ toward the medulla through the repulsive migration mechanisms mediated by the low dose CCL19 gradient with a uniform background of CCL21 presented in the TCZ periphery region. Once exited from the TCZ, T-cells maintain their random motility instead of chemotaxis in response to the dual CCL21 and CCL19 gradients originated from the TCZ, which is possibly enabled by the down-regulated cell surface CCR7 expression. This prevents the exited T-cells from being attracted back to TCZ, and thus effectively bridge the S1P1 mediated T-cells exit from LNs that takes place in the medullary sinuses. The results from Chapter 4 further indicate that the combinatorial guiding mechanism is unique to the physiological CCR7 ligands fields, but will be invalid if super-physiological CCR7 ligands fields are applied. On the other hand, the

selection of the exact low dose CCL19 gradient does not affect the general predictions of the combinatorial model.

The key feature in the combinatorial guiding mechanism is the CCL21 and CCL19 fields mediated T-cells exit from TCZ to the medulla, thus facilitating their egress through the S1P1-based mechanism. S1P1-based T-cells exit mechanism operates in the medullary sinuses and cortical sinusoids (Cyster, 2005; Matloubian et al., 2004; Sensken et al., 2011; Thangada et al., 2010). S1P1 signals compete with CCR7 signals and T-cells yield to S1P1 signals by overcoming CCR7 signals during their egress from the LNs (Dustin and Chakraborty, 2008). S1P expressed by the ECs of cortical sinusoids and medullary sinuses forms a gradient and guides the T-cells entry into the medullary sinuses and cortical sinusoids for T-cells egress through the efferent lymphatic vessel (Dustin and Chakraborty, 2008; Pappu et al., 2007). However, the region in the LNs, where S1P1 signal overtakes CCR7 signal is not clear. Blocking the interaction between S1P and S1P1 using S1P agonist does not prevent T-cells from reaching the medulla and staying at the abluminal side of the medullary sinuses (Dustin and Chakraborty, 2008; Mandala et al., 2002). Other studies also showed that S1P1 is not involved in T-cells migration in TCZ (Halin et al., 2005; Huang et al., 2007; Worbs and Förster, 2009). Consistently, *ex vivo* imaging studies by two photon microscopy showed the accumulation of T-cells between the medullary cords and empty sinuses upon blocking the S1P-S1P1 interaction (Wei et al., 2005). Nevertheless, arresting the S1P-S1P1 interaction blocks the entry of the T-cells into the medullary sinuses. Apart from S1P, CXCL12 is also produced in LNs, which is a potent chemoattractant for T-cells. However, the role of CXCL12 is limited to the medullary region of LNs and does not affect T-cells motility in LNs in the

presence of CCL21 and CCL19 (Asperti-Boursin et al., 2007; Okada and Cyster, 2007; Worbs and Förster, 2009). These results support the proposed CCR7 ligands fields mediated mechanism for facilitating T-cells exit from TCZ to the vicinity of the egress port. The physiological low expression of CCL19 in TCZ plays an important role in tuning T-cells migration patterns in LNs sub-regions and facilitating effective T-cells exit from LNs. Evidently, the absence of CCL19 in CCL19 knockout mice does not block recruitment of adoptively transferred T-cells to LNs, and surprisingly, it further increases T-cells retention in LNs, which is possibly due to the loss of CCL21 and CCL19 field mediated T-cells exit mechanism (Link et al., 2007).

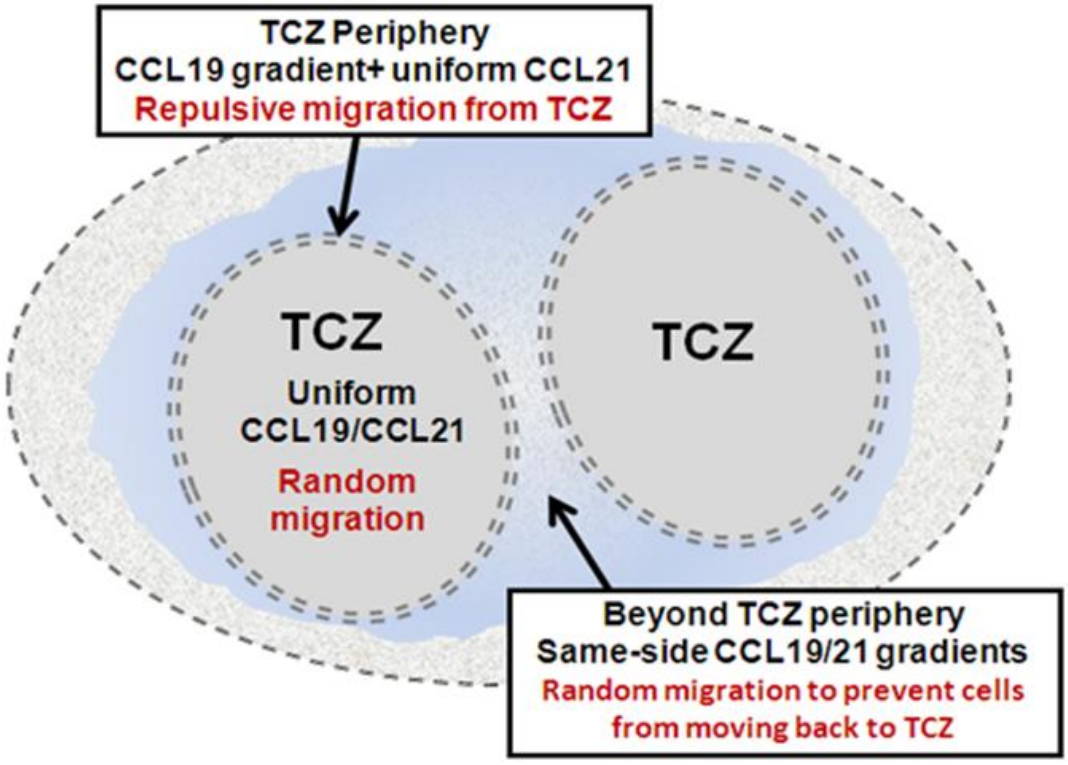

Figure 4.6. Illustration of the updated combinatorial guidance model for T-cells sub-regional migration in LNs and T-cells exit from TCZ.

4.5. Conclusion

In conclusion, in this chapter, I have further investigated the combinatorial guiding mechanism and discussed its relevance to T-cells exit from LNs. The immunofluorescence staining and confocal microscopy results for the CCL21 and CCL19 distribution profiles in mouse LNs sections support the hypothesized LNs sub-region CCL21 and CCL19 field profiles. Furthermore, I studied T-cells migration in the physiological or super-physiological CCL21 and CCL19 fields relevant to LNs sub-regions in microfluidic devices. The results support the roles of physiologically-relevant CCL21 and CCL19 fields in T-cells migration in LNs sub-regions. The results also demonstrated the critical role of the combined physiological CCL21 and CCL19 fields in assisting T-cells exit from LNs by repulsing T-cells from TCZ and preventing the re-entry of outgoing T-cells to TCZ. Additionally, cell surface CCR7 expression analysis shows the role of LNs sub-region relevant CCL21 and CCL19 fields in modulating the surface CCR7 expression level in T-cells. Collectively, the research in this chapter further formulates the combinatorial guiding mechanism and provides new insights into the process of T-cells exit from LNs.

CHAPTER 5

CONCLUSION, SIGNIFICANCE AND FUTURE DIRECTIONS

Microfluidic devices provide a useful platform to mimic the complex physiological microenvironments for *in vitro* quantitative immune cell migration analysis. In this thesis, I constructed different LNs sub-region relevant CCL21 and CCL19 fields using microfluidic devices based on the previous literatures and my own data of CCL21 and CCL19 distributions in mouse LNs sections. Activated human blood T-cells were quantitatively examined for their migration in these chemokine fields. The results suggested a novel combinatorial guiding mechanism for T-cells migration in LNs sub-region relevant CCL21 and CCL19 fields. As a particularly important part of this mechanism, T-cells migrate away from the low dose CCL19 gradient with a uniform background of high dose CCL21, which mimics the condition in the TCZ boundary. This interesting repulsive migration was explained by a receptor desensitization-based mathematical model. Furthermore, the random migration of T-cells in the dual same-side CCL21 and CCL19 gradients prevents cells from being attracted back to the TCZ. Thus, this combinatorial model suggests a CCR7 ligands fields mediated mechanism for T-cells migration from TCZ to the egress port (medullary sinuses) for their exit from LNs. I show that such a combinatorial guiding mechanism is unique to the physiological CCL21 and CCL19 fields configurations and is possibly associated with cell surface CCR7 down-regulation by exposure to LNs sub-regional CCR7 ligands fields.

In conclusion, enabled by microfluidic devices, this thesis achieved the proposed objectives by quantitatively characterizing the T-cells migration in CCL21 and CCL19 fields relevant to LNs sub-regions, which provides interesting new insight into the

guiding mechanisms for T-cells trafficking and organization in LNs. In addition, the combinatorial guiding mechanism revealed in this thesis will have important implications to other physiological and pathological systems mediated by CCR7 and its ligands. For example, CCR7 and CCL21 mediated excessive T-cells recruitment to the site of inflammation can cause further tissue damage (Pickens et al., 2012). In addition to T-cells, CCR7 signalling is also important for B-cells and DCs trafficking and organization in SLTs for secondary immune responses. Moreover, CCR7 and its dual ligands are involved in the recruitment of neutrophils and NK-cells to LNs (Beauvillain et al., 2011; Cyster, 2005; Pulendran et al., 2011). Similar roles of CCR7 and its ligands are also indicated in cancer metastasis (Kim et al., 2012). CCL21 and CCL19 expression is indicated in CNS related inflammation (Krumbholz et al., 2007; Pashenkov et al., 2003). Understanding how CCL21 and CCL19 coordinate the migration of different cell types through CCR7 signalling will inspire new approaches for manipulating adaptive immunity and for treating various relevant physiological problems and diseases. For example, the research findings from this thesis will support the development of new therapeutic method targeting CCL19 to control T-cells egress from LNs instead of or in combination with the existing drugs targeting the S1P axis for treating relevant diseases such as multiple sclerosis (MS). Finally, the effective use of microfluidic devices in this thesis will have positive impact on the development of microfluidics-based applications for studying cellular behaviours in complex microenvironments with relevance to physiological systems.

In this thesis, activated human blood T-cells were used as the sole model cell system for cell migration experiments, which mimic acutely activated T cells upon interaction with

DCs in LNs. In the future, the general or cell-type dependent combinatorial guiding mechanism should be further tested for different T-cells subsets such as CD4, CD8, naive and central memory T cells, as well as other SLTs relevant CCR7 expressing cells such as B-cells and DCs. In addition, I have proposed that the differential CCR7 desensitization by CCL21 and CCL19 serves as a potential molecular mechanism underlying the combinatorial guidance model. Our lab has started further exploring this mechanism by testing CCR7 mutants (aims to modify CCR7 desensitization). Other molecular techniques such as protein over-expression or RNA interference (RNAi) can be employed to test the dependence of the combinatorial guiding mechanism on CCR7 expression in T-cells. The observed cell surface CCR7 down-regulation in correlation with cell exposure to different CCL21 and CCL19 fields also needs to be further investigated. Furthermore, to study the role of CCL21 and CCL19 mediated T-cells exit mechanism, T-cells migration in competing gradients of S1P and CCL21 (with or without a superimposed same-side CCL19 gradient) should be examined. Ultimately, it will be important to test the combinatorial guiding mechanism in physiological models. Toward this direction, a possible approach is to directly examine T-cells migration in mouse LNs sub-regions using advanced intravital microscopy such as 2-photon microscopy in combination with inhibition of CCL19. The similar approach can be applied to CCL19 knockout mice model.

REFERENCES

Abhyankar, V.V., Lokuta, M.A., Huttenlocher, A., and Beebe, D.J. (2006). Characterization of a membrane-based gradient generator for use in cell-signalling studies. Lab on a Chip *6*, 389-393.

Afzali, B., Lombardi, G., Lechler, R.I., and Lord, G.M. (2007). The role of T helper 17 (Th17) and regulatory T-cells (Treg) in human organ transplantation and autoimmune disease. Clinical & Experimental Immunology *148*, 32-46.

Alblas, J., Ulfman, L., Hordijk, P., and Koenderman, L. (2001). Activation of RhoA and ROCK Are Essential for Detachment of Migrating Leukocytes. Mol. Biol. Cell *12*, 2137-2145.

Albrecht-Buehler, G. (1977). The phagokinetic tracks of 3T3 cells. Cell *11*, 395-404.

Amarie, D., Glazier, J.A., and Jacobson, S.C. (2007). Compact Microfluidic Structures for Generating Spatial and Temporal Gradients. Analytical Chemistry *79*, 9471-9477.

Ambravaneswaran, V., Wong, I.Y., Aranyosi, A.J., Toner, M., and Irimia, D. (2010). Directional decisions during neutrophil chemotaxis inside bifurcating channels. Integrative Biology *2*, 639-647.

Andrew, N., and Insall, R.H. (2007). Chemotaxis in shallow gradients is mediated independently of PtdIns 3-kinase by biased choices between random protrusions. Nat Cell Biol. *9*, 193-200.

Asperti-Boursin, F.o., Real, E., Bismuth, G., Trautmann, A., and Donnadieu, E. (2007). CCR7 ligands control basal T cell motility within lymph node slices in a phosphoinositide-3-kinase independent manner. The Journal of Experimental Medicine *204*, 1167-1179.

Atencia, J., Morrow, J., and Locascio, L.E. (2009). The microfluidic palette: A diffusive gradient generator with spatio-temporal control. Lab on a Chip *9*, 2707-2714.

Ayala, R., Shu, T., and Tsai, L.H. (2007). Trekking across the brain: the journey of neuronal migration. Cell *128*, 29-43.

Banchereau, J., Briere, F., Caux, C., Davoust, J., Lebecque, S., Liu, Y.-J., Pulendran, B., and Palucka, K. (2000). Immunobiology of Dendritic Cells. Annual Review of Immunology *18*, 767-811.

Banchereau, J., and Steinman, R.M. (1998). Dendritic cells and the control of immunity. Nature *392*, 245-252.

Barratt-Boyes, S.M., Zimmer, M.I., Harshyne, L.A., Meyer, E.M., Watkins, S.C., Capuano, S., Murphey-Corb, M., Falo, L.D., and Donnenberg, A.D. (2000). Maturation and Trafficking of Monocyte-Derived Dendritic Cells in Monkeys: Implications for Dendritic Cell-Based Vaccines. J Immunol. *164*, 2487-2495.

Bazan, J.F., Bacon, K.B., Hardiman, G., Wang, W., Soo, K., Rossi, D., Greaves, D.R., Zlotnik, A., and Schall, T.J. (1997). A new class of membrane-bound chemokine with a CX3C motif. Nature *385*, 640-644.

Beauvillain, C.l., Cunin, P., Doni, A., Scotet, M., Jaillon, S.b., Loiry, M.-L., Magistrelli, G., Masternak, K., Chevailler, A., Delneste, Y., and Jeannin, P. (2011). CCR7 is involved in the migration of neutrophils to lymph nodes. Blood *117*, 1196-1204.

Beebe, D.J., Mensing, G.A., and Walker, G.M. (2002). physics and applications of microfluidics in biology. Annual Review of Biomedical Engineering *4*, 261-286.

Behar, T., Schaffner, A., Colton, C., Somogyi, R., Olah, Z., Lehel, C., and Barker, J. (1994). GABA-induced chemokinesis and NGF-induced chemotaxis of embryonic spinal cord neurons. J. Neurosci. *14*, 29-38.

Berthier, E., Surfus, J., Verbsky, J., Huttenlocher, A., and Beebe, D. (2010). An arrayed high-content chemotaxis assay for patient diagnosis. Integrative Biology *2*, 630-638.

Bleul, C.C., Farzan, M., Choe, H., Parolin, C., Clark-Lewis, I., Sodroski, J., and Springer, T.A. (1996). The lymphocyte chemoattractant SDF-1 is a ligand for LESTR/fusin and blocks HIV-1 entry. Nature *382*, 829-833.

Borregaard, N. (2010). Neutrophils, from Marrow to Microbes. Immunity *33*, 657-670.

Braun, A., Worbs, T., Moschovakis, G.L., Halle, S., Hoffmann, K., Bolter, J., Munk, A., and Förster, R. (2011). Afferent lymph-derived T cells and DCs use different chemokine receptor CCR7-dependent routes for entry into the lymph node and intranodal migration. Nat Immunol. *12*, 879-887.

Breitfeld, D., Ohl, L., Kremmer, E., Ellwart, J., Sallusto, F., Lipp, M., and Förster, R. (2000). Follicular B Helper T Cells Express Cxc Chemokine Receptor 5, Localize to B

cell Follicles, and Support Immunoglobulin Production. The Journal of Experimental Medicine *192*, 1545-1552.

Bretscher, M.S. (2008). On the shape of migrating cells--a `front-to-back' model. Journal of Cell Science *121*, 2625-2628.

Britschgi, M.R., Favre, S., and Luther, S.A. (2010). CCL21 is sufficient to mediate DC migration, maturation and function in the absence of CCL19. European Journal of Immunology *40*, 1266-1271.

Britschgi, M.R., Link, A., Lissandrin, T.K.A., and Luther, S.A. (2008). Dynamic Modulation of CCR7 Expression and Function on Naive T-lymphocytes *In vivo*. J Immunol. *181*, 7681-7688.

Brown, M.N., Fintushel, S.R., Lee, M.H., Jennrich, S., Geherin, S.A., Hay, J.B., Butcher, E.C., and Debes, G.F. (2010). Chemoattractant Receptors and Lymphocyte Egress from Extralymphoid Tissue: Changing Requirements during the Course of Inflammation. J Immunol. *185*, 4873-4882.

Butler, K.L., Ambravaneswaran, V., Agrawal, N., Bilodeau, M., Toner, M., Tompkins, R.G., Fagan, S., and Irimia, D. (2010). Burn Injury Reduces Neutrophil Directional Migration Speed in Microfluidic Devices. PLoS ONE *5*, e11921.

Cai, G., Lian, J., Shapiro, S.S., and Beacham, D.A. (2000). Evaluation of endothelial cell migration with a novel in vitro assay system. Methods in Cell Science *22*, 107-114.

Calderón, L., and Boehm, T. (2011). Three chemokine receptors cooperatively regulate homing of hematopoietic progenitors to the embryonic mouse thymus. Proceedings of the National Academy of Sciences *108*, 7517-7522.

Campbell, K., and Groisman, A. (2007). Generation of complex concentration profiles in microchannels in a logarithmically small number of steps. Lab on a Chip *7*, 264-272.

Carlsen, H.S., Haraldsen, G., Brandtzaeg, P., and Baekkevold, E.S. (2005). Disparate lymphoid chemokine expression in mice and men: no evidence of CCL21 synthesis by human high endothelial venules. Blood *106*, 444-446.

Carreau, A., Kieda, C., and Grillon, C. (2011). Nitric oxide modulates the expression of endothelial cell adhesion molecules involved in angiogenesis and leukocyte recruitment. Experimental Cell Research *317*, 29-41.

Cheng, S.-Y., Heilman, S., Wasserman, M., Archer, S., Shuler, M.L., and Wu, M. (2007). A hydrogel-based microfluidic device for the studies of directed cell migration. Lab on a Chip *7*, 763-769.

Choi, E., Chang, H.-k., Young Lim, C., Kim, T., and Park, J. (2012). Concentration gradient generation of multiple chemicals using spatially controlled self-assembly of particles in microchannels. Lab on a Chip *12*, 3968-3975.

Comer, F.I., and Parent, C.A. (2002). PI 3-Kinases and PTEN: How Opposites Chemoattract. Cell *109*, 541-544.

Cyster, J.G. B cell follicles and antigen encounters of the third kind. Nat Immunol *11*, 989-996.

Cyster, J.G. (2005). Chemokines, sphingosine-1-phosphate, and cell migration in secondary lymphoid organs. Annual Review of Immunology *23*, 127-159.

Dale, D.C., Boxer, L., and Liles, W.C. (2008). The phagocytes: neutrophils and monocytes. Blood *112*, 935-945.

Debes, G.F., Arnold, C.N., Young, A.J., Krautwald, S., Lipp, M., Hay, J.B., and Butcher, E.C. (2005). Chemokine receptor CCR7 required for T-lymphocyte exit from peripheral tissues. Nat Immunol. *6*, 889-894.

Dekker, L.V., and Segal, A.W. (2000). Signals to Move Cells. Science *287*, 982-985.

Dertinger, S.K.W., Chiu, D.T., Jeon, N.L., and Whitesides, G.M. (2001). Generation of Gradients Having Complex Shapes Using Microfluidic Networks. Analytical Chemistry *73*, 1240-1246.

Dittrich, P., and Manz, A. (2005). Single-molecule fluorescence detection in microfluidic channels--the Holy Grail muTAS? Analytical and Bioanalytical Chemistry *382*, 1771-1782.

Dustin, M.L., and Chakraborty, A.K. (2008). Tug of War at the Exit Door. *28*, 15-17.

Ehrengruber, M.U., Coates, T.D., and Deranleau, D.A. (1995). Shape oscillations: a fundamental response of human neutrophils stimulated by chemotactic peptides? FEBS Letters *359*, 229-232.

Förster, R., Davalos-Misslitz, A.C., and Rot, A. (2008). CCR7 and its ligands: balancing immunity and tolerance. Nat Rev Immunol. *8*, 362-371.

Foxman, E.F., Campbell, J.J., and Butcher, E.C. (1997). Multistep Navigation and the Combinatorial Control of Leukocyte Chemotaxis. The Journal of Cell Biology *139*, 1349-1360.

Foxman, E.F., Kunkel, E.J., and Butcher, E.C. (1999). Integrating Conflicting Chemotactic Signals. The Journal of Cell Biology *147*, 577-588.

Friedl, P., Borgmann, S., and Bröcker, E.-B. (2001). Amoeboid leukocyte crawling through extracellular matrix: lessons from the Dictyostelium paradigm of cell movement. Journal of Leukocyte Biology *70*, 491-509.

Friedl, P., and Weigelin, B. (2008). Interstitial leukocyte migration and immune function. Nat Immunol. *9*, 960-969.

Friedl, P., and Wolf, K. (2010). Plasticity of cell migration: a multiscale tuning model. The Journal of Cell Biology *188*, 11-19.

Fukata, M., Nakagawa, M., and Kaibuchi, K. (2003). Roles of Rho-family GTPases in cell polarizFation and directional migration. Current Opinion in Cell Biology *15*, 590-597.

Geng, J.G. (2001). Directional migration of leukocytes: their pathological roles in inflammation and strategies for development of anti-inflammatory therapies. Cell Res *11*, 85-88.

Girard, J.-P., and Springer, T.A. (1995). High endothelial venules (HEVs): specialized endothelium for lymphocyte migration. Immunology Today *16*, 449-457.

Glawdel, T., Elbuken, C., Lee, L.E.J., and Ren, C.L. (2009). Microfluidic system with integrated electroosmotic pumps, concentration gradient generator and fish cell line (RTgill-W1)-towards water toxicity testing. Lab on a Chip *9*, 3243-3250.

Grabovsky, V., Feigelson, S., Chen, C., Bleijs, D.A., Peled, A., Cinamon, G., Baleux, F., Arenzana-Seisdedos, F., Lapidot, T., van Kooyk, Y., *et al.* (2000). Subsecond Induction of α4 Integrin Clustering by Immobilized Chemokines Stimulates Leukocyte Tethering and Rolling on Endothelial Vascular Cell Adhesion Molecule 1 under Flow Conditions. The Journal of Experimental Medicine *192*, 495-506.

Guermonprez, P., Valladeau, J., Zitvogel, L., Théry, C., and Amigorena, S. (2002). Antigen presentation and t cell stimulation by dendritic cells. Annual Review of Immunology *20*, 621-667.

Gunn, M., Kyuwa, S., Tam, C., Kakiuchi, T., Matsuzawa, A., Williams, L., and Nakano, H. (1999). Mice lacking expression of secondary lymphoid organ chemokine have defects in lymphocyte homing and dendritic cell localization. J Exp Med. *189*, 451 - 460.

Gunn, M.D., Tangemann, K., Tam, C., Cyster, J.G., Rosen, S.D., and Williams, L.T. (1998). A chemokine expressed in lymphoid high endothelial venules promotes the adhesion and chemotaxis of naive T-lymphocytes. Proceedings of the National Academy of Sciences *95*, 258-263.

Haessler, U., Pisano, M., Wu, M., and Swartz, M.A. (2011). Dendritic cell chemotaxis in 3D under defined chemokine gradients reveals differential response to ligands CCL21 and CCL19. Proceedings of the National Academy of Sciences *108*, 5614-5619.

Halin, C., Scimone, M.L., Bonasio, R., Gauguet, J.-M., Mempel, T.R., Quackenbush, E., Proia, R.L., Mandala, S., and von Andrian, U.H. (2005). The S1P-analog FTY720 differentially modulates T-cells homing via HEV: T-cells-expressed S1P1 amplifies integrin activation in peripheral lymph nodes but not in Peyer patches. Blood *106*, 1314-1322.

Hammond, M., Lapointe, G., Feucht, P., Hilt, S., Gallegos, C., Gordon, C., Giedlin, M., Mullenbach, G., and Tekamp-Olson, P. (1995). IL-8 induces neutrophil chemotaxis predominantly via type I IL-8 receptors. J Immunol. *155*, 1428-1433.

Han, S., Yan, J.-J., Shin, Y., Jeon, J.J., Won, J., Eun Jeong, H., Kamm, R.D., Kim, Y.-J., and Chung, S. (2012). A versatile assay for monitoring in vivo-like transendothelial migration of neutrophils. Lab on a Chip *12*, 3861-3865.

Hatten, M.E. (2002). New directions in neuronal migration. Science *297*, 1660-1663.

Herzmark, P., Campbell, K., Wang, F., Wong, K., El-Samad, H., Groisman, A., and Bourne, H.R. (2007). Bound attractant at the leading vs. the trailing edge determines chemotactic prowess. Proceedings of the National Academy of Sciences *104*, 13349-13354.

Hoffman, J., Linderman, J., and Omann, G. (1996). Receptor up-regulation, internalization, and interconverting receptor states. Critical components of a quantitative description of N-formyl peptide-receptor dynamics in the neutrophil. J Biol Chem. *271*, 18394-18404.

Höpken, U.E., Wengner, A.M., Loddenkemper, C., Stein, H., Heimesaat, M.M., Rehm, A., and Lipp, M. (2007). CCR7 deficiency causes ectopic lymphoid neogenesis and disturbed mucosal tissue integrity. Blood *109*, 886-895.

Horwitz, R., and Webb, D. (2003). Cell migration. Current Biology *13*, R756-R759.

Huang, C., Jacobson, K., and Schaller, M.D. (2004). MAP kinases and cell migration. Journal of Cell Science *117*, 4619-4628.

Huang, J.H., Cárdenas-Navia, L.I., Caldwell, C.C., Plumb, T.J., Radu, C.G., Rocha, P.N., Wilder, T., Bromberg, J.S., Cronstein, B.N., Sitkovsky, M., *et al.* (2007). Requirements for T-lymphocyte Migration in Explanted Lymph Nodes. J Immunol. *178*, 7747-7755.

Irimia, D., Geba, D.A., and Toner, M. (2006a). Universal Microfluidic Gradient Generator. Analytical Chemistry *78*, 3472-3477.

Irimia, D., Liu, S.-Y., Tharp, W.G., Samadani, A., Toner, M., and Poznansky, M.C. (2006b). Microfluidic system for measuring neutrophil migratory responses to fast switches of chemical gradients. Lab on a Chip *6*, 191-198.

Ismagilov, R.F., Stroock, A.D., Kenis, P.J.A., Whitesides, G., and Stone, H.A. (2000). Experimental and theoretical scaling laws for transverse diffusive broadening in two-phase laminar flows in microchannels. Applied Physics Letters *76*, 2376-2378.

Jeon, N.L., Dertinger, S.K.W., Chiu, D.T., Choi, I.S., Stroock, A.D., and Whitesides, G.M. (2000). Generation of Solution and Surface Gradients Using Microfluidic Systems. Langmuir *16*, 8311-8316.

Junger, W.G. (2011). Immune cell regulation by autocrine purinergic signalling. Nat Rev Immunol. *11*, 201-212.

Kaiser, A., Donnadieu, E., Abastado, J.-P., Trautmann, A., and Nardin, A. (2005). CC Chemokine Ligand 19 Secreted by Mature Dendritic Cells Increases Naive T Cell Scanning Behavior and Their Response to Rare Cognate Antigen. J Immunol. *175*, 2349-2356.

Keenan, T.M., and Folch, A. (2008). Biomolecular gradients in cell culture systems. Lab on a Chip *8*, 34-57.

Keese, C.R., Wegener, J., Walker, S.R., and Giaever, I. (2004). Electrical wound-healing assay for cells in vitro. Proceedings of the National Academy of Sciences of the United States of America *101*, 1554-1559.

Kelner, G., Kennedy, J., Bacon, K., Kleyensteuber, S., Largaespada, D., Jenkins, N., Copeland, N., Bazan, J., Moore, K., Schall, T., and *et al.* (1994). Lymphotactin: a cytokine that represents a new class of chemokine. Science *266*, 1395-1399.

Kim, S.-J., Shin, J.-Y., Lee, K.-D., Bae, Y.-K., Sung, K., Nam, S., and Chun, K.-H. (2012). MicroRNA let-7a suppresses breast cancer cell migration and invasion through downregulation of C-C chemokine receptor type 7. Breast Cancer Research *14*, R14.

Kim, S., Kim, H.J., and Jeon, N.L. (2010). Biological applications of microfluidic gradient devices. Integrative Biology *2*, 584-603.

Kinashi, T., and Katagiri, K. (2005). Regulation of immune cell adhesion and migration by regulator of adhesion and cell polarization enriched in lymphoid tissues. Immunology *116*, 164-171.

Klemke, M., Kramer, E., Konstandin, M.H., Wabnitz, G.H., and Samstag, Y. (2010). An MEK-cofilin signalling module controls migration of human T cells in 3D but not 2D environments. EMBO J *29*, 2915-2929.

Klemke, R.L., Cai, S., Giannini, A.L., Gallagher, P.J., Lanerolle, P.d., and Cheresh, D.A. (1997). Regulation of Cell Motility by Mitogen-activated Protein Kinase. The Journal of Cell Biology *137*, 481-492.

Knapp, D.M., Helou, E.F., and Tranquillo, R.T. (1999). A Fibrin or Collagen Gel Assay for Tissue Cell Chemotaxis: Assessment of Fibroblast Chemotaxis to GRGDSP. Experimental Cell Research *247*, 543-553.

Koduru, S., Kumar, L., Massaad, M.J., Ramesh, N., Le Bras, S.v., Ozcan, E., Oyoshi, M.K., Kaku, M., Fujiwara, Y., Kremer, L., *et al.* (2010). Cdc42 interacting protein 4 (CIP4) is essential for integrin-dependent T-cells trafficking. Proceedings of the National Academy of Sciences *107*, 16252-16256.

Kohout, T.A., Nicholas, S.L., Perry, S.J., Reinhart, G., Junger, S., and Struthers, R.S. (2004). Differential Desensitization, Receptor Phosphorylation, βArrestin Recruitment, and ERK1/2 Activation by the Two Endogenous Ligands for the CC Chemokine Receptor 7. Journal of Biological Chemistry *279*, 23214-23222.

Kroeze, W.K., Sheffler, D.J., and Roth, B.L. (2003). G-protein-coupled receptors at a glance. Journal of Cell Science *116*, 4867-4869.

Krumbholz, M., Theil, D., Steinmeyer, F., Cepok, S., Hemmer, B., Hofbauer, M., Farina, C., Derfuss, T., Junker, A., Arzberger, T., *et al.* (2007). CCL19 is constitutively expressed in the CNS, up-regulated in neuroinflammation, active and also inactive multiple sclerosis lesions. Journal of Neuroimmunology *190*, 72-79.

Kunkel, E.J., and Butcher, E.C. (2002). Chemokines and the Tissue-Specific Migration of Lymphocytes. Immunity *16*, 1-4.

Kunkel, E.J., and Butcher, E.C. (2003). Plasma-cell homing. Nat Rev Immunol. *3*, 822-829.

Laing, K.J., and Secombes, C.J. (2004). Chemokines. Developmental & Comparative Immunology *28*, 443-460.

Laudanna, C., and Bolomini-Vittori, M. (2009). Integrin activation in the immune system. Wiley Interdisciplinary Reviews: Systems Biology and Medicine *1*, 116-127.

Lauffenburger, D.A. (1982). Influence of external concentration fluctuations on leukocyte chemotactic orientation. Cell Biophysics *4*, 177-209.

Lauffenburger, D.A., and Zigmond, S.H. (1981). Chemotactic factor concentration gradients in chemotaxis assay systems. J Immunol Methods *40*, 45-60.

Li, J., Zhu, L., Zhang, M., and Lin, F. (2012). Microfluidic device for studying cell migration in single or co-existing chemical gradients and electric fields. Biomicrofluidics *6*, 024121.

Li Jeon, N., Baskaran, H., Dertinger, S.K.W., Whitesides, G.M., Van De Water, L., and Toner, M. (2002). Neutrophil chemotaxis in linear and complex gradients of interleukin-8 formed in a microfabricated device. Nat Biotech. *20*, 826-830.

Limame, R., Wouters, A., Pauwels, B., Fransen, E., Peeters, M., Lardon, F., De Wever, O., and Pauwels, P. (2012). Comparative Analysis of Dynamic Cell Viability, Migration and Invasion Assessments by Novel Real-Time Technology and Classic Endpoint Assays. PLoS ONE *7*, e46536.

Lin, F., Baldessari, F., Gyenge, C.C., Sato, T., Chambers, R.D., Santiago, J.G., and Butcher, E.C. (2008). Lymphocyte Electrotaxis In-vitro and In-vivo. J Immunol. *181*, 2465-2471.

Lin, F., and Butcher, E.C. (2006). T cell chemotaxis in a simple microfluidic device. Lab on a Chip *6*, 1462-1469.

Lin, F., and Butcher, E.C. (2008). Modelling the role of homologous receptor desensitization in cell gradient sensing. J Immunol. *181*, 8335-8343.

Lin, F., Nguyen, C.M.-C., Wang, S.-J., Saadi, W., Gross, S.P., and Jeon, N.L. (2004). Effective neutrophil chemotaxis is strongly influenced by mean IL-8 concentration. Biochemical and Biophysical Research Communications *319*, 576-581.

Lin, F., Nguyen, C.-C., Wang, S.-J., Saadi, W., Gross, S., and Jeon, N. (2005). Neutrophil Migration in Opposing Chemoattractant Gradients Using Microfluidic Chemotaxis Devices. Annals of Biomedical Engineering *33*, 475-482.

Link, A., Vogt, T.K., Favre, S., Britschgi, M.R., Acha-Orbea, H., Hinz, B., Cyster, J.G., and Luther, S.A. (2007). Fibroblastic reticular cells in lymph nodes regulate the homeostasis of naive T cells. Nat Immunol. *8*, 1255-1265.

Liu, Y., Sai, J., Richmond, A., and Wikswo, J. (2008). Microfluidic switching system for analyzing chemotaxis responses of wortmannin-inhibited HL-60 cells. Biomedical Microdevices *10*, 499-507.

Lokuta, M.A., Nuzzi, P.A., and Huttenlocher, A. (2003). Calpain regulates neutrophil chemotaxis. Proceedings of the National Academy of Sciences *100*, 4006-4011.

Luster, A.D. (2001). Chemotaxis: Role in Immune Response. In eLS (John Wiley & Sons, Ltd).

Luster, A.D., Alon, R., and von Andrian, U.H. (2005). Immune cell migration in inflammation: present and future therapeutic targets. Nat Immunol. *6*, 1182-1190.

Luther, S.A., Bidgol, A., Hargreaves, D.C., Schmidt, A., Xu, Y., Paniyadi, J., Matloubian, M., and Cyster, J.G. (2002). Differing Activities of Homeostatic Chemokines CCL19, CCL21, and CXCL12 in Lymphocyte and Dendritic Cell Recruitment and Lymphoid Neogenesis. J Immunol. *169*, 424-433.

Luther, S.A., Tang, H.L., Hyman, P.L., Farr, A.G., and Cyster, J.G. (2000). Coexpression of the chemokines ELC and SLC by T zone stromal cells and deletion of

the ELC gene in the plt/plt mouse. Proceedings of the National Academy of Sciences of the United States of America *97*, 12694-12699.

Mandala, S., Hajdu, R., Bergstrom, J., Quackenbush, E., Xie, J., Milligan, J., Thornton, R., Shei, G.-J., Card, D., Keohane, C., *et al.* (2002). Alteration of Lymphocyte Trafficking by Sphingosine-1-Phosphate Receptor Agonists. Science *296*, 346-349.

Manzo, A., Bugatti, S., Caporali, R., Prevo, R., Jackson, D.G., Uguccioni, M., Buckley, C.D., Montecucco, C., and Pitzalis, C. (2007). CCL21 Expression Pattern of Human Secondary Lymphoid Organ Stroma Is Conserved in Inflammatory Lesions with Lymphoid Neogenesis. Am J Pathol. *171*, 1549-1562.

Martin, A.P., Marinkovic, T., Canasto-Chibuque, C., Latif, R., Unkeless, J.C., Davies, T.F., Takahama, Y., Furtado, G.C., and Lira, S.A. (2009). CCR7 Deficiency in NOD Mice Leads to Thyroiditis and Primary Hypothyroidism. J Immunol. *183*, 3073-3080.

Mathias, J.R., Perrin, B.J., Liu, T.-X., Kanki, J., Look, A.T., and Huttenlocher, A. (2006). Resolution of inflammation by retrograde chemotaxis of neutrophils in transgenic zebrafish. Journal of Leukocyte Biology *80*, 1281-1288.

Matloubian, M., Lo, C.G., Cinamon, G., Lesneski, M.J., Xu, Y., Brinkmann, V., Allende, M.L., Proia, R.L., and Cyster, J.G. (2004). Lymphocyte egress from thymus and peripheral lymphoid organs is dependent on S1P receptor 1. Nature *427*, 355-360.

Menon, S., and Beningo, K.A. (2011). Cancer Cell Invasion Is Enhanced by Applied Mechanical Stimulation. PLoS ONE *6*, e17277.

Miller, M.J., Wei, S.H., Cahalan, M.D., and Parker, I. (2003). Autonomous T cell trafficking examined in-vivo with intravital two-photon microscopy. Proceedings of the National Academy of Sciences of the United States of America *100*, 2604-2609.

Moghe, P.V., Nelson, R.D., and Tranquillo, R.T. (1995). Cytokine-stimulated chemotaxis of human neutrophils in a 3-D conjoined fibrin gel assay. Journal of Immunological Methods *180*, 193-211.

Mosadegh, B., Huang, C., Park, J.W., Shin, H.S., Chung, B.G., Hwang, S.-K., Lee, K.-H., Kim, H.J., Brody, J., and Jeon, N.L. (2007). Generation of Stable Complex Gradients Across Two-Dimensional Surfaces and Three-Dimensional Gels. Langmuir *23*, 10910-10912.

Mosser, D.M., and Edwards, J.P. (2008). Exploring the full spectrum of macrophage activation. Nat Rev Immunol. *8*, 958-969.

Muller, W.A. (2009). Mechanisms of Transendothelial Migration of Leukocytes. Circulation Research *105*, 223-230.

Murdoch, C., and Finn, A. (2000). Chemokine receptors and their role in inflammation and infectious diseases. Blood *95*, 3032-3043.

Murphy, P.M., Baggiolini, M., Charo, I.F., Hébert, C.A., Horuk, R., Matsushima, K., Miller, L.H., Oppenheim, J.J., and Power, C.A. (2000). International Union of Pharmacology. XXII. Nomenclature for Chemokine Receptors. Pharmacological Reviews *52*, 145-176.

Nandagopal, S., Wu, D., and Lin, F. (2011). Combinatorial Guidance by CCR7 Ligands for T Lymphocytes Migration in Co-Existing Chemokine Fields. PLoS ONE 6(3), e18183.

Narasaraju, T., Yang, E., Samy, R.P., Ng, H.H., Poh, W.P., Liew, A.-A., Phoon, M.C., van Rooijen, N., and Chow, V.T. (2011). Excessive Neutrophils and Neutrophil Extracellular Traps Contribute to Acute Lung Injury of Influenza Pneumonitis. The American Journal of Pathology *179*, 199-210.

Nelson, R.D., Quie, P.G., and Simmons, R.L. (1975). Chemotaxis Under Agarose: A New and Simple Method for Measuring Chemotaxis and Spontaneous Migration of Human Polymorphonuclear Leukocytes and Monocytes. J Immunol. *115*, 1650-1656.

Ngo, V.N., Lucy Tang, H., and Cyster, J.G. (1998). Epstein-Barr Virus-induced Molecule 1 Ligand Chemokine Is Expressed by Dendritic Cells in Lymphoid Tissues and Strongly Attracts Naive T Cells and Activated B cells. The Journal of Experimental Medicine *188,* 181-191.

Norgauer, J., Eberle, M., Fay, S., Lemke, H., and Sklar, L. (1991). Kinetics of N-formyl peptide receptor up-regulation during stimulation in human neutrophils. J Immunol *146*, 975-980.

Okada, T., and Cyster, J.G. (2006). B cell migration and interactions in the early phase of antibody responses. Current Opinion in Immunology *18*, 278-285.

Okada, T., and Cyster, J.G. (2007). CC Chemokine Receptor 7 Contributes to Gi-Dependent T Cell Motility in the Lymph Node. J Immunol. *178*, 2973-2978.

Okada, T., Miller, M.J., Parker, I., Krummel, M.F., Neighbors, M., Hartley, S.B., O'Garra, A., Cahalan, M.D., and Cyster, J.G. (2005). Antigen-Engaged B cells Undergo Chemotaxis toward the T Zone and Form Motile Conjugates with Helper T Cells. PLoS Biol *3*, e150.

Otero, C., Groettrup, M., and Legler, D.F. (2006). Opposite Fate of Endocytosed CCR7 and Its Ligands: Recycling versus Degradation. J Immunol *177*, 2314-2323.

Ott, T.R., Lio, F.M., Olshefski, D., Liu, X.-J., Ling, N., and Struthers, R.S. (2006). The N-terminal domain of CCL21 reconstitutes high affinity binding, G protein activation, and chemotactic activity, to the C-terminal domain of CCL19. Biochemical and Biophysical Research Communications *348*, 1089-1093.

Pappu, R., Schwab, S.R., Cornelissen, I., Pereira, J.o.P., Regard, J.B., Xu, Y., Camerer, E., Zheng, Y.-W., Huang, Y., Cyster, J.G., and Coughlin, S.R. (2007). Promotion of Lymphocyte Egress into Blood and Lymph by Distinct Sources of Sphingosine-1-Phosphate. Science *316*, 295-298.

Pashenkov, M., Söderström, M., and Link, H. (2003). Secondary lymphoid organ chemokines are elevated in the cerebrospinal fluid during central nervous system inflammation. Journal of Neuroimmunology *135*, 154-160.

Pham, T.H.M., Okada, T., Matloubian, M., Lo, C.G., and Cyster, J.G. (2008). S1P1 Receptor Signalling Overrides Retention Mediated by G[alpha]i-Coupled Receptors to Promote T Cell Egress. Immunity *28*, 122-133.

Pickens, S.R., Chamberlain, N.D., Volin, M.V., Pope, R.M., Talarico, N.E., Mandelin, A.M., and Shahrara, S. (2012). Role of the CCL21 and CCR7 pathways in rheumatoid arthritis angiogenesis. Arthritis & Rheumatism *64*, 2471-2481.

Poznansky, M.C., Olszak, I.T., Evans, R.H., Wang, Z., Foxall, R.B., Olson, D.P., Weibrecht, K., Luster, A.D., and Scadden, D.T. (2002). Thymocyte emigration is mediated by active movement away from stroma-derived factors. The Journal of Clinical Investigation *109*, 1101-1110.

Pulendran, B., Katsikis, P.D., Schoenberger, S.P., Marcenaro, E., Carlomagno, S., Pesce, S., Moretta, A., and Sivori, S. (2011). Bridging Innate NK Cell Functions with Adaptive Immunity. In Crossroads between Innate and Adaptive Immunity III (Springer New York), pp. 45-55.

Qin, S., Rottman, J.B., Myers, P., Kassam, N., Weinblatt, M., Loetscher, M., Koch, A.E., Moser, B., and Mackay, C.R. (1998). The chemokine receptors CXCR3 and CCR5 mark subsets of T cells associated with certain inflammatory reactions. The Journal of Clinical Investigation *101*, 746-754.

Raffaghello, L., and Pistoia, V. (2009). Editorial: In-and-out blood vessels: new insights into T cell reverse transmigration. Journal of Leukocyte Biology *86*, 1271-1273.

Raftopoulou, M., and Hall, A. (2004). Cell migration: Rho GTPases lead the way. Developmental Biology *265*, 23-32.

Ramos, C.D.L., Canetti, C., Souto, J.T., Silva, J.o.S., Hogaboam, C.M., Ferreira, S.H., and Cunha, F.Q. (2005). MIP-1α [CCL3] acting on the CCR1 receptor mediates

neutrophil migration in immune inflammation via sequential release of TNFα and LTB4. Journal of Leukocyte Biology *78*, 167-177.

Randolph, D.A., Huang, G., Carruthers, C.J.L., Bromley, L.E., and Chaplin, D.D. (1999). The Role of CCR7 in TH1 and TH2 Cell Localization and Delivery of B cell Help in-vivo. Science *286*, 2159-2162.

Ricart, B.G., John, B., Lee, D., Hunter, C.A., and Hammer, D.A. (2011). Dendritic Cells Distinguish Individual Chemokine Signals through CCR7 and CXCR4. J Immunol. *186*, 53-61.

Ridley, A.J., Schwartz, M.A., Burridge, K., Firtel, R.A., Ginsberg, M.H., Borisy, G., Parsons, J.T., and Horwitz, A.R. (2003). Cell Migration: Integrating Signals from Front to Back. Science *302*, 1704-1709.

Rosen, E.M., Meromsky, L., Setter, E., Vinter, D.W., and Goldberg, I.D. (1990). Quantitation of cytokine-stimulated migration of endothelium and epithelium by a new assay using microcarrier beads. Experimental Cell Research *186*, 22-31.

Roux, P.P., and Blenis, J. (2004). ERK and p38 MAPK-Activated Protein Kinases: a Family of Protein Kinases with Diverse Biological Functions. Microbiol. Mol. Biol. Rev. *68*, 320-344.

Sánchez-Martín, L., Estecha, A., Samaniego, R., Sánchez-Ramón, S., Vega, M.Á., and Sánchez-Mateos, P. (2011). The chemokine CXCL12 regulates monocyte-macrophage differentiation and RUNX3 expression. Blood *117*, 88-97.

Saadi, W., Rhee, S., Lin, F., Vahidi, B., Chung, B., and Jeon, N. (2007). Generation of stable concentration gradients in 2D and 3D environments using a microfluidic ladder chamber. Biomedical Microdevices *9*, 627-635.

Sackmann, E.K., Berthier, E., Young, E.W.K., Shelef, M.A., Wernimont, S.A., Huttenlocher, A., and Beebe, D.J. (2012). Microfluidic kit-on-a-lid: a versatile platform for neutrophil chemotaxis assays. Blood *120*, e45-e53.

Sanchez-Madrid, F., and Angel del Pozo, M. (1999). Leukocyte polarization in cell migration and immune interactions. EMBO J *18*, 501-511.

Schaerli, P., and Moser, B. (2005). Chemokines. Immunologic Research *31*, 57-74.

Schiffmann, E., Corcoran, B.A., and Wahl, S.M. (1975). N-formylmethionyl peptides as chemoattractants for leucocytes. Proceedings of the National Academy of Sciences *72*, 1059-1062.

Schumann, K., Lämmermann, T., Bruckner, M., Legler, D.F., Polleux, J., Spatz, J.P., Schuler, G., Förster, R., Lutz, M.B., Sorokin, L., and Sixt, M. (2010). Immobilized Chemokine Fields and Soluble Chemokine Gradients Cooperatively Shape Migration Patterns of Dendritic Cells. Immunity *32*, 703-713.

Sensken, S.-C., Nagarajan, M., Bode, C., and Gräler, M.H. (2011). Local Inactivation of Sphingosine 1-Phosphate in Lymph Nodes Induces Lymphopenia. J Immunol. *186*, 3432-3440.

Shamloo, A., Ma, N., Poo, M.M., Sohn, L.L., and Heilshorn, S.C. (2008). Endothelial cell polarization and chemotaxis in a microfluidic device. Lab on a Chip *8*, 1292-1299.

Shankaran, H., Wiley, H.S., and Resat, H. (2007). Receptor downregulation and desensitization enhance the information processing ability of signalling receptors. BMC Systems Biology *1*, 48.

Shannon, L.A., Calloway, P.A., Welch, T.P., and Vines, C.M. (2010). CCR7/CCL21 Migration on Fibronectin Is Mediated by Phospholipase Cgamma1 and ERK1/2 in Primary T-lymphocytes. Journal of Biological Chemistry *285*, 38781-38787.

Shaykhiev, R., and Bals, R. (2007). Interactions between epithelial cells and leukocytes in immunity and tissue homeostasis. Journal of Leukocyte Biology *82*, 1-15.

Sip, C.G., Bhattacharjee, N., and Folch, A. (2011). A modular cell culture device for generating arrays of gradients using stacked microfluidic flows. Biomicrofluidics *5*, 022210-022219.

Sklar, L., Bokoch, G., Button, D., and Smolen, J. (1987). Regulation of ligand-receptor dynamics by guanine nucleotides. Real-time analysis of interconverting states for the neutrophil formyl peptide receptor. J Biol Chem. *262*, 135-139.

Smith, J.A. (1994). Neutrophils, host defense, and inflammation: a double-edged sword. Journal of Leukocyte Biology *56*, 672-686.

Stein, J.V., and Nombela-Arrieta, C. (2005). Chemokine control of lymphocyte trafficking: a general overview. Immunology *116*, 1-12.

Takahama, Y. (2006). Journey through the thymus: stromal guides for T-cell development and selection. Nat Rev Immunol. *6*, 127-135.

Tedder, T., Steeber, D., Chen, A., and Engel, P. (1995). The selectins: vascular adhesion molecules. The FASEB Journal *9*, 866-873.

Thangada, S., Khanna, K.M., Blaho, V.A., Oo, M.L., Im, D.-S., Guo, C., Lefrancois, L., and Hla, T. (2010). Cell-surface residence of sphingosine 1-phosphate receptor 1 on lymphocytes determines lymphocyte egress kinetics. The Journal of Experimental Medicine *207*, 1475-1483.

Tharp, W.G., Yadav, R., Irimia, D., Upadhyaya, A., Samadani, A., Hurtado, O., Liu, S.-Y., Munisamy, S., Brainard, D.M., Mahon, M.J., *et al.* (2006). Neutrophil chemorepulsion in defined interleukin-8 gradients in-vitro and in-vivo. Journal of Leukocyte Biology *79*, 539-554.

Tran, C.N., Lundy, S.K., and Fox, D.A. (2005). Synovial biology and T cells in rheumatoid arthritis. Pathophysiology *12*, 183-189.

Tranquillo, R.T., Lauffenburger, D.A., and Zigmond, S.H. (1988). A stochastic model for leukocyte random motility and chemotaxis based on receptor binding fluctuations. J. Cell Biol. *106*, 303-309.

Van Haastert, P.J.M., and Veltman, D.M. (2007). Chemotaxis: Navigating by Multiple Signalling Pathways. Sci. STKE *2007*, pe40-.

Vianello, F., Olszak, I., and Poznansky, M. (2005). Fugetaxis: active movement of leukocytes away from a chemokinetic agent. Journal of Molecular Medicine *83*, 752-763.

von Andrian, U.H., and Mempel, T.R. (2003). Homing and cellular traffic in lymph nodes. Nat Rev Immunol. *3*, 867-878.

Wan, B., Nie, H., Liu, A., Feng, G., He, D., Xu, R., Zhang, Q., Dong, C., and Zhang, J.Z. (2006). Aberrant Regulation of Synovial T Cell Activation by Soluble Costimulatory Molecules in Rheumatoid Arthritis. J Immunol. *177*, 8844-8850.

Wardlaw, A.J., Moqbel, R., Cromwell, O., and Kay, A.B. (1986). Platelet-activating factor. A potent chemotactic and chemokinetic factor for human eosinophils. The Journal of Clinical Investigation *78*, 1701-1706.

Wareing, M.D., Shea, A.L., Inglis, C.A., Dias, P.B., and Sarawar, S.R. (2007). CXCR2 Is Required for Neutrophil Recruitment to the Lung during Influenza Virus Infection, But Is Not Essential for Viral Clearance. Viral Immunology *20*, 369-378.

Wei, S.H., Rosen, H., Matheu, M.P., Sanna, M.G., Wang, S.-K., Jo, E., Wong, C.-H., Parker, I., and Cahalan, M.D. (2005). Sphingosine 1-phosphate type 1 receptor agonism inhibits transendothelial migration of medullary T cells to lymphatic sinuses. Nat Immunol. *6*, 1228-1235.

Weninger, W., and von Andrian, U.H. (2003). Chemokine regulation of naïve T cell traffic in health and disease. Seminars in Immunology *15*, 257-270.

Wessels, D., Lusche, D.F., Kuhl, S., Heid, P., and Soll, D.R. (2007). PTEN plays a role in the suppression of lateral pseudopod formation during Dictyostelium motility and chemotaxis. Journal of Cell Science *120*, 2517-2531.

Wolf, K., Mazo, I., Leung, H., Engelke, K., von Andrian, U.H., Deryugina, E.I., Strongin, A.Y., Bröcker, E.-B., and Friedl, P. (2003). Compensation mechanism in tumor cell migration. The Journal of Cell Biology *160*, 267-277.

Worbs, T., and Förster, R. (2009). T Cell Migration Dynamics Within Lymph Nodes During Steady State: An Overview of Extracellulr and Intracellular Factors Influencing the Basal Intranodal T Cell Motility. In Visualizing Immunity, pp. 71-105.

Worbs, T., Mempel, T.R., Bölter, J., von Andrian, U.H., and Förster, R. (2007). CCR7 ligands stimulate the intranodal motility of T-lymphocytes in-vivo. The Journal of Experimental Medicine *204*, 489-495.

Wright, G.A., Costa, L., Terekhov, A., Jowhar, D., Hofmeister, W., and Janetopoulos, C. (2012). On-Chip Open Microfluidic Devices for Chemotaxis Studies. Microscopy and Microanalysis *18*, 816-828.

Xu, J., Wang, F., Van Keymeulen, A., Herzmark, P., Straight, A., Kelly, K., Takuwa, Y., Sugimoto, N., Mitchison, T., and Bourne, H.R. (2003). Divergent Signals and Cytoskeletal Assemblies Regulate Self-Organizing Polarity in Neutrophils. Cell *114*, 201-214.

Yarrow, J., Perlman, Z., Westwood, N., and Mitchison, T. (2004). A high-throughput cell migration assay using scratch wound healing, a comparison of image-based readout methods. BMC Biotechnology *4*, 21.

Zagzag, D., Shiff, B., Jallo, G.I., Greco, M.A., Blanco, C., Cohen, H., Hukin, J., Allen, J.C., and Friedlander, D.R. (2002). Tenascin-C Promotes Microvascular Cell Migration and Phosphorylation of Focal Adhesion Kinase. Cancer Research *62*, 2660-2668.

Zhao, M., Song, B., Pu, J., Wada, T., Reid, B., Tai, G., Wang, F., Guo, A., Walczysko, P., Gu, Y., *et al.* (2006). Electrical signals control wound healing through phosphatidylinositol-3-OH kinase-[gamma] and PTEN. Nature *442*, 457-460.

Zicha, D., Dunn, G.A., and Brown, A.F. (1991). A new direct-viewing chemotaxis chamber. Journal of Cell Science *99*, 769-775.

Zigmond, S.H. (1977). Ability of polymorphonuclear leukocytes to orient in gradients of chemotactic factors. The Journal of Cell Biology *75*, 606-616.

APPENDIX

A.1. Sub-region analysis of T-cells migration in same-side dual CCL21 and CCL19 gradients

I analyzed T-cells migration in different regions of the superimposed gradients of 5nM CCL19 and 100nM CCL21 along the same direction. The results (Figure A.1.) show that in the high concentration region of the CCL19 and CCL21 gradients, cells exhibit repulsive migration away from the gradients; In contrast, in the low concentration region of the CCL19 and CCL21 gradients cells chemotax to the gradients; in the middle region of the gradient fields, cells migrate randomly. This experiment demonstrates the differential cell migratory behaviours in different combinations of CCL19 and CCL21 fields in a single experimental setup.

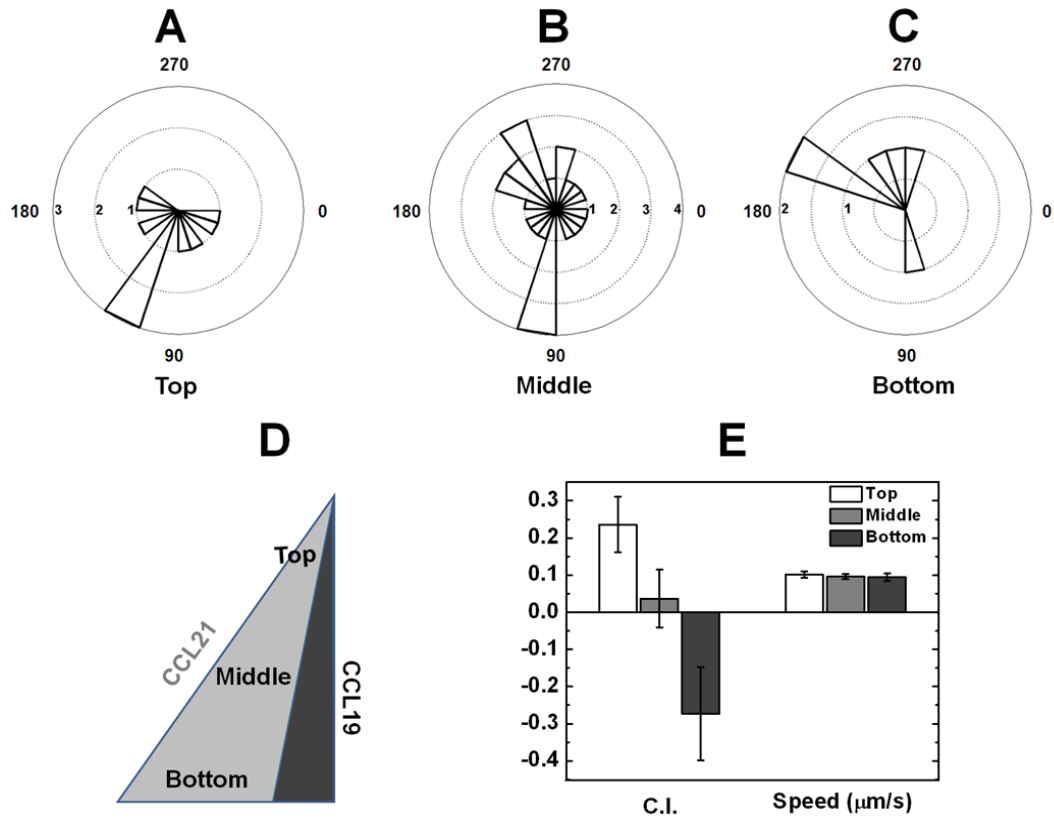

Figure A.1. Sub-region analysis of T-cells migration in same-side gradient fields of 5nM CCL19 and 100nM CCL21. (A) Angular histogram shows that T-cells in the top region orient towards the CCL19/CCL21gradients; **(B)** Angular histogram shows that T-cells in the middle region orient randomly; **(C)** Angular histogram shows that T-cells in the bottom region orient away from the CCL19/CCL21 gradients; **(D)** Schematic illustration of the same side gradient configuration and the sub-regions for analysis; **(E)** Comparison of chemotactic index (C.I.) and the speed of cells in different sub-regions of the same-side gradient fields. The error bars represent the standard error of the mean (s.e.m.). Positive C.I. indicates cells migrate toward the gradients and negative C.I. indicates cells migrate away from the gradients.

A.2. Analysis of cell surface CCR7 expression upon exposure to different CCL21 and CCL19 gradients

A.2. 1. Methodologies

The PDMS microfluidic device was prepared as described in Chapter 2 of this thesis. Instead of using coverslides, thin glass coverslips were used as the substrate for the device to allow higher magnification imaging. T-cells were exposed to single or superimposed CCL21 and CCL19 fields or medium alone for 20 minutes in the microfluidic devices, followed by immediate fixation using 4% formaldehyde solution. The fixed cells in the microfluidic devices were washed and blocked with 10% donkey serum for 45 minutes at room temperature. Cells were then stained with anti-human CCR7 primary antibody (mouse IgG, R&D Systems, MN) and incubated for 2 hours. After washing, the cell samples were stained with secondary anti-mouse antibody (donkey IgG, Northenlights-NL493, R&D Systems, MN) and incubated for 1 hour in dark at room temperature. Next, the cell samples were washed again followed by nuclear staining with DAPI and incubated for 15 minutes in dark at room temperature. Finally, the cell samples were washed and then imaged for CCR7 and DAPI staining using a confocal microscope.

The confocal images were analyzed using NIH ImageJ (v.1.34s). The total intensity (total integrated density) of CCR7 (staining) was measured for 10 or more cells in each condition. The average total intensity of each condition was normalised to positive control (positive control value was considered as 100%). The positive control, isotype control and negative control refer to the cell samples exposed to medium alone and treated with primary CCR7 antibody (positive control), mouse serum (isoptype control),

and no treatment (negative control), respectively, followed by the secondary antibody staining. The isoptype control and negative control showed undetectable staining (0%).

A.2. 2. Results and Discussion

Alteration of CCR7 expression is important for T-cells retention in LNs or exit from LNs (Cyster, 2005; Pham et al., 2008). However, the effect of CCR7 ligands fields on altering T cell surface CCR7 expression is not clear. Here, I in the first time, examined T-cells surface CCR7 expression upon exposure to different precisely defined single or superimposed CCL19 and CCL21 fields relevant to LNs sub-regions using microfluidic devices.

As shown in Figure A.2., surface CCR7 expression level in T-cells is generally reduced upon exposure to different CCL19 and CCL21 fields compared with the positive control without chemokine fields exposure. Particularly, gradients or uniform fields of CCL19 more significantly reduces surface CCR7 expression compared with gradients or uniform fields of CCL21. Evidently, even a low dose CCL19 fields can significantly reduce cell surface CCR7 expression level. These results are consistent with the known higher ability of CCL19 than CCL21 for desensitizing and internalizing CCR7 (Britschgi et al., 2008; Kohout et al., 2004; Otero et al., 2006). As expected, the dual uniform fields of CCL19 and CCL21 resulted in a more significant net reduction of surface CCR7 expression than single uniform field of CCL19 or CCL21 alone. Surprisingly, exposure to a low dose CCL19 gradient with a high dose uniform field of CCL21 that mimic the LNs TCZ periphery region resulted in almost undetectable surface CCR7 expression. Similarly, exposure to the dual same-side CCL19 and CCL21 gradients also resulted in very low surface CCR7 expression. These interesting results are consistent with the

observed random T-cells migration in the dual same-side CCL19 and CCL21 gradients (in the scenario when cells enter the dual same-side CCL19 and CCL21 gradients with or without significant previous exposure to the CCL19 and CCL21 fields in the TCZ periphery region). On the other hand, the molecular mechanism responsible for such dramatic change of surface CCR7 expression is not clear, which is beyond the focus of this thesis. Another interesting observation is that exposure of cells to single or dual gradients of CCL19 or/and CCL21 resulted in higher level of reduction of cell surface CCR7 expression compared with the corresponding single or dual uniform fields of CCL19 or/and CCL21. Further studies are required to clarify these experimental observations. In summary, the CCR7 staining analysis showed the differential ability of CCL19 and CCL21 fields for altering T-cells surface CCR7 expression, which may help explain the observed T-cells migration in different CCL19 and CCL21 fields in the experiments and the proposed combinatorial guiding mechanism.

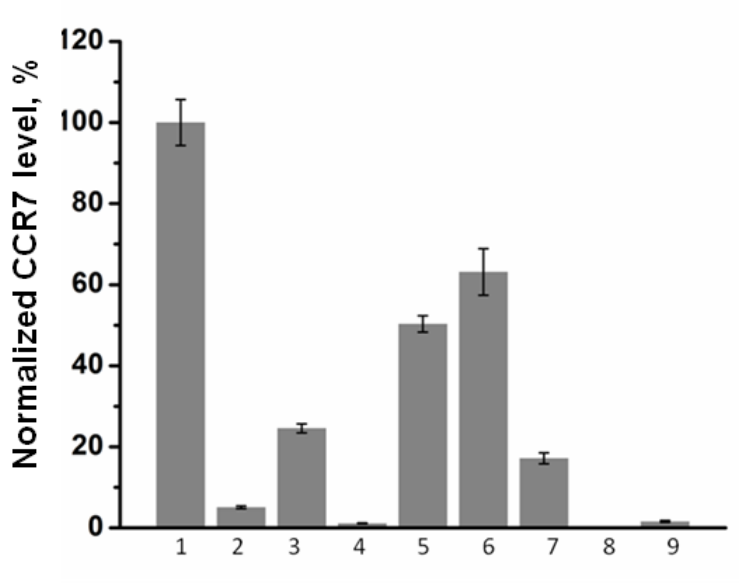

Figure A.2. Surface CCR7 expression in activated human blood T cells upon exposure to different CCL21 and CCL19 fields. The plot is based on the data from one set of representative experiments. The error bars represent the standard error of the mean (s.e.m.).